

**CHARACTERIZATION OF ASH (*FRAXINUS* SPP.) DISTRIBUTION IN A RIPARIAN FOREST IN
SOUTHEAST MICHIGAN USING SPECTRAL AND PHYSICAL VARIABLE MODELS**

by

Patrick M. Williams

**A thesis submitted
in partial fulfillment of the requirements
for the degree of
Master of Science
(Natural Resources and Environment)
at the University of Michigan
December 2012**

Faculty advisors:

Professor Michael J. Wiley, Chair

Professor Daniel G. Brown

ABSTRACT

The emerald ash borer (*Agrilus planipennis* Fairmarie) has killed tens of millions of ash (*Fraxinus* spp.) trees in Michigan alone. Riparian and lowland areas typically contain large proportions of ash and have been especially affected in Southeast Michigan. The loss of up to 20-60% of the overstory has significant implications for forest succession and floodplain stability. The goal of this study was to identify the proportion and evaluate the status of ash in a Southeast Michigan riparian forest community and to develop a minimally field-intensive GIS/ remote sensing method for identifying dominant ash populations employing multiple linear regression (MLR) and binary logistic regression (LR).

I gathered a local sample of nearly 1000 ash trees at 60 locations within the Sharonville State Game Area, Washtenaw County, Michigan, and combined this data with Landsat remotely sensed imagery and physical map-based variables in an effort to model ash population distributions. Landsat imagery and derived products were evaluated for their ability to segregate an ash spectral signature, while the map-based variables were evaluated for their ability to represent local hydrologic conditions interpreted from the autecology of ash species. An existing, ash containing lowland deciduous forest classification for Michigan (IFMAP) was also evaluated for its ability to predict ash presence/ absence.

Ash mortality comprised a total of 17% of the sampled deciduous forest with virtually all trees deceased and symptomatic of emerald ash borer infestation. The MLR and LR predictive models generally out-performed IFMAP in predicting ash

presence/absence. A single Landsat scene was generally unable to distinguish an ash related spectral signature, though elevation based variables contributed to successful prediction of ash presence with up to 91.7% accuracy. For the successful prediction of ash percent coverage, hyperspectral remotely sensed imagery would likely be necessary.

ACKNOWLEDGMENTS

I would like to thank the University of Michigan School of Natural Resources and Environment for lending equipment used for field sampling, notably the Environmental and Spatial Analysis lab and the Wiley lab. Shannon Brines, manager of the Environmental Spatial Analysis lab, deserves special recognition for his advice, assistance, and encouragement during this study's infancy. I especially thank my advisors Mike Wiley and Dan Brown for their encouragement, expert advice, and editorial critiques. Lastly and most of all, I thank my loving wife, Kerry Girardin Williams, for all of her support and patience, without which this thesis would never have come to fruition.

TABLE OF CONTENTS

Abstract	ii
Acknowledgements	iv
Table of Contents	v
List of Figures	vi
List of Tables	viii
Introduction	1
Methods	4
1. Study area	4
2. Study organisms	5
3. Integrated Forest Monitoring, Assessment and Prescription (IFMAP)	7
4. Remotely sensed imagery processing	8
5. Field methods	11
6. Spectral transformations	12
7. Physical predictive variables	14
8. Statistical analyses	15
Results	20
Discussion	23
Figures and Tables	34
Literature Cited	59
Appendix A. Master list of response variable regression tables	
Appendix B. Master list of all investigated regression tables	
Appendix C. Field Sample Plot Data	

LIST OF FIGURES

Figure 1. Study area is confined to the Washtenaw County portion of the Sharonville State Game Area. Map by the State of Michigan Department of Natural Resources (Map 1304, revised 09/2003).	34
Figure 2. Landsat 7 ETM+ scene from July 15, 1999	35
Figure 3. Landsat scene with sample subset overlay	35
Figure 4. Normalized Difference Vegetation Index (NDVI)	36
Figure 5. Tasseled Cap Layer 1: Brightness	36
Figure 6. Tasseled Cap Layer 2: Greenness	37
Figure 7. Tasseled Cap Layer 3: Wetness	37
Figure 8. 30m digital elevation model with 1m elevation increment	39
Figure 9. Slope terrain variable expressed in percent slope	39
Figure 10. Topographic Wetness Index (TWI) produced from ArcGIS Model Builder	40
Figure 11. ArcGIS Model Builder model producing Topographic Wetness Index terrain variable. The map algebra equation is equivalent to $TWI = \ln \left(\frac{A_s}{S} \right)$	40
Figure 12. Available water capacity (cm water/ cm soil)	41
Figure 13. (a) Field data normality test output. (b) Arcsine transformed field data normality test output.	43
Figure 14. Standardized normal probability plot of the multiple linear regression residuals.	45
Figure 15. Model map canopy coverage output from the multivariate regression.	46
Figure 16. Scatter plot of field measured and multiple linear regression (MLR) model percent cover values.	47
Figure 17. Presence model map output from the multivariate regression reclassified to probability of 0.002.	49

Figure 18. Presence >10% model map output from the multivariate regression reclassified to probability of 0.10.	50
Figure 19. Presence >20% model map output from the multivariate regression reclassified to probability of 0.20.	51
Figure 20. Presence at all percentages model map output from the logistic regression.	52
Figure 21. Presence >10% model map output from the logistic regression.	53
Figure 22. Presence >20% model map output from the logistic regression.	54
Figure 23. ROC curves for logistic regression models for a) ash presence, b) ash presence > 10%, and c) ash presence > 20%.	55
Figure 24. IFMAP Lowland Deciduous Forest Class	56

LIST OF TABLES

Table 1. Tasseled cap feature coefficients used by ERDAS IMAGINE 2010 for Landsat 7 ETM+ bands in the tasseled cap transformation.38

Table 2. Model predictions and associated abbreviations42

Table 3. Number of sample plots by community type42

Table 4. Prediction models with regression coefficients and model fit statistics44

Table 5. Two-sample Kolomogorov-Smirnov test for equality of distribution functions between field data and model generated data (percent cover). Critical value = $\frac{1.92}{\sqrt{60}} = 0.2479$ (Birnbaum and Hall 1960)46

Table 6. Summary table of each presence prediction’s overall accuracy, Kappa, user’s and producer’s accuracy, and the commission and omission error48

Table 7. Multivariate model for ash presence classification table reporting the user’s and producer’s accuracy, the commission and omission error, overall accuracy, and Kappa.49

Table 8. Multivariate model for ash presence greater than 10% cover classification table reporting the user’s and producer’s accuracy, the commission and omission error, overall accuracy, and Kappa.50

Table 9. Multivariate model for ash presence greater than 20% cover classification table reporting the user’s and producer’s accuracy, the commission and omission error, overall accuracy, and Kappa.51

Table 10. Logistic model for ash presence at all percent cover classification table reporting the user’s and producer’s accuracy, the commission and omission error, overall accuracy, and Kappa.52

Table 11. Logistic model for ash presence >10% cover classification table reporting the user’s and producer’s accuracy, the commission and omission error, overall accuracy, and Kappa.53

Table 12. Logistic model for ash presence >20% cover classification table reporting the user’s and producer’s accuracy, the commission and omission error, overall accuracy, and Kappa.54

Table 13. IFMAP lowland deciduous forest classification and ash presence table reporting the user's and producer's accuracy, the commission and omission error, overall accuracy, and Kappa.56

Table 14. IFMAP lowland deciduous forest classification and ash presence >10% table reporting the user's and producer's accuracy, the commission and omission error, overall accuracy, and Kappa.57

Table 15. IFMAP lowland deciduous forest classification and ash presence >20% table reporting the user's and producer's accuracy, the commission and omission error, overall accuracy, and Kappa.58

INTRODUCTION

Discovered in southeastern Michigan in June 2002, the emerald ash borer (*Agrilus planipennis* Fairmarie; henceforth referred to as EAB) has since killed tens of millions of ash trees (*Fraxinus* spp.) and spread as far as Minnesota, Missouri, Virginia, and Quebec Province (EAB 2012, McCullough and Siegert 2007, Smitely et al. 2008). Although ash is present in upland forest communities such as oak-hickory and northern hardwood, riparian areas typically encompass larger populations of ash (Pontius et al. 2008), with some forest ecotypes containing up to 60% dominance by ash, though more frequently 20 to 30% (Baker and Wiley 2004). Along with riparian areas containing larger populations of ash trees, the species most likely to occur in lowland areas (*F. pennsylvanica* [green ash] and *F. nigra* [black ash]) are preferred hosts of EAB (McCullough et al. 2008). Furthermore, there is evidence that stressed trees are more likely to be infested by EAB (McCullough et al. 2009). Ash in riparian areas subjected to regular flooding stress may be more prone for infestation; however, there is not empirical evidence at this time to support flooding stress as a factor increasing occurrence of EAB infestation.

The mortality of 20 to 60% of a riparian forest community overstory creates a significant community disturbance, including canopy gaps, tree fall, and reduced groundwater uptake from the loss of mature trees (Busch et al. 1992, Schilling and Jacobson 2009), which potentially prolongs flooding. In the wake of a large overstory disturbance, understory recruitment of shade tolerant woody species taking advantage of gaps is a common feature of secondary succession; however, in riparian floodplains

the flooding regime favors succession toward shade intolerant but flood tolerant species (Battaglia and Sharitz 2006, Mann et al. 2008, Hale et al. 2008). Furthermore, dynamic riparian ecosystems characteristically experience rapid and substantial geomorphological changes following the loss of stabilizing overstory trees, which can in turn influence forest community composition (Kupfer and Malanson 1993). These effects beg the question of the fate of ash dominated riparian forests following EAB infestation.

While efforts have been made to map the spread of EAB and improve early detection in the field, little information can be found on the effects of significant overstory ash tree loss on the forest community (Iverson et al. 2006, McCullough and Siegert 2007, Pontius et al. 2008, Smitely et al. 2008). To monitor the spread of EAB and to work towards containment, remote sensing has been successfully employed, albeit using expensive high spatial resolution hyperspectral data collection methodologies and intensive data processing by a team of experts (Pontius et al. 2008, Hallett pers. comm.). This study tests a method to identify riparian areas with high ash dominance utilizing free, readily available, digital physical and remotely sensed data.

In this study I have coupled easily acquired physical variables (e.g. elevation, available water capacity, etc.) with Landsat imagery to describe and predict ash dominated riparian and lowland forest communities in southeast Michigan. With the ultimate goal of mapping the proportion of ash canopy per pixel across a forested landscape, I explored multiple linear and binary logistic regressions to produce models for ash presence. The ability to model percent coverage and presence of ash is the first

step in identifying forest communities that should be monitored for EAB and estimating the potential for development of forest canopy gaps due to infestation. The main objectives of this study are to:

1. Determine the proportion of ash in a riparian forest community in a southeast Michigan river system;
2. Evaluate the status of ash within the area's riparian forest community; and
3. Evaluate a less field-intensive, GIS/remote sensing method for identifying forested communities with dominant ash populations and compare that method with an existing mapped vegetation classification.

METHODS

1. Study area

The Sharonville State Game Area (SSGA) is located at 42.17 N Latitude, 84.12 W Longitude in the southwest corner of Washtenaw County and the southeast corner of Jackson County, Michigan, approximately 5 miles (8 kilometers) northwest of Manchester, MI. The study area was the Washtenaw County, Sharon Township portion of the SSGA (T3S, R3E, Sections 30 and 31), approximately 1.36 square miles (3.52 square kilometers; Figure 1). This area lies at the cusp of the Ann Arbor Moraines and the Jackson Interlobate sub-subsections of the Washtenaw subsection of Albert's regional landscape ecosystem classification system (1995). This region is characterized by coarse-textured to loamy ground and end moraines, outwash, and ice-contact physiography. Total relief of the site is less than 50 m (46 m), ranging from 276 m to 322 m above sea level (USGS 2009). The growing season is approximately 150 days with approximately 32 inches of precipitation, 40 inches of snow, and annual mean temperature of 48°F (Albert 1995, RRWC et al. 2009).

The Upper River Raisin flows northeast through the center of the study area. Average annual flow of the Upper River Raisin is 107 cubic feet per second (cfs) with a drainage area of 132 square miles as measured at the U.S. Geological Survey stream gauge approximately two miles downstream of the study area (RRWC et al. 2009, USGS 2012). During the period of record (1970-1981, 1985-present), March has the greatest average monthly discharge, 197 cfs, and August the least, 48 cfs. The greatest peak flow

event on record was 869 cfs and the least peak flow event was 252 cfs, with an average annual peak flow event of 403 cfs, median 388 cfs (USGS 2012).

The study area is predominantly deciduous forest, mixed deciduous and coniferous forest, mixed with land used for the agricultural production of row crops. Only the areas dominated by deciduous forest were investigated. Upland forested areas consisted of oak-hickory and beech-sugar maple communities. Typical overstory dominant species included red oak (*Quercus rubra*), white oak (*Quercus alba*), pignut hickory (*Carya glabra*), shagbark hickory (*Carya ovata*), black cherry (*Prunus serotina*), sugar maple (*Acer saccharum*), American beech (*Fagus grandifolia*), black walnut (*Juglans nigra*), and basswood (*Tilia americana*). Lowland forested areas consisted of river floodplain and deciduous swamp species. Typical overstory dominant species included silver maple (*Acer saccharinum*), green ash (*Fraxinus pennsylvanica*), American sycamore (*Platanus occidentalis*), American elm (*Ulmus americana*), and Eastern Cottonwood (*Populus deltoides*) (Barnes and Wagner 2002). Public ownership of the SSGA and the presence of a relatively unmodified stream and riparian forest community with ash dominance contributed significantly to selection of the site for this study.

2. Study organisms

Green ash (also known as red ash; *Fraxinus pennsylvanica* Marshall) is the overwhelming dominant ash species in the study area, particularly in the lowland riparian areas of the River Raisin. Where I refer to “ash,” it may be understood as green ash. Green ash is the most widely distributed ash species in North America, ranging from southern Nova Scotia to southern Saskatchewan at its northern limits to Texas and

northern Florida at its southern limits (Wright 1959). Green ash is named for its opposite, pinnately compound leaves as they are green on top and bottom. There are generally seven to nine leaflets with serrate margins. When leaves are not available, green ash may be identified by its stout twigs, pubescent or glabrous, and if glabrous, not peeling or flaking. A medium sized tree, it is generally 40-50 feet (12-16 m) tall and 12-24 inches (30-60 cm) in diameter at breast height (DBH) at maturity (Barnes and Wagner 2002). A dioecious species (male and female flowers on different trees), the flowers appear before or with leaves in May, and the leaves drop in early fall (Wright 1959, Barnes and Wagner 2002). Green ash grows commonly in alluvial soils associated with streams and rivers that endure flooding, but not continuously wet like swamps where black ash (*F. nigra*) grows. Green ash is shade intolerant to moderately shade tolerant and is often a pioneer species after disturbance. It also often succeeds strongly shade intolerant floodplain species like black willow (*Salix nigra*) and eastern cottonwood (*Populus deltoides*) (Wright 1959, Barnes and Wagner 2002).

An introduced pest to ash, the emerald ash borer (*Agrilus planipennis* Fairmarie) (Coleoptera: Buprestidae) is a phloem-feeding beetle native to Asia (Poland and McCullough 2006, McCullough and Siegert 2007, McCullough et al. 2008). Discovered in June of 2002 in southeastern Michigan, the EAB is estimated to have been introduced in North America from solid wood packing material in the early 1990s (Poland and McCullough 2006, McCullough and Siegert 2007, Smitely et al. 2008). Since its introduction, the EAB has killed tens of millions of ash trees in Michigan, Illinois, Indiana, Kentucky, Maryland, Minnesota, Missouri, New York, Ohio, Ontario, Pennsylvania,

Tennessee, Quebec, Virginia, West Virginia, and Wisconsin (EAB 2012). Aside from the EAB estimated ability to travel 11 km/year, the spread of EAB has been exacerbated by human transport of infected nursery stock, logs, and firewood (McCullough and Siegert 2007, McCullough et al. 2008, Smitely et al. 2008). EAB adults are long and narrow beetles, approximately one-third to one-half inch (7.5 to 13.5 mm) long. Overall, they are gold to bronze in color, with metallic emerald green wing covers. While the adults feed on ash foliage, the devastation to ash populations is caused by the EAB larvae. Passing through four instars, the larva reach a length up to one and one-quarter inches (32mm) (McCullough et al. 2008). While the life cycle of the EAB is generally one year, instars may overwinter and emerge the following year (McCullough and Siegert 2007, McCullough et al. 2008). In fact, EAB has been shown to emerge from cut ash logs two summers after harvest (Petrice and Haack 2007). The phloem-feeding larvae create serpentine galleries within the ash sapwood, effectively girdling and eventually killing the tree. Early infestation is difficult to detect, but over time the following signs of infestation appear: D-shaped exit holes, splitting and sloughing bark, woodpecker activity, serpentine bark galleries, crown die-back, and epicormic branching (McCullough and Siegert 2007, McCullough et al. 2008).

3. Integrated Forest Monitoring, Assessment and Prescription (IFMAP)

I evaluated how well an existing map classification of lowland deciduous forest predicted the presence of ash based on the ground truth field data (described below), and as a basis for comparison with the predictions from the multiple linear regression and logistic regression models produced in this study. The IFMAP Michigan Statewide

Map was released by the Michigan Department of Natural Resources in 2003. A stated purpose for this map was to aid in assessment of natural resources and planning at the ecosystem level (MDNR 2003). This is a statewide land cover map identified with Landsat Thematic Mapper (TM) satellite imagery, primarily to the third level (e.g. Level 1 = Wetland, Level 2 = Lowland Forest, Level 3 = Lowland Deciduous Forest). The Lowland Deciduous Forest is the narrowest classification including “lowland ash,” a Level 4 classification that is spatially undefined. IFMAP defines “lowland” as “land that is periodically flooded and/or on hydric soils.” Further, a “lowland deciduous forest” is an area where the “proportion of trees exceeds 25%” and “the proportion of deciduous trees exceeds 60% of the canopy” (MDNR 2003). The land-cover classes were identified using images from 1997-2001 across three seasons, spring (leaf-off), summer, and fall (leaf senescence). The Lowland Forest land cover class was filtered using a three-by-three majority kernel filter, which was conducted to generalize the map to improve interpretation at the forest stand level (MDNR 2003).

4. Remotely sensed imagery processing

One Landsat 7 ETM+ scene from July 15, 1999 (Figure 2) was utilized for this study, acquired from USGS Earth Explorer (USGS 2010). The scene was clipped to the SSGA boundaries using ArcGIS 9.3.1 ArcEditor (ESRI 2009). The scene date corresponds with peak leaf-out (Barnes and Wagner 2002), and it is also prior to significant ash dieback from EAB (EAB 2012, McCullough and Siegert 2007, Smitely et al. 2008). Digital number values extracted from bands 1, 2, 3, 4, 5, and 7 were used for analysis (thermal band 6 and panoramic band 8 were excluded; band 7 was renamed to “etm6” in

statistical analyses). Prior to any image enhancement, the scene was radiometrically and atmospherically corrected using dark number subtraction and the COST method without the tau parameter (Chavez 1996, Bergen and Wang 2010).

Unsupervised classification was conducted to identify deciduous riparian forest within the SSGA using the ISODATA method with a total of twenty-five classes. Classification iterations continued until 95% convergence of classes was achieved. Classes were then visually compared with a 1 m resolution Michigan Georef National Agricultural Imagery Program Digital Ortho Photo Image (RS&GIS 2005) and the IFMAP lowland deciduous forest class. Relevant classes were combined into a deciduous riparian forest class to be used subsequently in supervised classification.

Supervised classification was performed to identify areas within mapped deciduous riparian forests that would have a high likelihood of containing ash and that could be sampled for further data collection in the field. An initial sample of eleven plots was generated randomly from within the deciduous riparian forest class generated from the unsupervised classification using the Hawth's Analysis Tools (Beyer 2006) add-on in ArcGIS. Sample plots measured 40 m x 40 m to account for GPS uncertainty, were aligned with the center of Landsat pixels, and were oriented on cardinal directions. At each of these sample plots, I collected data in the field on ash abundance to ensure that ash was represented at a variety of percent areal coverages.

All ash boles 10 cm or greater were measured for diameter at breast height (DBH). The 10 cm DBH minimum was used as the allometric equation for crown diameter estimation was based on trees minimally 10 cm DBH (Anderson et. al 2000).

Ash canopy area for each tree was estimated from the allometric equation (Equation 1), derived from bottomland green ash in Arkansas (Anderson et al. 2000). The predominant ash species in this study is green ash, although black ash and white ash (*F. americana*) are also represented. Percent cover was determined by summing all tree areas and dividing the total ash canopy area by plot area (1,600 m²), without accounting for canopy overlap.

$$\text{Crown diameter} = -6.1 + 0.99 \cdot \text{DBH} \quad (\text{Equation 1})$$

Six of the eleven plots contained at least 5% canopy coverage by ash (5.8%, 9.4%, 14.5%, 21.4%, 24.7%, and 34.7%). Landsat pixels corresponding with these six locations were used as seed pixels for the supervised classification. Spectrally similar and spatially contiguous pixels to the ground truth plots were identified by using a three-by-three pixel filter with a threshold spectral Euclidian distance of 10.0 digital numbers, generating a maximum of 1000 pixels for each seed pixel. Based on the pixels identified in this way, I created a spectral signature for ash, which was subsequently applied to the SSGA Landsat image as a whole using the same rules specified above for spectrally similar and spatially contiguous pixels. The liberal rules were used to narrow down the image to those pixels most likely to contain ash, but to be broadly inclusive so that the subsequent analysis could refine the subset to those that did and did not contain ash using a statistical model. Pixels that were part of the classified subset (Figure 3) were subsequently used to structure sample plots for the more detailed analysis. All image processing was completed in Erdas Imagine 2010 (Leica 2009).

5. Field methods

With supervised classification completed, and a subset of deciduous forest locations most likely to contain ash identified, I selected a set of field sample plots. The goal was to support a classification of the image into two categories: ash present and ash absent. The number of sample plots was determined by the following formula:

$$n = \frac{B}{4b^2} \quad \text{(Equation 2)}$$

where n = the number of sample plots, B = the upper $(\alpha/k) \times 100^{\text{th}}$ percentile of the Chi-square distribution with one degree of freedom (α = the desired confidence level; k = the number of categories; 0.95 and 2 respectively; $B = 5.024$), and b = the precision (0.05) (Congalton and Green 1999). This equation yielded a target number of 503 sample plots. As the project area is so small, containing fewer than 5,850 pixels, 503 sample plots centered on pixel centers would constitute nearly 9% of the entire project area. However, because I planned to sample plots that were four times the size of the 30 x 30 m pixels (i.e., 60 x 60 m), the area covered would be nearly 36% of all pixels. To meet practical and logistical constraints associated with collecting these data, the target was adjusted 10% of this estimated number of sample plots (i.e. fifty). Ten additional sample plots were added to total sixty, accounting for over 4% of the total project area (Brown pers. comm.)

Plots were squares measuring 60 m x 60 m centered on the Landsat pixels and oriented along cardinal directions. The plot size was increased from the original 40 m x 40 m plots to account for any potential Landsat registration errors. Sample plot locations were randomly generated using the Hawth's Analysis Tools ArcGIS add-on.

Once the plot center was located in the field using a hand held Garmin GPS 12 XL unit, the most easily accessed plot corner was established. Using a compass, the diagonal azimuth from the plot center was used, and a tape measure was used to measure the 42.4 m distance to the corner of the 60 m x 60 m plot. The remaining plot corners were established using a compass and tape measure from the first plot corner. Within the plot, all ash boles 10 cm or greater were measured at DBH. In order to prevent double-counting, each individual tree was marked with chalk at the time of measurement. Each tree was inspected for signs of EAB infestation, such as D-shaped exit holes, splitting and sloughing bark, woodpecker activity, serpentine bark galleries, and epicormic branching (McCullough and Siegert 2007, McCullough et al. 2008). Ash canopy area for each tree was estimated from Equation 1. Percent cover was determined by summing all tree areas and dividing the total ash canopy area by plot area (3,600 m²), without accounting for canopy overlap.

I tested the normality of the field data by producing frequency histograms, P-P plots, and detrended P-P plots in SPSS (SPSS 2010). The percentage data were transformed using an arcsine square-root transformation (Equation 3) as proportion data have non-constant variance (Gotelli and Ellison 2004, Zar 1999, Ahrens et al. 1990, Haukos et al. 1998).

$$p' = \arcsine(\sqrt{p}), \text{ where } p = \text{proportion} \quad (\text{Equation 3})$$

6. Spectral transformations

In addition to the spectral bands of the ETM+ image, I calculated four spectrally transformed features for input as predictor variables in the statistical model. The

normalized difference vegetation index (NDVI, Figure 2) is produced by Equation 4, where IR equals the infrared band values and R equals the red band values of the electromagnetic spectrum (Leica 2008).

$$\frac{IR-R}{IR+R} \quad \text{(Equation 4)}$$

The NDVI reports the percent of vegetation greenness on a scale from 0 to 1, with 1 being the greatest value (Figure 4). This vegetation index was chosen because its sensitivity to vegetation structure and productivity might result in a quantitative difference between ash dominated pixels compared to other deciduous vegetation.

I also calculated the tasseled cap transformation, which reduces band features from six correlated bands to three uncorrelated features, each orthogonal to the others. By rotating the plane formed by two bands, functionally little information is lost. The three primary features produced by the tasseled cap transformation correspond to the scene physical characteristics of brightness, greenness, and a transition between the two representing wetness (Kauth and Thomas 1976, Crist and Cicone 1984a,b, Crist and Kauth 1986, Huang et al. 2002, Lillesand et al. 2008). The brightness, greenness, and wetness features minimally capture 95% of the data variation (Crist and Kauth 1986). Each feature is a combination of weighted sums of the ETM+ spectral bands (Kauth and Thomas 1976, Crist and Cicone 1984a,b, Crist and Kauth 1986, Huang et al. 2002, Lillesand et al. 2008); the coefficients used by ERDAS Imagine (Leica 2009) are listed in Table 1. Images of brightness, greenness, and wetness are displayed in Figures 5-7.

7. Physical predictor variables

A 1 arc-second (resampled to 30m) digital elevation model (DEM) was used to create two terrain-related variables for inclusion in the statistical model. The DEM has 1m vertical resolution (Figure 8; USGS 2009) and is a gridded lattice representing point elevations at the pixel center (Gallant and Wilson 2000). In the relatively small project area, the DEM relates to the relative location of ash within the landscape; ash is likely to be located in lower elevations (Wright 1959, Barnes and Wagner 2002).

Slope, represented as percent slope, was calculated to measure the rate of elevation change in the steepest direction. Slope plays a critical role in the movement of water and materials (Figure 9; Gallant and Wilson 2000), and ash typically inhabits lowlands and bottomlands that have lower percent slopes and lower elevations (Wright 1959, Barnes and Wagner 2002). The topographic wetness index (TWI, Figure 10) is a combination of specific catchment area and slope steepness representing the potential for soil saturation from surface flows (Sorenson et al. 2006, Sorenson and Seibert 2007, Brown 2010). Local low points with larger catchment areas will have a greater potential for soil saturation and often correspond to lowland areas where ash thrive. TWI is produced by Equation 5 where A_s is the specific catchment area and S is slope:

$$TWI = \ln \left(\frac{A_s}{S} \right) \quad (\text{Equation 5})$$

This equation was applied spatially in ArcGIS Model Builder (Figure 11). Starting with the DEM, the sinks, or local minima, that have no lower neighbor cells are filled. From the filled DEM, the percent slope and flow direction were calculated, followed by the

flow accumulation, or specific catchment area, calculated from flow direction. The percent slope and flow accumulation were then used in Equation 5 to produce the TWI.

In addition to elevation-based terrain variables, available water capacity, a soil-based variable was included in analysis (AWC, Figure 12). AWC is the amount of water available to plants between field capacity and permanent wilting point expressed by the unitless volume fraction of cm water/ cm soil (NRCS undated, Brady and Weil 2002). As ash grows in alluvial soils with higher soil organic carbon associated with rivers and streams, it follows that these areas will have greater AWC (Wright 1959, Brady and Weil 2002).

8. Statistical analyses

Eight different regression models were estimated to predict ash. First, one multiple linear regression (MLR) that predicted percent canopy cover of ash and three separate binary logistic regressions (LR) for predicting presence of ash at three percentages of canopy cover (>0%, >10% and >20%) were estimated. These models used Landsat spectral information and physical variables as predictors. A total of seven predictions were made from these four models: percent canopy cover from the MLR and classifications of presence from these predictions at three different levels (>0%, >10% and >20%), as well as predictions of presence from each of the three LR models. The four MLR and LR models were re-estimated using the presence of the IFMAP lowland deciduous forest classification as a predictor variable in place of the spectral information from the satellite image. These models were used to create four additional predictions: percent canopy cover from the MLR and predictions of presence from each

of the three LR models. In addition, the IFMAP lowland deciduous forest classification (IFMAP) is effectively a stand-alone presence model and prediction map containing an unknown proportion of ash and evaluated at three different levels (>0%, >10% and >20%). Each of these predictions was compared with field data to evaluate their predictive accuracy. See Table 2 for a list of model prediction abbreviations.

A multiple linear regression (MLR; $y = b_0 + b_1X_1 + b_2X_2 \dots b_nX_n$) using automatic backward stepwise variable selection was performed using all predictor variables (DEM, slope, TWI, AWC, NDVI, brightness, greenness, wetness, Landsat ETM+ bands 1-5, and 7) to predict the response variable arcsine square-root transformed percent ash canopy coverage (MLR). A predictive map of proportion ash canopy coverage was produced after the arcsine square-root transformation was transformed back using Equation 6:

$$\hat{p} = \sqrt{\sin(\hat{p}')} \quad (\text{Equation 6})$$

ETM+ bands were input singly without any other spectral features (i.e. NDVI and tasseled cap) to avoid multiple-collinearity among the bands. NDVI and greenness were also evaluated separately due to high correlation (0.8973). The two-sample Kolomogorov-Smirnov test for equality of distribution functions was performed to evaluate how well the predicted proportions match the percent canopy coverages measured in the field (Borkowski undated, Birnbaum and Hall 1960).

H_0 : Field Percentage(p) = Model Percentage(\hat{p}) for all p vs.

H_a : Field Percentage(p) \neq Model Percentage(\hat{p}) for at least one p .

The model residuals were tested for normality using a standardized normal probability plot.

Three additional prediction maps were created from the above MLR for the following: ash presence ($MLR > 0\%$), ash presence at proportions greater than 10% coverage ($MLR > 10\%$), and ash presence at proportions greater than 20% coverage ($MLR > 20\%$). These predictive maps were created by reclassifying the *MLR* predictive map based on the probabilities of >0 , >0.10 , and >0.20 respectively. The purpose of including these three additional MLR predictions was to evaluate which regression model, the MLR or the LR, produced more accurate ash presence predictions.

A binary logistic regression (LR; $y = \text{Exp}(b_0 + b_1X_1 + b_2X_2 \dots b_nX_n) / (1 + \text{Exp}(b_0 + b_1X_1 + b_2X_2 \dots b_nX_n))$) using automatic backward stepwise variable selection was performed using all predictor variables (DEM, slope, TWI, AWC, NDVI, brightness, greenness, wetness, Landsat ETM+ bands 1-5, and 7) to predict the response variable ash presence ($LR > 0\%$), regardless of ash abundance. This LR sought to fit a model distinguishing where ash existed from where it was not present. ETM+ bands were input singly without any other spectral features (i.e. NDVI and tasseled cap) to avoid multiple-collinearity among the bands. NDVI and greenness were also evaluated separately due to high correlation (0.8973). Two additional LR models were estimated where presence was defined at canopy coverage percentages greater than 10% ($LR > 10\%$) and greater than 20% ($LR > 20\%$). With these regressions, I sought to identify locations of ash containing pixels where ash was present in larger percentages of canopy coverage. The ability to identify pixels with larger proportions of ash is desirable for assessing areas with greater canopy disturbance. A predictive map of ash presence was produced for each respective LR response variable. Classification tables and relative

operating characteristic (ROC) curves were produced to evaluate performance of the LR models of ash presence.

In the interest of producing the best possible predictive model, IFMAP presence/absence was also incorporated as a predictor variable in MLR and LR models. As IFMAP was created from Landsat TM imagery, regressions were processed without spectral variables and only the IFMAP classification and the physical variables: DEM, slope, TWI, and AWC. A MLR ($y = b_0 + b_1X_1 + b_2X_2 \dots b_nX_n$) using automatic backward stepwise variable selection was performed using only the aforementioned IFMAP presence/absence and the physical predictive variables to predict the response variable arcsine square-root transformed percent ash canopy coverage (*IFMAP_MLR*). Binary logistic regressions ($y = \text{Exp}(b_0 + b_1X_1 + b_2X_2 \dots b_nX_n) / (1 + \text{Exp}(b_0 + b_1X_1 + b_2X_2 \dots b_nX_n))$) using automatic backward stepwise variable selection were performed using only the aforementioned IFMAP presence/absence and physical predictive variables to predict the response variables ash presence (*IFMAP_LR>0%*), presence of canopy coverage greater than 10% (*IFMAP_LR>10%*), and presence of canopy coverage greater than 20% (*IFMAP_LR>20%*). A prediction map was produced for each occurrence when IFMAP was a significant variable producing a novel regression result.

All prediction maps were evaluated with user's and producer's accuracies, the commission and omission errors, overall accuracy, and Kappa statistic. The IFMAP lowland deciduous forest class was evaluated against field collected ash percent canopy coverage data that were processed as three response variables assessing how IFMAP predicted ash presence at any proportion (*IFMAP>0%*), ash at proportions greater than

10% (IFMAP>10%), and ash at proportions greater than 20% (IFMAP>20%). All statistical analyses were performed in STATA (StataCorp 2011).

RESULTS

The SSGA deciduous forest communities are fairly healthy with the exception of the ash component; generally there is low to moderate incidence of invasive shrubs like common and glossy buckthorn (*Rhamnus cathartica*, *R. frangula*), bush honeysuckle (*Lonicera* spp.), autumn olive (*Elaeagnus umbellata*), and Japanese barberry (*Berberis thunbergii*) which are common in Southeast Michigan forests. Ash is predominantly located within the riparian area along the River Raisin and wetland depressions/deciduous swamps within the study area. The sixty sample plots were distributed among the following community types: 27 oak-hickory, 4 beech-maple, 11 floodplain, 12 deciduous swamp, 5 mixed forest, and 1 open field with a treed hedgerow (Table 3; Barnes and Wagner 2002). Some plots were a mixture of communities and may have contained lowland areas with ash (e.g. part oak-hickory terrace and part floodplain).

The mature ash trees are virtually all dead within the study area, with the exception of the occasional root collar sprout and saplings <2cm DBH. Despite this exceptional mortality, very few ash trees had fallen at the time of sampling. While the majority of site visits were conducted during the late fall and winter to minimize GPS disruption by leafed out canopy, several site visits were conducted during leaf out and no mature ash was observed with a live canopy. All ash trees had evidence of EAB infestation including at least one of the following symptoms: D-shaped exit holes, splitting and sloughing bark, woodpecker activity, serpentine bark galleries, and epicormic branching (McCullough and Siegert 2007, McCullough et al. 2008). A total of 974 ash trees were sampled. The average ash tree was 23.9 cm DBH (range = 10.0 to

94.1 cm) with a crown of 17.6 m² (range = 3.8 to 87.1 m²). Within the twenty-eight ash containing plots, there was a total of 17% ash canopy coverage, with average canopy coverage of 14.9% per plot.

Both the field data on percentage ash cover, and arcsine square-root transformed data, displayed non-normal distributions (Figure 13). Both frequency histograms were right skewed, though the transformed data were marginally more normal. Both the normal P-P and detrended P-P plots of residuals indicated non-normality of these data. The multiple linear regression was performed using the arcsine square-root transformed percentage ash canopy cover, then back transformed for creation of the predictive maps.

Table 4 presents the multiple linear regression and logistic regression predictor variables, regression coefficients, coefficients of determination, and model significance values. The multiple linear regression (*MLR*) model of arcsine square-root transformed ash percent canopy coverage in field sample plots included only DEM and TWI as significant predictor variables ($p < 0.001$ and $p = 0.001$ respectively, $R^2 = 0.51$). The regression residuals appear normal and should not adversely affect my results and application toward predictive maps (Figure 14). A predictive map depicting ash canopy coverage percentages predicted values ranged from 0 to 34% (Figure 15). A two-sample Kolomogorov-Smirnov pairwise test for equality of distribution functions indicated that the distributions of field data and model predictions were significantly different ($p < 0.001$, Table 5). A scatter plot of the percent cover values of the field data and model data illustrates the inequality of the distributions (Figure 16).

The binary logistic regression LR>0% model included DEM and greenness as significant predictor variables ($p = 0.002$ and 0.038 respectively; Pseudo- $R^2 = 0.63$). LR>10% included DEM and Slope as significant independent variables ($p = 0.004$ and 0.020 respectively; Pseudo- $R^2 = 0.49$). LR>20% included DEM as the only significant independent variable ($p = 0.005$; Pseudo- $R^2 = 0.44$). The logistic regressions had the following areas under the ROC curve: 0.96, 0.93, and 0.94 respectively (Figure 23).

Table 6 presents a summary of each model presence prediction's overall accuracy, Kappa, user's and producer's accuracies, and the commission and omission errors. The presence predictions varied in their performance in the following ways, from best classification to poorest (taking into account overall accuracy and the Kappa statistic):

Presence of ash >0%:

LR (Fig. 20, Table 10) > **IFMAP** (Fig. 24, Table 13) > **MLR** (Fig. 17, Table 7)

Presence of ash >10% cover:

MLR (Fig. 18, Table 8) > **LR** (Fig. 21, Table 11) > **IFMAP** (Table 14)

Presence of ash > 20% cover:

LR (Fig. 22, Table 12) > **MLR** (Fig. 19, Table 9) > **IFMAP** (Table 15)

Full regression tables of the response variables are presented in Appendix B. Full regression tables of all investigated regressions are presented in Appendix C.

DISCUSSION

After spending some time at the Sharonville State Game Area near the River Raisin, it is clearly evident that the emerald ash borer has devastated the local ash population. Nearly 1,000 ash trees were sampled and virtually all are dead; no ash tree larger than two cm DBH was observed to be alive, minimally evidenced by no viable buds for the next spring. All observed trees have some readily visible sign of infestation, with many trees so long dead that the bark is sloughing off, exposing the serpentine galleries that ushered in their death. Sample plots varied in the amount of ash present from 0.2% canopy cover by ash to as high as 66.7%, with an average of 14.9%. Overall, 17% of the sampled riparian forest canopy has been killed, and little evidence of any woody trees taking ash's place can be observed.

A loss of nearly 20% of the riparian forest in the SSGA raises crucial questions about the successional fate of the forest community. Such a large-scale disturbance is rare in non-coastal floodplains not subjected to hurricanes (King and Antrobus 2005, Battaglia and Sharitz 2006). At the time of field investigation, little woody vegetation was observed establishing in the wake of canopy gaps; however, seedling regeneration may have been overlooked because of leaf-off conditions exacerbated by snow cover. Ash is considered both a pioneer and secondary succession species as it is shade intolerant and flood tolerant, though more shade tolerant than other pioneer species like black willow and eastern cottonwood (Wright 1959, Barnes and Wagner 2002, King and Antrobus 2005). In fact, ash could regenerate to fill gaps from deceased parent

trees; however, ash is at a disadvantage since the ash seed bank must compete with other species in the seed bank and from living, productive adult trees.

The gaps could instead be filled by existing co-dominants such as silver maple, sycamore, and eastern cottonwood—all are shade-intolerant species that are tolerant to flooding (Barnes and Wagner 2002, King and Antrobus 2005). American elm is an associate with ash within the study area, and it is a common gap filler since it is moderately shade-tolerant and flood tolerant (Barnes and Wagner 2002, King and Antrobus 2005); however, its success as a dominant appears to be limited by Dutch elm disease since most elms within the study area appear to be deceased before reaching the upper canopy. Alternatives to existing co-dominants filling the gaps are the establishment of lesser floodplain species or invasive species. Hale et al. (2008) discuss the increase of the historically non-dominant species bitternut hickory (*Carya cordiformis*) and northern hackberry (*Celtis occidentalis*) in the Lower Wisconsin River riparian forests. Both of these species are present in the SSGA and tend to be later successional species (Hale et al. 2008). While less flood tolerant, both are fairly shade tolerant and the gap openings may provide opportunity to move into the canopy. As for invasive species, glossy buckthorn and bush honeysuckle are common in Michigan forests and can tolerate floodplain conditions (Barnes and Wagner 2002). The bottom line here is that what vegetation will take the place of ash is not easily foreseen.

The question of what will replace ash in southeastern Michigan floodplains is a primary driver of my interest in classifying ash-containing communities. Resource managers and ecologists alike would benefit from the knowledge of where and how

much dead ash exists within riparian areas. I used two statistical modeling techniques to predict the percent coverage of ash and the presence of ash for 30 m pixels in the study area: multiple linear regression and binary logistic regression. The goal was to maximize predictive accuracy over generality, with models designed to be precise and realistic because of the large scale—or small extent—of the study area (Guisan and Zimmerman 2000). These models cannot be expected to represent other regions with the same level of accuracy as that found in the study area; however, similar patterns are a reasonable expectation if the methods are duplicated for other areas similar in scale and flora. While the use of multiple linear regression and binary logistic regression models was appropriate for this question (Guisan and Zimmerman 2000), the model results indicate only limited success in modeling ash percent coverage and moderate success in modeling ash presence.

The MLR model of percent cover produced reasonable predicted values (0-33.8%), but did not capture the full range collected in the field (up to 66.7%). The model was statistically significant but accuracy was low; for example, the plot with the greatest amount of ash coverage (66.7%) had a predicted value of only 5.4%. The weak fit of the model is reflected in the coefficient of determination value of 0.51. Coefficients for both the DEM and TWI variables were in the directions expected: the DEM was negative, predicting ash at lower relative elevations and the TWI was positive, predicting ash at locations with a greater wetness index value. While these variables certainly contribute to ash presence, one might expect spectral variables to be useful when assigning values related to the amount of ash. Variables like NDVI and the tasseled cap

greenness, which are directly related to the amount of “green” in an area, might be expected to be significant too, but they were not. This outcome reasonably leads to the conclusion that Landsat ETM+ does not have spectral sensitivity to differentiate ash from other deciduous vegetation with only one scene.

One issue that likely contributed to the MLR model having limited success predicting percent cover is that there were not enough sample points, or a sufficient range in values. The number of sample points was calculated based on two classes, ash present and ash absent (Congalton and Green 1999). These classes are appropriate for evaluating presence/absence of ash, but not percent cover. A minimum of eight classes should have been included in the sample point calculation, representing classes of 10% increments up to 70%: 0% , >0-10%, >10-20%, >20-30%, >30-40%, >40-50%, >50-60%, >60-70%. This range of percent cover values would cover the expected maximum ash canopy coverage of ~60% (Baker and Wiley 2004), which was ultimately validated by the field data. As previously mentioned, although the predicted percent cover values were limited in their accuracy, the predictive map appeared to detect ash presence fairly well, which was why the MLR predictive map was resampled and evaluated for ash presence. The degree of success achieved by this model in predicting ash presence/absence is discussed below in comparison to the logistic regression and the IFMAP lowland deciduous forest classification.

Each of the binary logistic regressions produced good results for estimating the presence of ash for greater than 0% ($LR>0\%$), greater than 10% ($LR>10\%$), and greater than 20% cover ($LR>20\%$). The regressions produced reasonable pseudo- R^2 values

(0.44-0.63), good to excellent classification percentages (83.3%-91.7%), and excellent ROC values (0.93-0.96). Even though the logistic models were fairly successful in predicting ash presence and absence, the significant variables were not identical among the different models. The DEM was significant in all models and was the only significant variable in the >20% model. Like the MLR, the DEM coefficients were all negative, indicating that ash were more likely to be present in the lower elevations of the study region. The model for presence classified at >0% also had greenness as a significant variable; it was the only model that included a spectral variable. This variable had a positive coefficient, indicating that greener pixels were more likely to contain ash. This makes intuitive sense as green ash is named for its green leaves; however, whether ash has a “greener” signature than other co-dominants cannot be known without having separate spectral signatures of all co-dominants, especially silver maple, which is the dominant species in most sample plots containing ash. The model for presence of >10% cover also had slope as a significant predictor variable, which had a negative coefficient indicating that ash had a greater probability of presence at lower slopes. The fact that the each logistic model had different significant predictor variables points to the relatively weak role of these secondary variables in predicting ash presence, a potentially arbitrary set of variables used for classifying ash presence as a whole with the exception of DEM, which consistently had greater significance than all other variables, and always $p \leq 0.005$.

The IFMAP lowland deciduous classification had weak to moderate success predicting ash presence: 63.3%-75% correctly classified and kappa of 15.1%-34.8%,

depending on how the field data were classified for evaluation. The low Kappa values indicate that the classifications had a much greater likelihood of chance agreement than true agreement. Of particular interest is that IFMAP was produced solely by Landsat TM classification, whereas the models developed here were driven solely by physical variables in all but one instance. The likely reason that IFMAP was able to have such success classifying ash presence and absence was the use of multiple years and three seasons in their analysis, while the presented models used only one scene from peak leaf-out. With the exception of the MLR presence >0% model, both the logistic and MLR models had better classification success than IFMAP. One reason for this is that the IFMAP lowland deciduous forest class is much patchier than the model maps produced by the presented models. Another reason may simply be that physical variables are better at predicting the presence of ash than analyses utilizing the limited spectral resolution of Landsat TM (and ETM+).

None of Landsat 7 ETM+ bands were found to be significant predictors; therefore, it can be presumed that the spectral resolution of Landsat taken at one point in time is not sufficient to differentiate ash containing pixels from other deciduous forest. Since the NDVI is derived from a direct ratio of the red and infrared bands which had no correlation with ash coverage, it was also not a significant predictor. The tasseled cap greenness variable was significant in one model, which is somewhat surprising as it is similar the NDVI in identifying green vegetation. The reason it was significant is likely due to greater variation being encompassed as it is derived from all Landsat bands, whereas the NDVI is derived from only two. In other respects, it is not

surprising that greenness was not significant in all models as it is better at differentiating broad classes like vegetation and soils as opposed to specific species or soil types (Crist and Kauth 1986).

The variables DEM, slope, and TWI were the only significant physical variables. The DEM was significant in all models, and the other two variables are dependent on the DEM, which indicates that elevation and related features are the best indicators of ash presence of all included variables. The derived slope variable was only significant in one model as lowland forests tend to have flatter slopes, and this site has expanses of low slope land in agricultural production. DEM picks up the lower elevations where lowland forests and riparian ash species occur, and TWI identifies wetter areas, also where riparian ash species occur. If one were to expand the analysis to more disparate riparian sites, it would be important to standardize the DEM values by site before comparison; otherwise the lower areas from sites with greater elevation may not be appropriately identified (Gotelli and Ellison 2004). It was surprising that AWC was not only insignificant, but not even close to significant in either the MLR or logistic regressions. Looking at the maps, it appears that the higher values for this variable correspond to the lowest areas, and that this location would make the variable significant, similar to the DEM and TWI. Perhaps the reason that AWC was not significant is it has low variability (0.07-0.4). All variables were analyzed in a correlation matrix, so cross-correlation should not have been a factor in AWC's insignificance.

A number of data issues may have potentially affected the results of this study. First, the sample points were chosen randomly as opposed to a grid layout, which may

have increased the spatial autocorrelation, although it is reasonable to assume that because of the small size of the study area, some spatial autocorrelation could not be avoided. This has the possible effect of over-estimating the significance of variables in the models. Another sample related issue is that there may not have been enough sample points. While 60 sample points was thought a suitable number based on the number of cells in the Landsat image and using two classes (presence/ absence), this number was too small when considering proportions, effectively 101 classes representing 0-100 percent, or at least 11 classes if going by categories of 10% values from 0 to 100% (Congalton and Green 1999). MLR residuals appear normal, therefore the model predictive map application should be valid (Figure14).

Two studies by Baker and Wiley (2004, 2009) included this study area in their analyses: the first study sought to encompass and describe the variation within Lower Michigan's riparian areas, while the second investigated the causal relationships of broad scale controls resulting in that variation. The 2004 study originally classified riparian areas into seven groups, labeling this study area as a [Silver] Maple-Elm-Sycamore ecotype. For the 2009 study, groups were reduced to five ecotypes and the Maple-Elm-Sycamore group was combined with the Silver Maple Swamp ecotype and renamed "Silver" [maple]. It is reasonable to assume that these two ecotypes from the 2004 study were combined because of their similar species composition with both silver maple and green ash as canopy dominants. These two ecotypes had a mean relative abundance of green ash between 18.7-28.0% which this study corroborates with an average of 17% relative abundance of ash (Baker and Wiley 2004).

Similar to Baker and Wiley, I used map-based, or latent, variables, albeit they used many more to encompass regional variability, such as temperature, precipitation, transport distance, runoff, groundwater, and multiple flood-based variables. The study area investigated does not have appreciable differences in temperature or precipitation, and the DEM and TWI variables in this study were intended to be proxies for runoff, groundwater, and flood variables. The analyses conducted in this study may have been bolstered by the inclusion of groundwater and floodplain elevation, but I did not have the data necessary to model these variables at such a fine scale. The goal of identifying riparian ecotypes also differs from the goal of identifying a single species, which is why spectral variables were included in this study.

Baker and Wiley (2009) identify latent, or unmeasured, variables in their analysis generated from geographic predictors, site wetness being one. A composite of precipitation/potential evapotranspiration, groundwater flux, and floodplain elevation, their site wetness variable contained parameters encompassing surface and subsurface contributors to site wetness. I used DEM as a proxy for site wetness, i.e. assuming lower relative elevations are both closer to the water table and more prone to flooding, and the TWI further provided the surface flow contribution to site wetness. My model, however, did not include an explicit groundwater component; therefore, DEM was at best a rough proxy without knowing the difference between ground elevation and the water table. I also included AWC as an additional proxy to site wetness; soils with finer particles and higher amount of soil organic carbon have higher AWC values, and water is retained longer for use by plants (Brady and Weil 2002). This variable, however, was

not significant in any models and did not contribute significantly to site wetness in these models.

The Silver Maple Swamp ecotype was successfully identified using regional to local level variables, while this study sought to tease out the green ash component of that ecotype assemblage using only local, fine scale (30 m) variables. This disparity brings into the discussion the question of scale. Baker and Wiley show that these ecotypes derive from drivers working across multiple scales, from catchment, to valley segment, to local extents (2004, 2009). While variables such as climate did not differ in this study area, broader scale factors like valley hydraulics not considered in this study may have significance in the presence of ash. Variables that cannot be effectively granulated at the 30 m pixel level play a role in the presence of the larger Silver Maple Swamp ecotype containing the species of interest, so too may the micro-site level presence of ash be driven by these coarser variables (Baker and Wiley 2004, 2009). If a broader, regional analysis for green ash were conducted including more variables similar to that of Baker and Wiley, it is anticipated that the outcome would be mapping of ash containing Silver Maple Swamp ecotypes, more so than identifying presence or percent cover of ash alone. Green ash grows in other ecotypes than the Silver Maple Swamp; in fact it was ubiquitous in all but one ecotype in Lower Michigan (Baker and Wiley 2004). Reciprocally, it can be argued that the models of this study identify a Silver Maple Swamp ecotype or a more fine tuned IFMAP-like lowland deciduous forest class.

This study's models are not successful enough for determining how much ash is present within a community, and therefore, how much of the overstory is dead or dying

following EAB infestation for the purpose of creating a minimally field-intensive model for predicting ash percent coverage and presence (even at >10-20% cover). It is not enough to know where ash is likely to grow, but to quantify the amount of dieback. Here enters the need for and utility of remotely sensed imagery to segregate a spectral signature for green ash. Landsat does not have the spectral resolution, and potentially not the spatial resolution, to isolate ash; therefore, the greater spectral resolution of sensors like Hyperion or AVIRIS should be investigated. By successfully quantifying the ash composition of a forest, the scale of community disturbance and question of forest succession can begin to be investigated more broadly. This study area contained 17% ash dominance, with other riparian ecotypes encompassing up to 60% ash dominance. In the wake of the EAB infestation in southeast Michigan, this dominant portion of the canopy is dead or dying, and this infestation is spreading to all of the Northeast United States and Southeast Canada. Additional studies are necessary to document the level of devastation to riparian ecosystems by this invasive pest and to assess the long-term effects of such a large community disturbance.

FIGURES AND TABLES

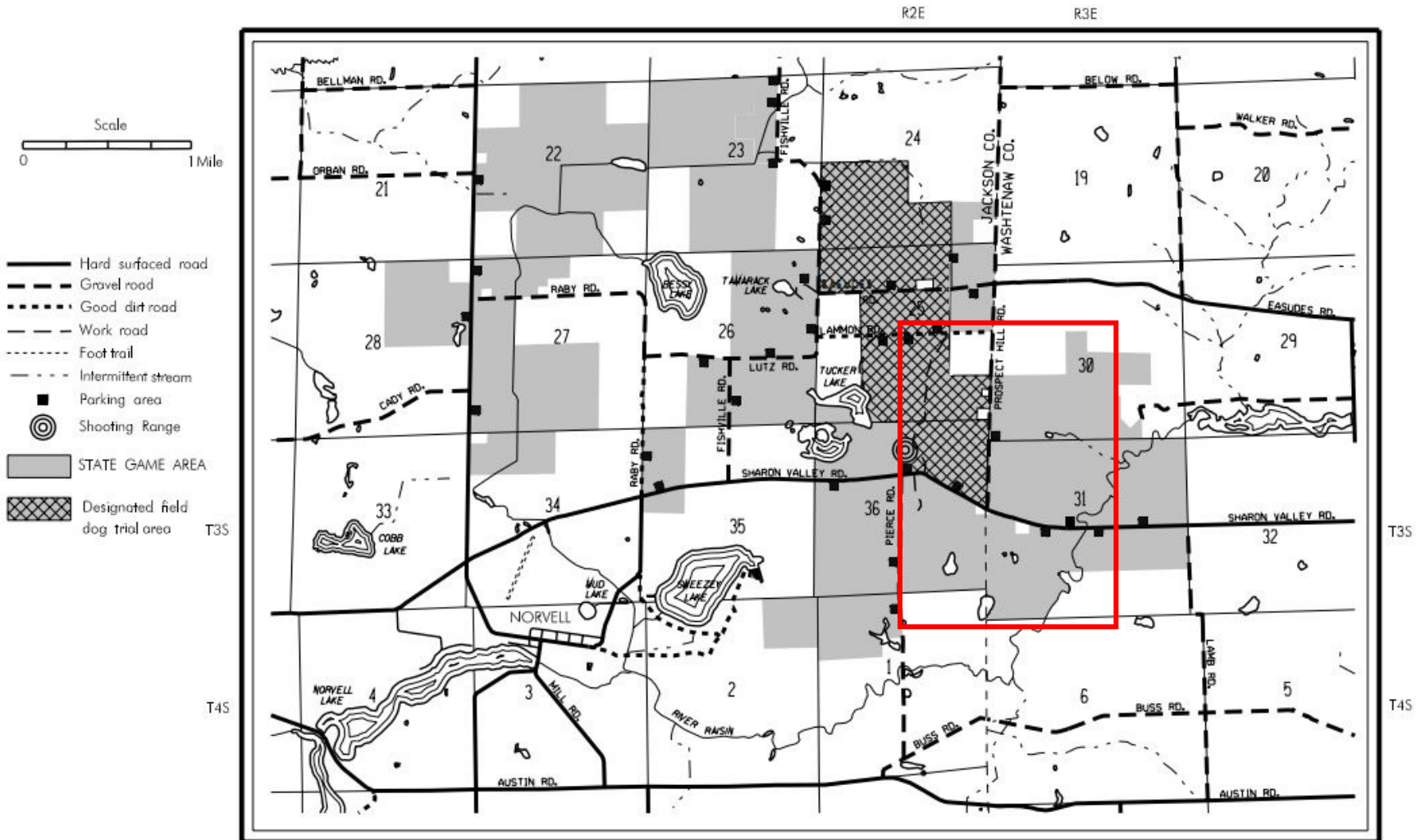


Figure 1. Study area is confined to the Washtenaw County portion of the Sharonville State Game Area. Map by the State of Michigan Department of Natural Resources (Map 1304, revised 09/2003).

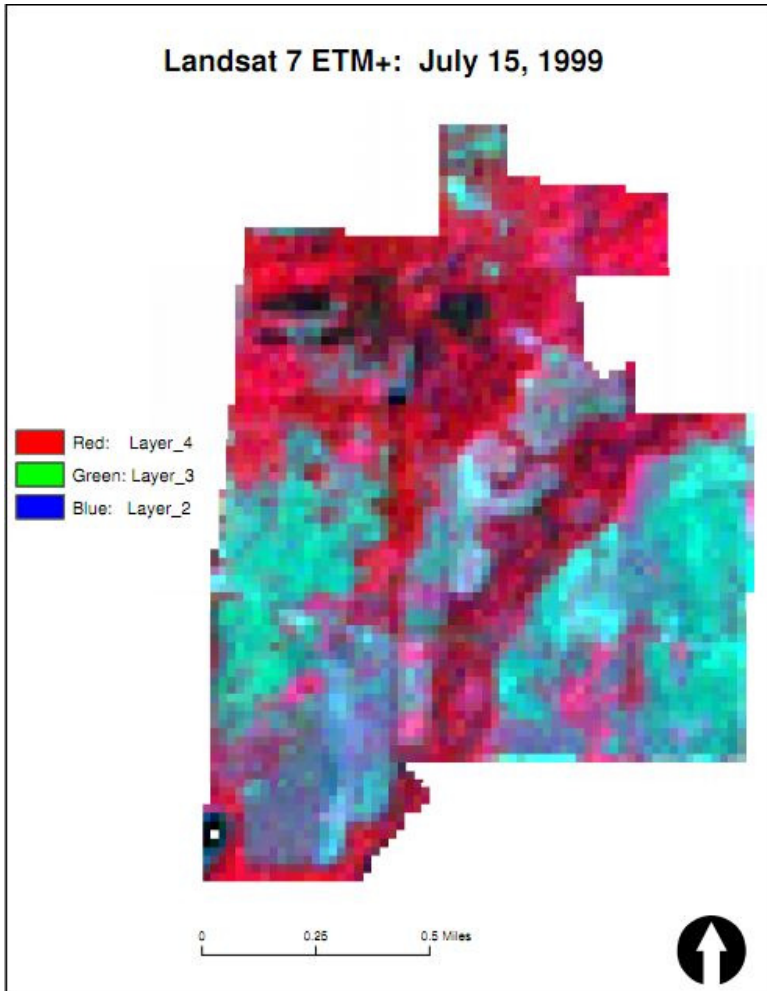


Figure 2. Landsat 7 ETM+ scene from July 15, 1999

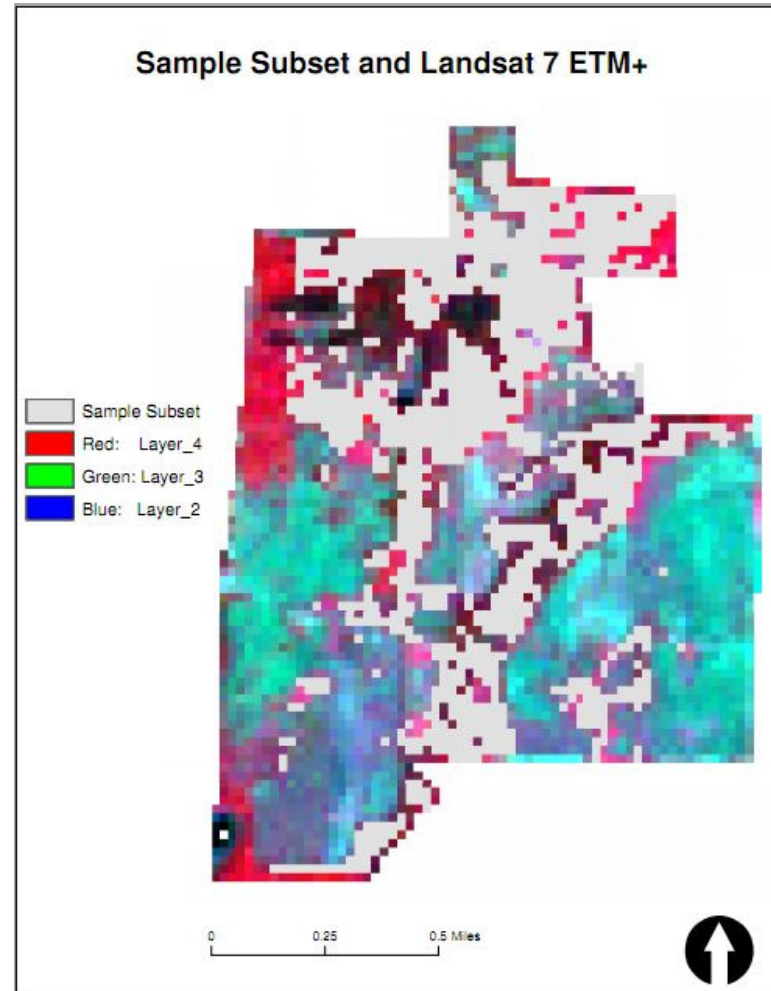


Figure 3. Landsat scene with sample subset overlay

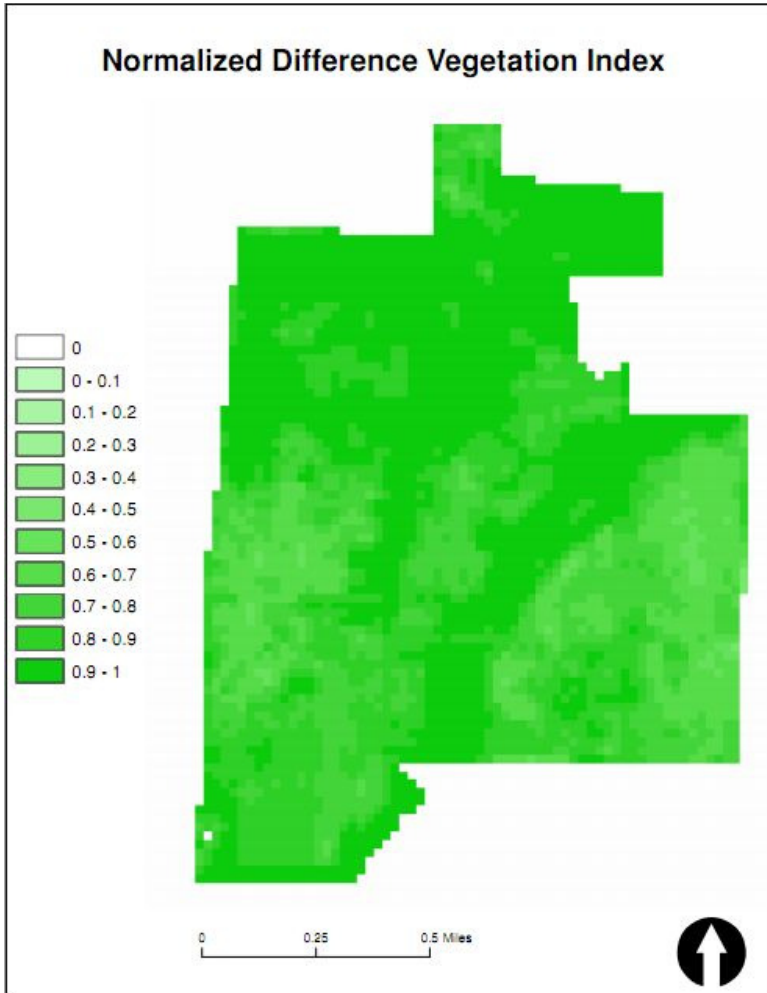


Figure 4. Normalized Difference Vegetation Index (NDVI)

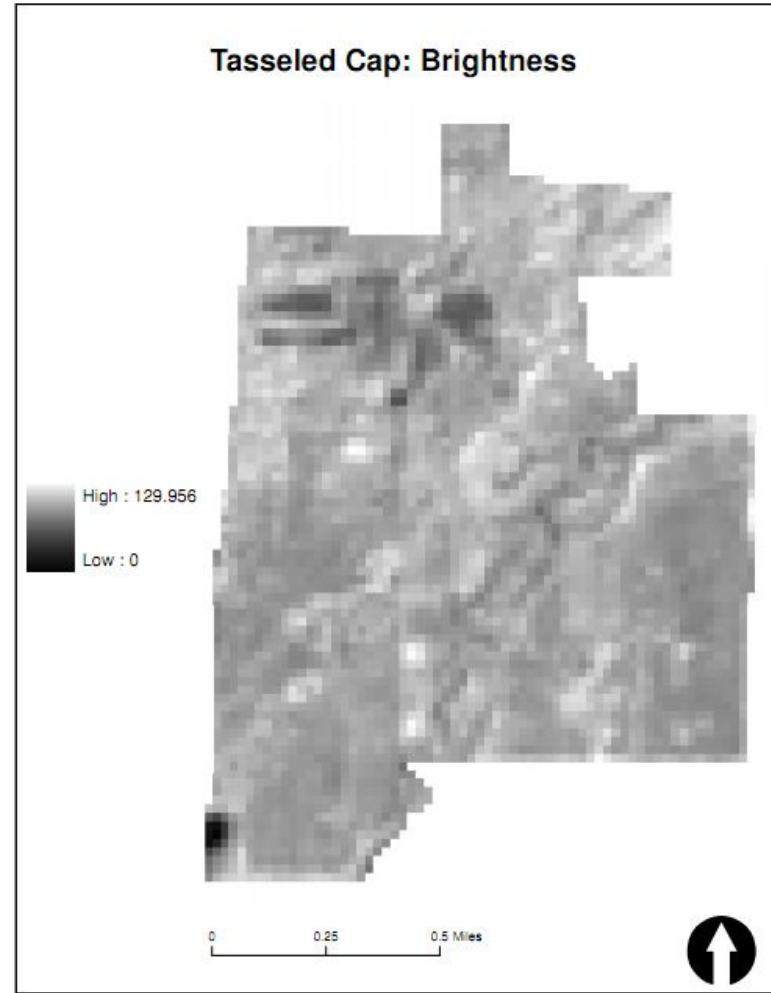


Figure 5. Tasseled Cap Layer 1: Brightness

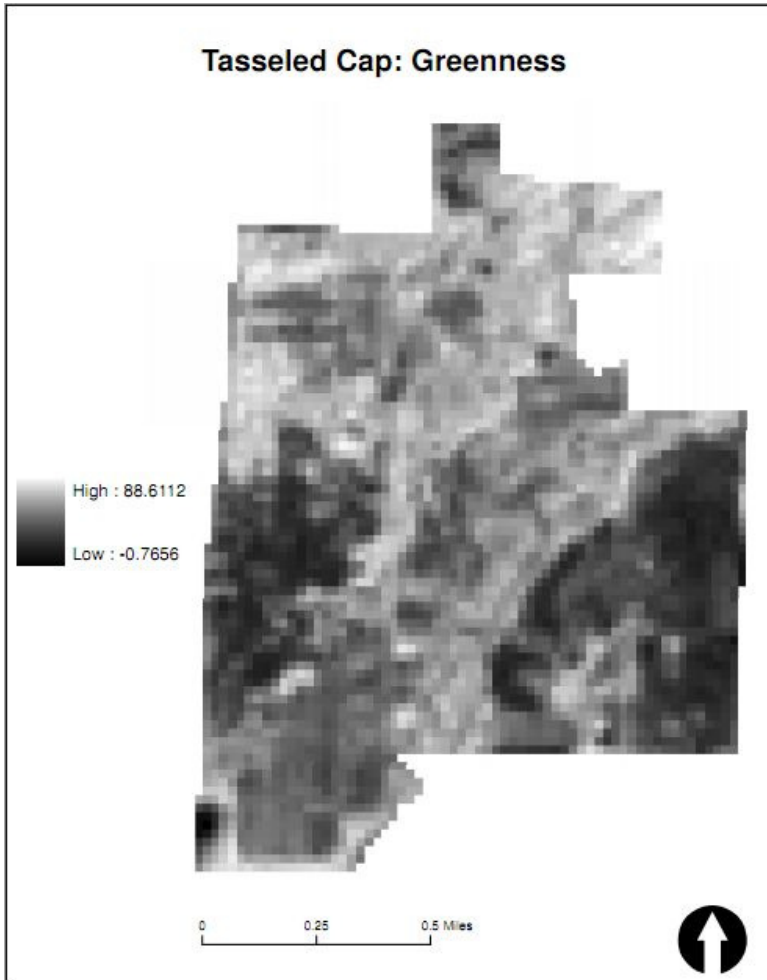


Figure 6. Tasseled Cap Layer 2: Greenness

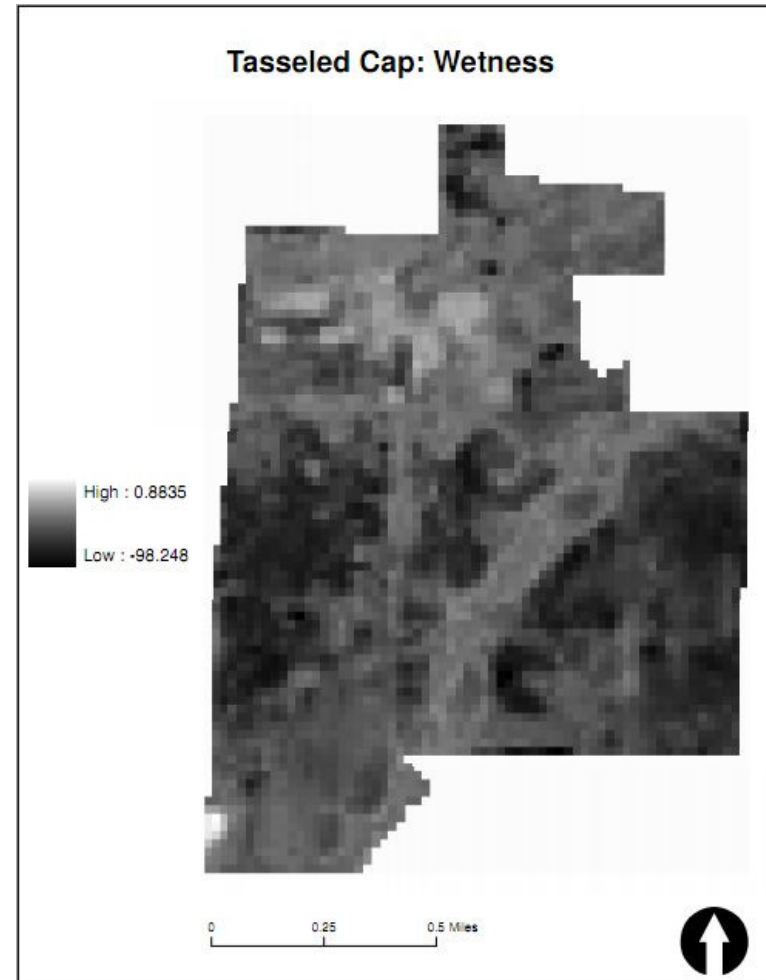


Figure 7. Tasseled Cap Layer 3: Wetness

Table 1. Tasseled cap feature coefficients used by ERDAS IMAGINE 2010 for Landsat 7 ETM+ bands in the tasseled cap transformation.

FEATURE	Band 1	Band 2	Band 3	Band 4	Band 5	Band 7
Brightness	0.3561	0.3972	0.3904	0.6966	0.2286	0.1596
Greenness	-0.3344	-0.3544	-0.4556	0.6966	-0.0242	-0.263
Wetness	0.2626	0.2141	0.0926	0.0656	-0.7629	-0.5388
Component 4	0.0805	-0.0498	0.195	-0.1327	0.5752	-0.7775
Component 5	-0.7252	-0.0202	0.6683	0.0631	-0.1494	-0.0274
Component 6	0.4	-0.8172	0.3832	0.0602	-0.1095	0.0985

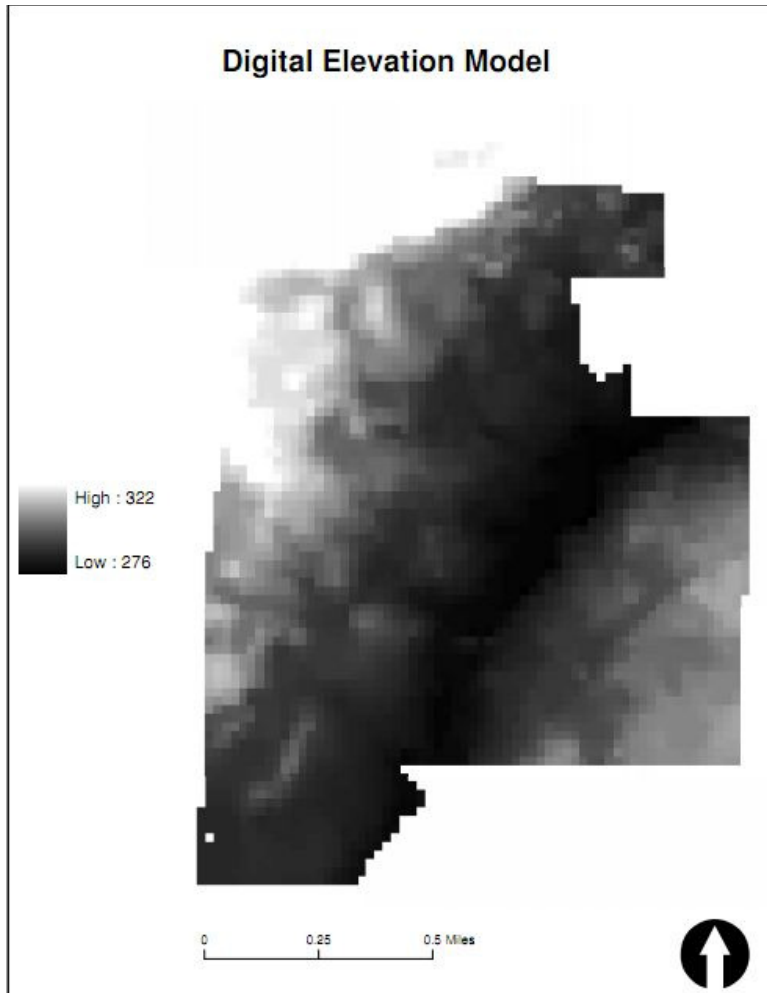


Figure 8. 30m digital elevation model with 1m elevation increment.

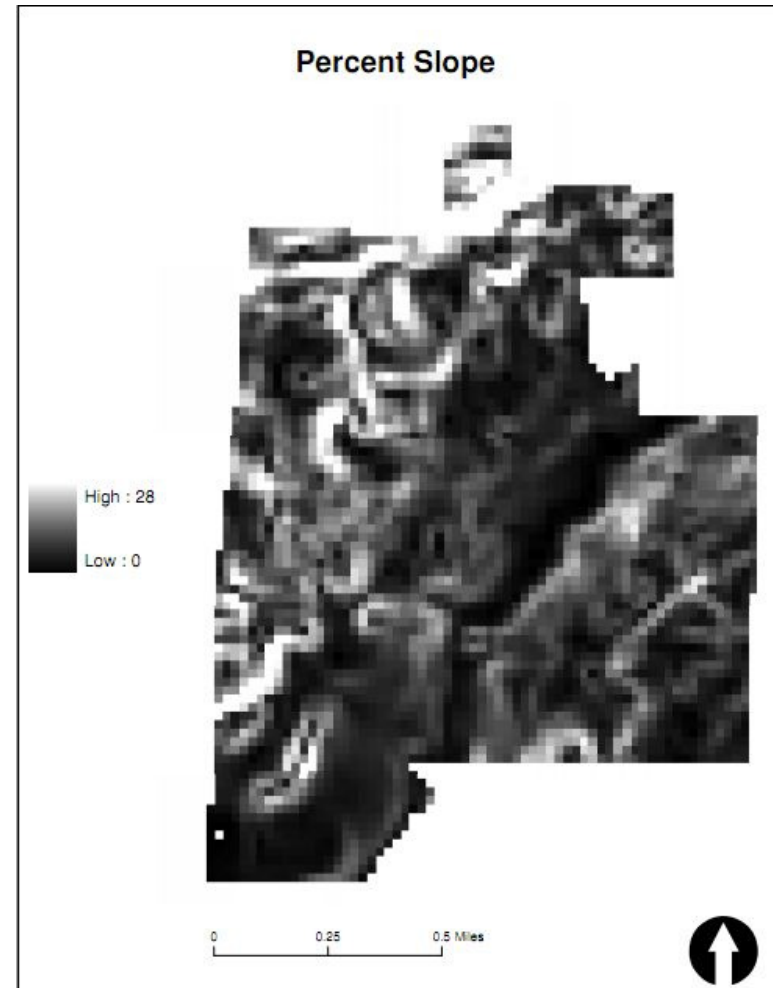


Figure 9. Slope terrain variable expressed in percent slope.

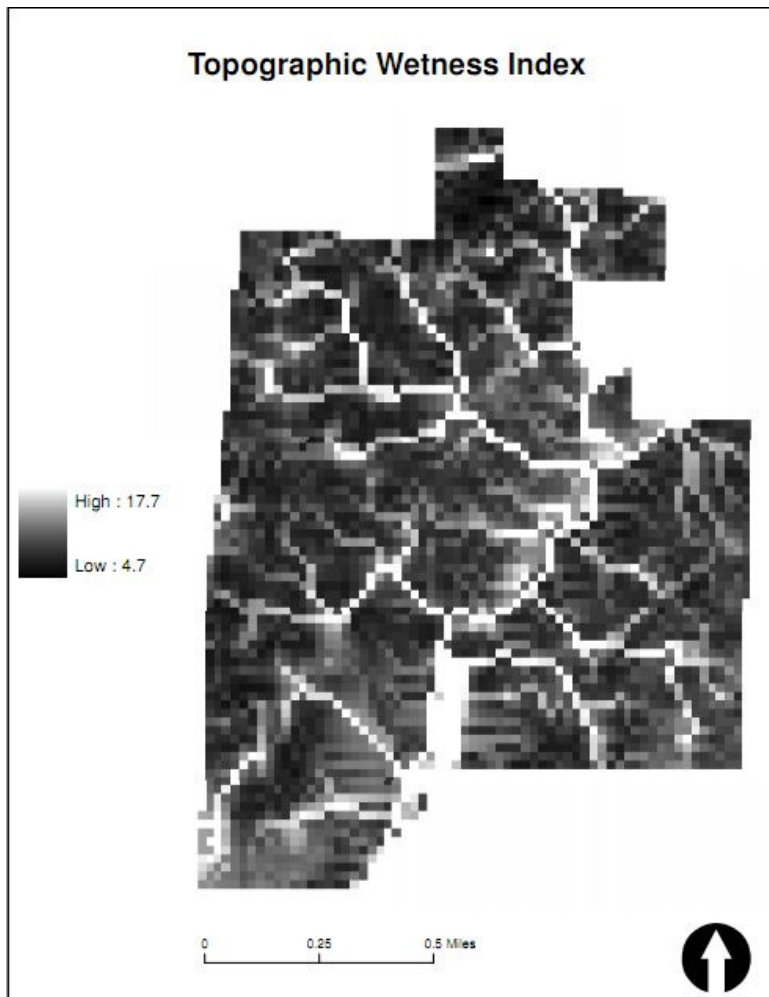


Figure 10. Topographic Wetness Index (TWI) produced from ArcGIS Model Builder.

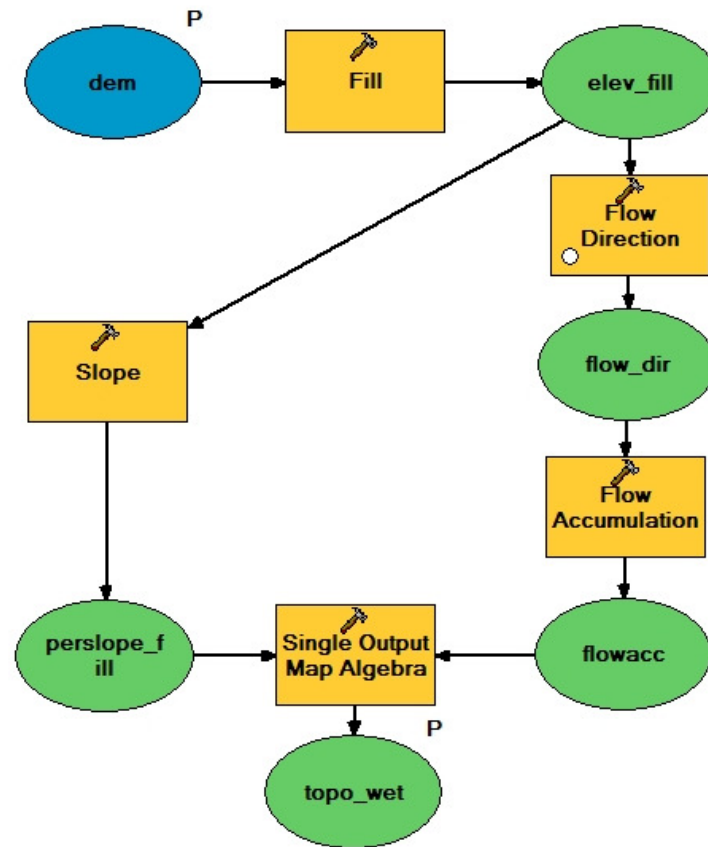


Figure 11. ArcGIS Model Builder model producing Topographic Wetness Index terrain variable. The map algebra equation is equivalent to $TWI = \ln \left(\frac{A_s}{S} \right)$.

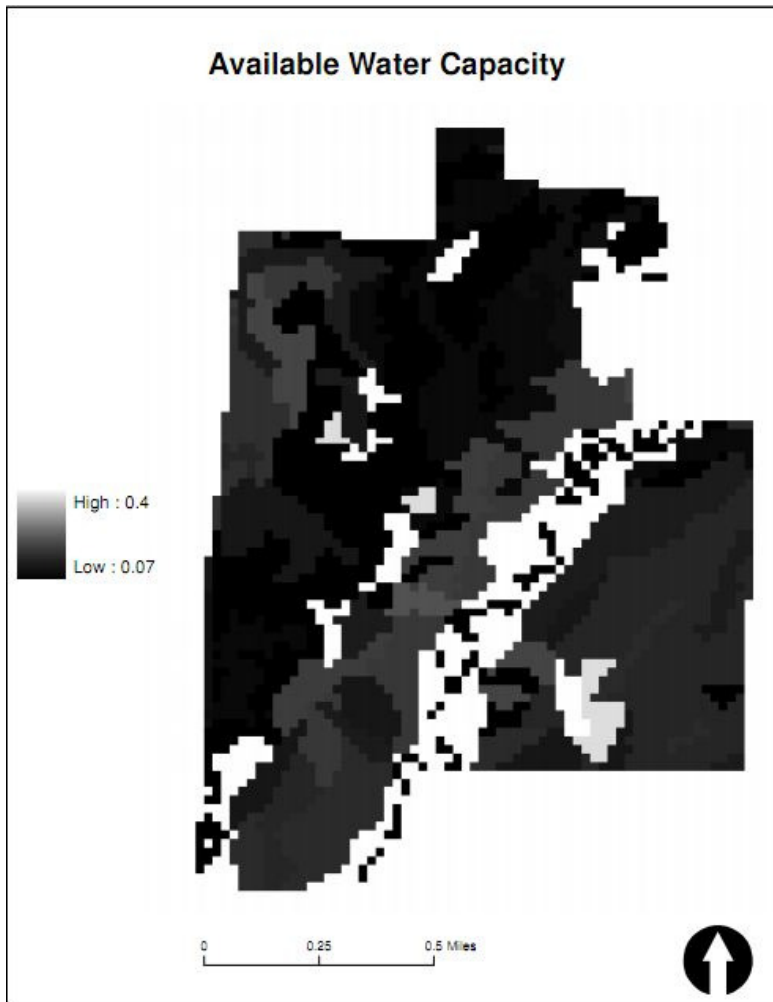


Figure 12. Available water capacity (cm water/ cm soil).

Table 2. Model predictions and associated abbreviations

Model	Prediction	Abbreviation
Multiple Linear Regression (MLR)*	MLR proportion	<i>MLR</i>
	MLR presence	<i>MLR>0%</i>
	MLR presence >10% canopy coverage	<i>MLR>10%</i>
	MLR presence >20% canopy coverage	<i>MLR>20%</i>
Logistic Regression (LR)*	LR presence	<i>LR>0%</i>
	LR presence >10% canopy coverage	<i>LR>10%</i>
	LR presence >20% canopy coverage	<i>LR>20%</i>
Multiple Linear Regression with IFMAP**	IFMAP MLR proportion	<i>IFMAP_MLR</i>
Logistic Regression with IFMAP**	IFMAP LR presence	<i>IFMAP_LR>0%</i>
	IFMAP LR presence >10% canopy coverage	<i>IFMAP_LR>10%</i>
	IFMAP LR presence >20% canopy coverage	<i>IFMAP_LR>20%</i>
IFMAP†	IFMAP presence	<i>IFMAP>0%, 10%, 20%</i>

* regression models using spectral and physical variables

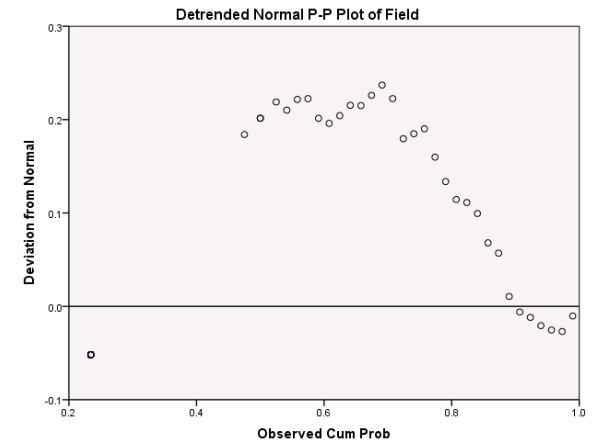
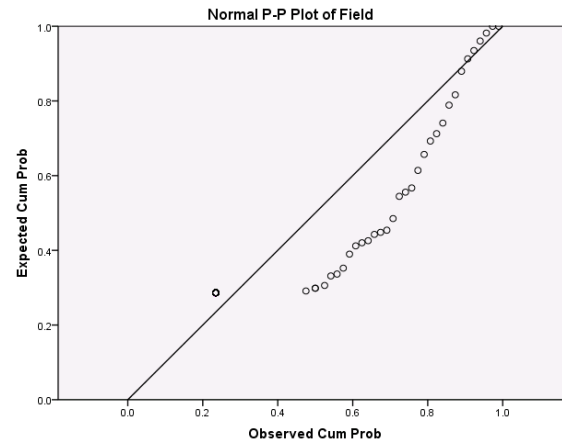
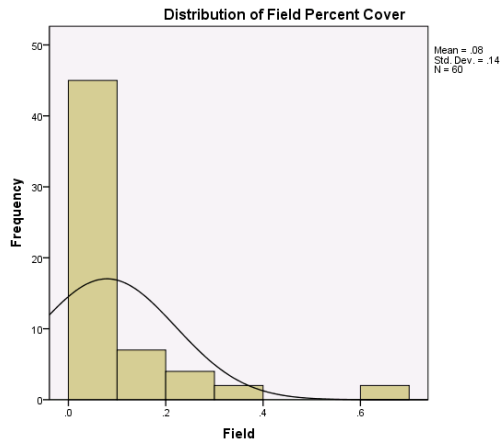
** regression models using IFMAP and physical variables

† lowland deciduous forest class

Table 3. Number of sample plots by community type.

Community Type	Number
Oak-hickory	27
Beech-maple	4
Floodplain	11
Deciduous swamp	12
Mixed forest	5
Open field with hedgerow	1

(a)



(b)

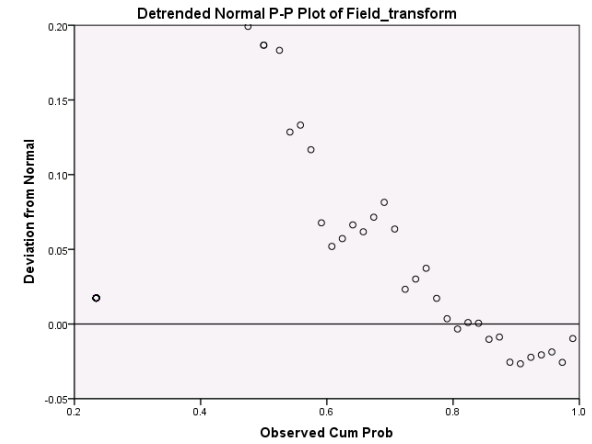
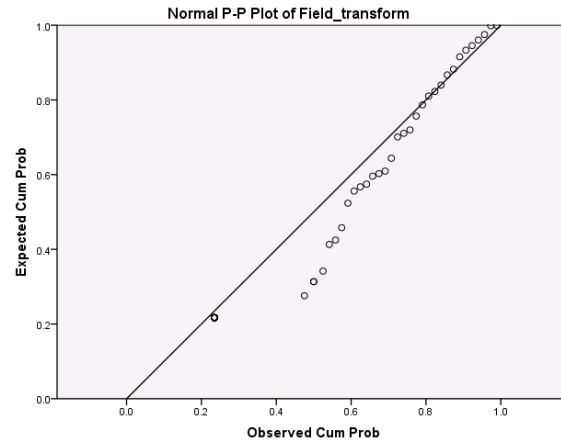
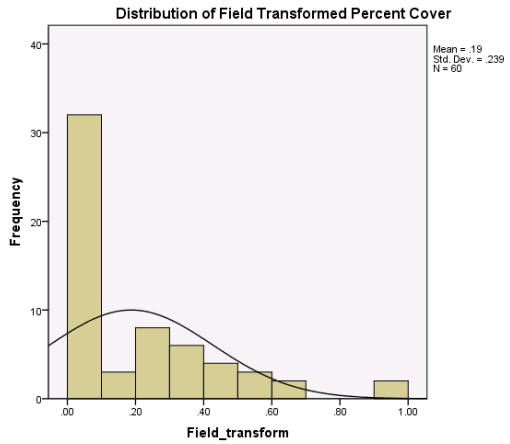


Figure 13. (a) Field data normality test output. (b) Arcsine transformed field data normality test output.

Table 4. Prediction models with regression coefficients and model fit statistics.

Multiple linear (MLR) and logistic regression (LR) models

Predictor variables and regression coefficients

Predicted variable	Intercept term	<i>b</i> variable 1	<i>b</i> variable 2	(Pseudo)R ² †	Model Significance‡
1. MLR	4.89588	-0.0174797 DEM**	0.0325878 TWI**	0.51	29.17
2. LR>0%	275.9972	-1.024682 DEM**	0.2327206 Greenness*	0.63	52.55
3. LR>10%	134.1341	-0.4729051 DEM**	-0.6212272 Slope*	0.49	33.38
4. LR>20%	172.3402	-0.619925 DEM**		0.44	20.60
5. IFMAP_MLR	4.89588	-0.0174797 DEM**	0.0325878 TWI**	0.51	29.17
6. IFMAP_LR>0%	209.1679	-0.7340369 DEM**		0.56	46.56
7. IFMAP_LR>10%	134.1341	-0.4729051 DEM**	-0.6212272 Slope*	0.49	33.38
8. IFMAP_LR>20%	172.3402	-0.619925 DEM**		0.44	20.60

* significant at the 0.05 probability level

** significant at the 0.01 probability level

† R² for MLR; Pseudo R² for LR; note: R² and Pseudo R² cannot be directly compared

‡ F-statistic for MLR; Chi² for LR; all models significant at the 0.01 probability level

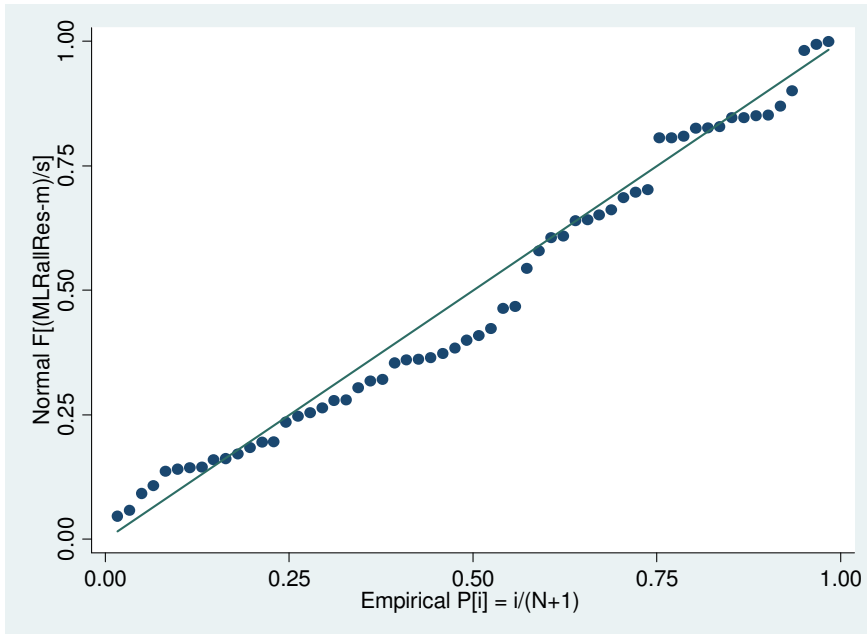


Figure 14. Standardized normal probability plot of the multiple linear regression residuals.

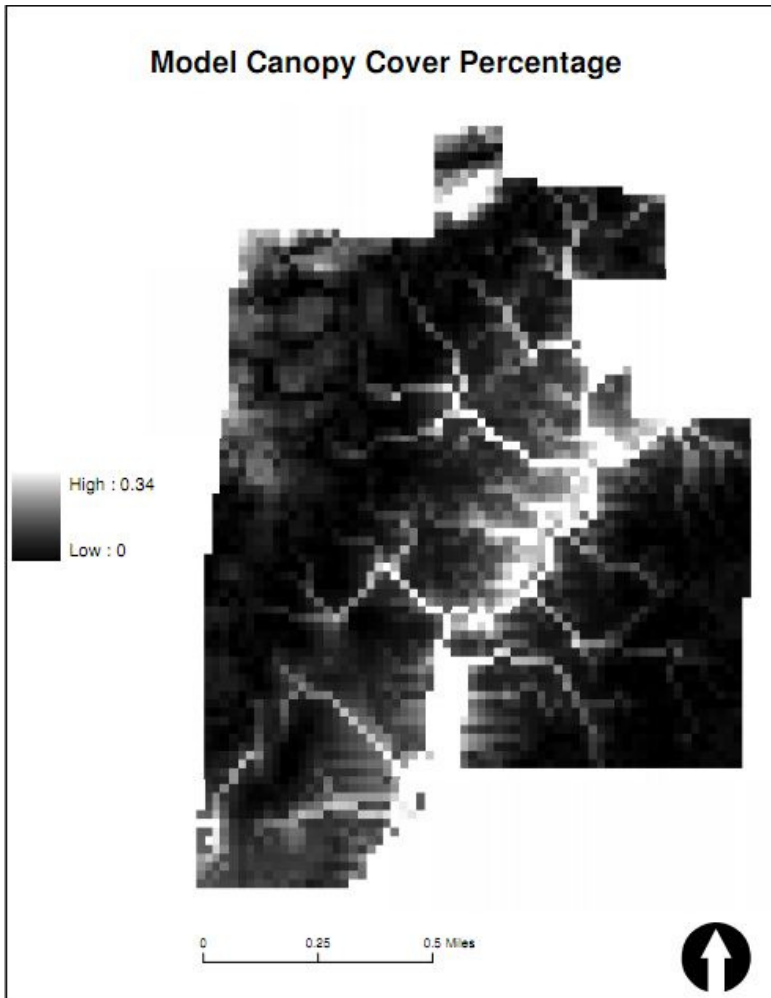


Table 5. Two-sample Kolmogorov-Smirnov test for equality of distribution functions between field data and model generated data (percent cover). Critical value = $\frac{1.92}{\sqrt{60}} = 0.2479$ (Birnbaum and Hall 1960)

Smaller Group	D	P-value	Exact P-value
Field	0.4667	>0.001	
Model	-0.1000	0.549	
Combined K-S	0.4667	>0.001	>0.001

Figure 15. Model map canopy coverage output from the multivariate regression.

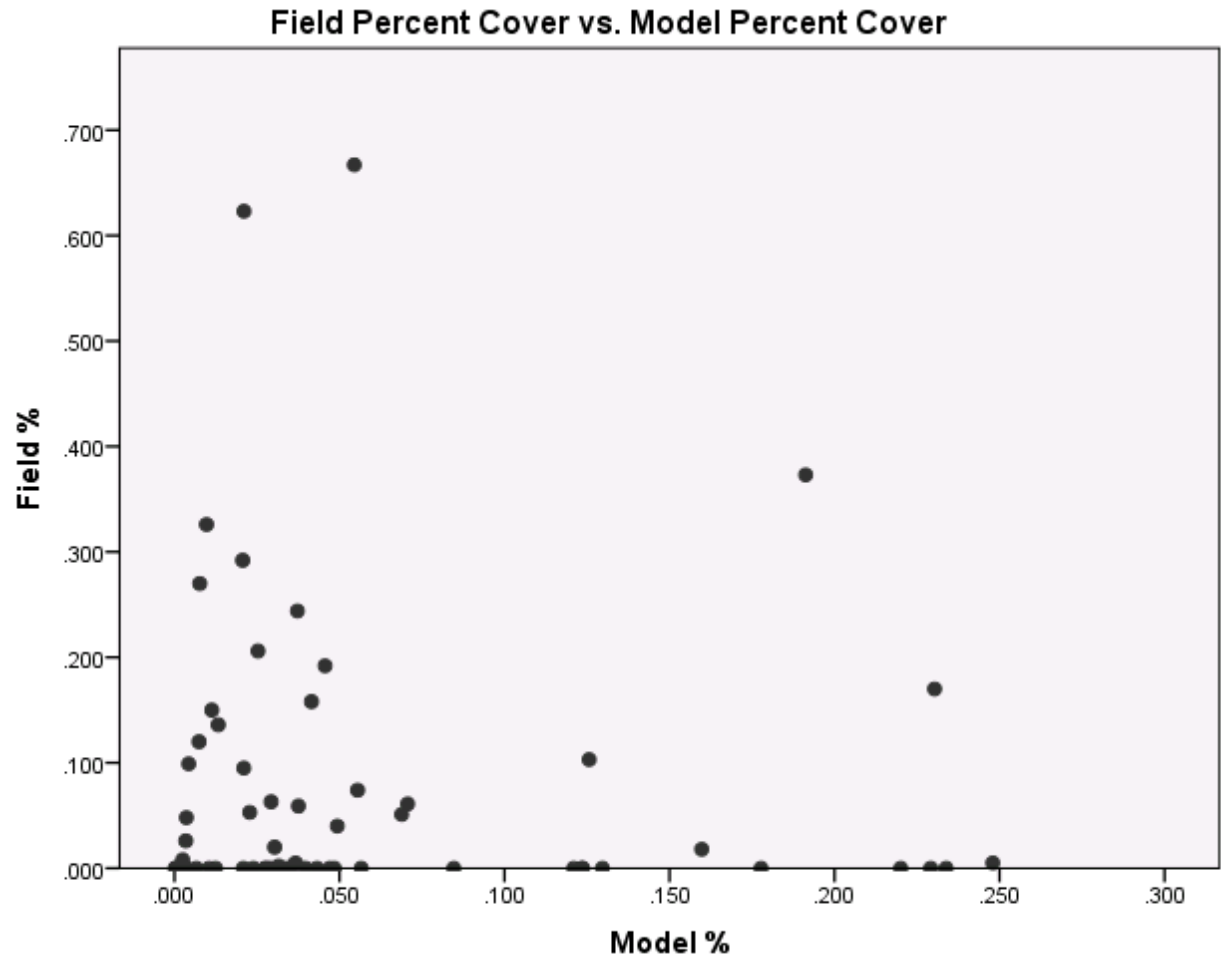


Figure 16. Scatter plot of field measured and multiple linear regression (MLR) model percent cover values.

Table 6. Summary table of each presence prediction’s overall accuracy, Kappa, user’s and producer’s accuracy, and the commission and omission error.

Presence Class	Prediction	Overall Accuracy	Kappa	User's Present	User's Absent	Producer's Present	Producer's Absent
>0%	MLR>0%	60.00%	11.30%	56.10%	100.00%	100.00%	10.70%
	LR>0%	90.00%	79.90%	90.60%	89.30%	90.60%	89.30%
	IFMAP>0%	63.30%	28.60%	77.80%	57.10%	43.80%	85.70%
>10%	MLR>10%	85.00%	57.10%	75.00%	87.50%	60.00%	93.30%
	LR>10%	83.30%	51.20%	72.70%	85.70%	53.00%	93.30%
	IFMAP>10%	75.00%	34.80%	50.00%	84.10%	53.30%	82.20%
>20%	MLR>20%	91.70%	57.10%	80.00%	92.70%	50.00%	98.10%
	LR>20%	91.70%	65.80%	66.70%	96.10%	75.00%	94.20%
	IFMAP>20%	70.00%	15.10%	22.20%	90.50%	50.00%	73.10%

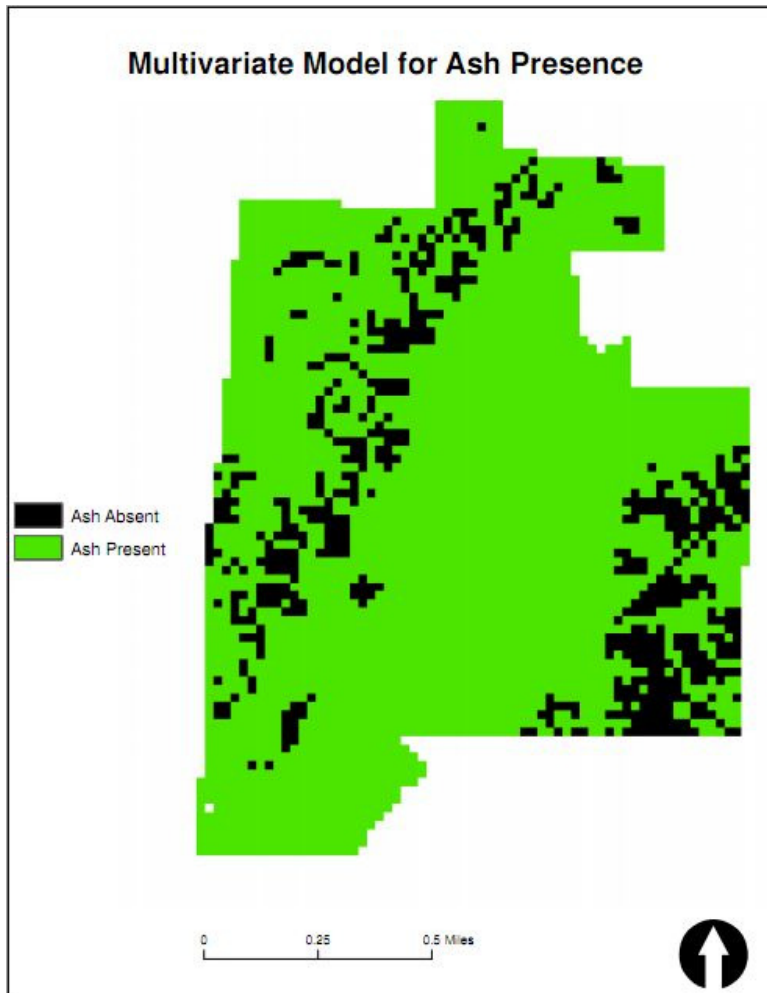


Figure 17. Presence model map output from the multivariate regression reclassified to probability of 0.002.

Table 7. Multivariate model for ash presence classification table reporting the user's and producer's accuracy, the commission and omission error, overall accuracy, and Kappa.

MLR>0%	Sample Plots				
	Ash Present	Ash Absent	Row Total	User's Accuracy	Commission Error
Ash Present	32	25	57	56.1%	43.9%
Ash Absent	0	3	3	100.0%	0.0%
Column Total	32	28	60		
Producer's Accuracy	100.0%	10.7%			
Omission Error	0%	89.3%			
Overall Accuracy	60%				
Kappa	11.3%				

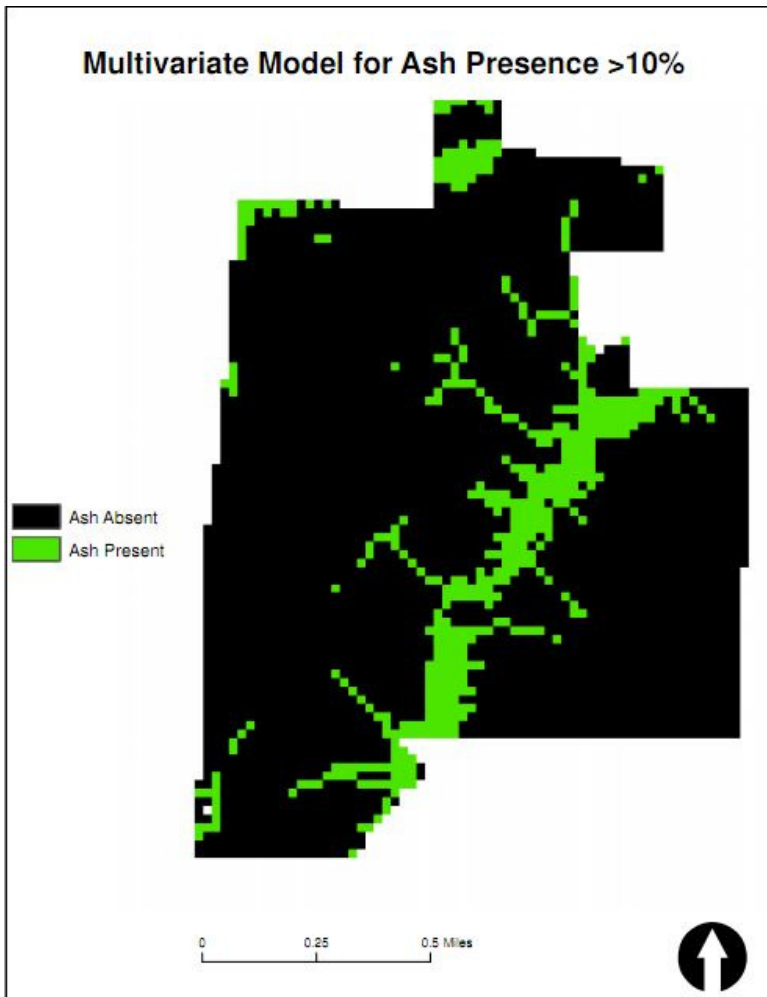


Figure 18. Presence >10% model map output from the multivariate regression reclassified to probability of 0.10.

Table 8. Multivariate model for ash presence greater than 10% cover classification table reporting the user's and producer's accuracy, the commission and omission error, overall accuracy, and Kappa.

MLR>10%	Sample Plots			User's Accuracy	Commission Error
	Ash Present	Ash Absent	Row Total		
Ash Present	9	3	12	75 %	25%
Ash Absent	6	42	48	87.5%	12.5%
Column Total	15	45	60		
Producer's Accuracy	60.0%	93.3%			
Omission Error	40%	6.7%			
Overall Accuracy	85%				
Kappa	57.1%				

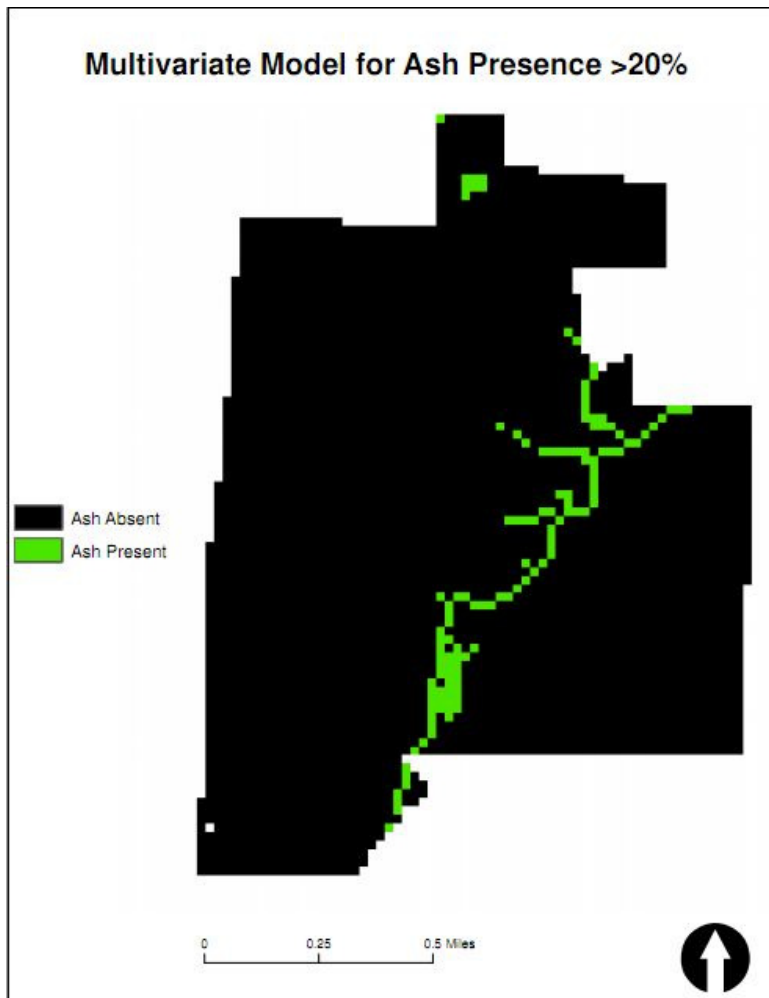


Table 9. Multivariate model for ash presence greater than 20% cover classification table reporting the user's and producer's accuracy, the commission and omission error, overall accuracy, and Kappa.

MLR>20%	Sample Plots				
Model Map	Ash Present	Ash Absent	Row Total	User's Accuracy	Commission Error
Ash Present	4	1	5	80%	20%
Ash Absent	4	51	55	92.7%	7.3%
Column Total	8	52	60		
Producer's Accuracy	50%	98.1%			
Omission Error	50%	1.9%			
Overall Accuracy	91.7%				
Kappa	57.1%				

Figure 19. Presence >20% model map output from the multivariate regression reclassified to probability of 0.20.

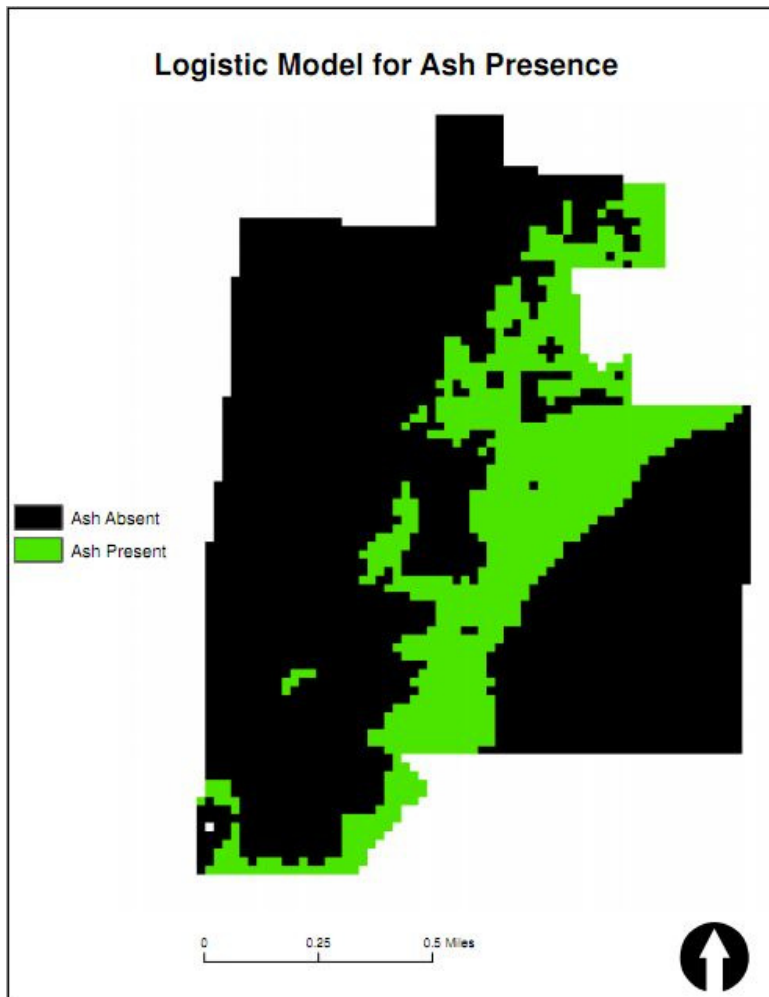


Figure 20. Presence at all percentages model map output from the logistic regression.

Table 10. Logistic model for ash presence at all percent cover classification table reporting the user's and producer's accuracy, the commission and omission error, overall accuracy, and Kappa.

LR>0%	Sample Plots				
Model Map	Ash Present	Ash Absent	Row Total	User's Accuracy	Commission Error
Ash Present	29	3	32	90.6%	9.4%
Ash Absent	3	25	28	89.3%	10.7%
Column Total	32	28	60		
Producer's Accuracy	90.6%	89.3%			
Omission Error	9.4%	10.7%			
Overall Accuracy	90%				
Kappa	79.9%				

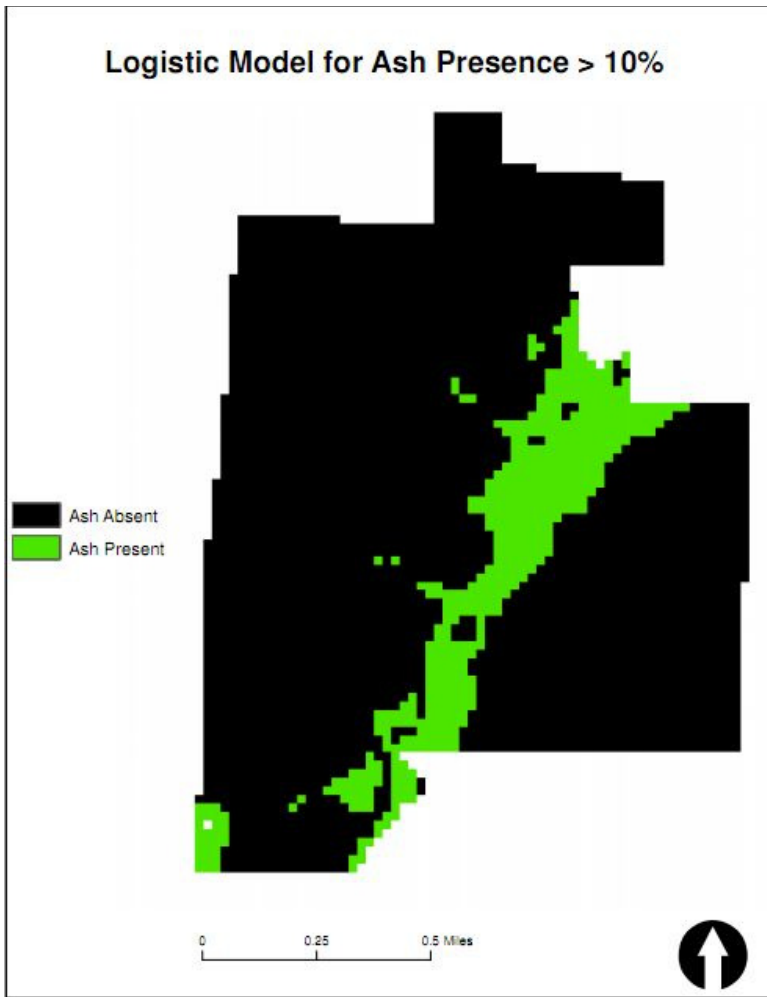


Figure 21. Presence >10% model map output from the logistic regression.

Table 11. Logistic model for ash presence >10% cover classification table reporting the user's and producer's accuracy, the commission and omission error, overall accuracy, and Kappa.

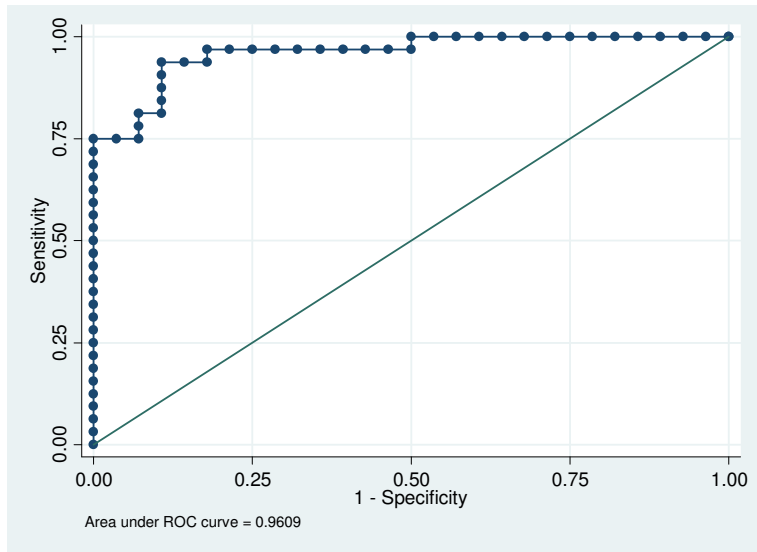
LR>10%	Sample Plots				
	Ash Present	Ash Absent	Row Total	User's Accuracy	Commission Error
Ash Present	8	3	11	72.7%	27.3%
Ash Absent	7	42	49	85.7%	14.3%
Column Total	15	45	60		
Producer's Accuracy	53%	93.3%			
Omission Error	47%	6.7%			
Overall Accuracy	83.3%				
Kappa	51.2%				



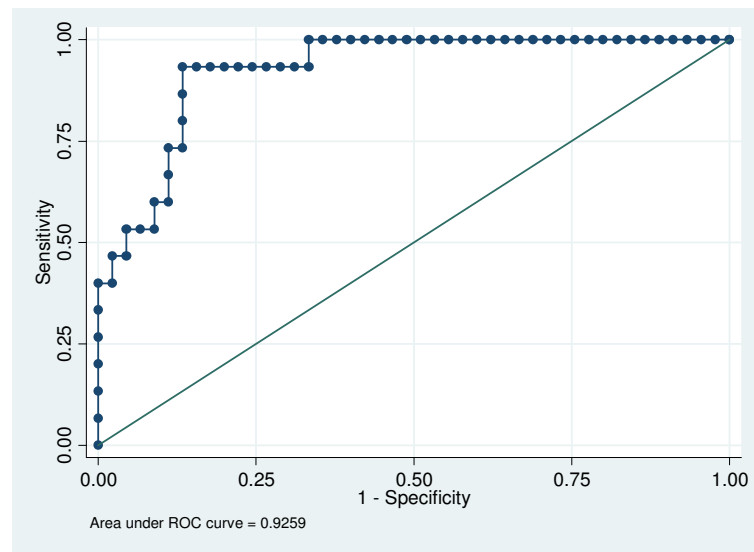
Figure 22. Presence >20% model map output from the logistic regression.

Table 12. Logistic model for ash presence >20% cover classification table reporting the user's and producer's accuracy, the commission and omission error, overall accuracy, and Kappa.

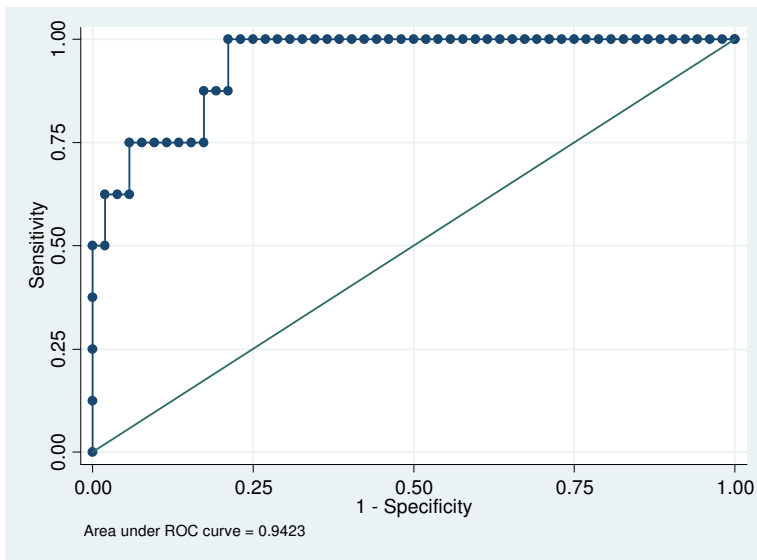
LR>20%	Sample Plots				
Model Map	Ash Present	Ash Absent	Row Total	User's Accuracy	Commission Error
Ash Present	6	3	9	66.7%	33.3%
Ash Absent	2	49	51	96.1%	3.9%
Column Total	8	52	60		
Producer's Accuracy	75%	94.2%			
Omission Error	25%	5.8%			
Overall Accuracy	91.7%				
Kappa	65.8%				



a)



b)



c)

Figure 23. ROC curves for logistic regression models for a) ash presence, b) ash presence > 10%, and c) ash presence > 20%.



Figure 24. IFMAP Lowland Deciduous Forest Class

Table 13. IFMAP lowland deciduous forest classification and ash presence table reporting the user's and producer's accuracy, the commission and omission error, overall accuracy, and Kappa.

IFMAP>0%	Sample Plots				
	Ash Present	Ash Absent	Row Total	User's Accuracy	Commission Error
Ash Present	14	4	18	77.8%	22.2%
Ash Absent	18	24	42	57.1%	42.9%
Column Total	32	28	60		
Producer's Accuracy	43.8%	85.7%			
Omission Error	56.2%	14.3%			
Overall Accuracy	63.3%				
Kappa	28.6%				

Table 14. IFMAP lowland deciduous forest classification and ash presence >10% table reporting the user's and producer's accuracy, the commission and omission error, overall accuracy, and Kappa.

IFMAP>10%	Sample Plots				
Model Map	Ash Present	Ash Absent	Row Total	User's Accuracy	Commission Error
Ash Present	8	8	16	50%	50%
Ash Absent	7	37	44	84.1%	15.9%
Column Total	15	45	60		
Producer's Accuracy	53.3%	82.2%			
Omission Error	46.7%	17.8%			
Overall Accuracy	75%				
Kappa	34.8%				

Table 15. IFMAP lowland deciduous forest classification and ash presence >20% table reporting the user's and producer's accuracy, the commission and omission error, overall accuracy, and Kappa.

IFMAP>20%	Sample Plots				
Model Map	Ash Present	Ash Absent	Row Total	User's Accuracy	Commission Error
Ash Present	4	14	18	22.20%	77.80%
Ash Absent	4	38	42	90.50%	9.50%
Column Total	8	52	60		
Producer's Accuracy	50.00%	73.10%			
Omission Error	50.00%	26.90%			
Overall Accuracy	70.00%				
Kappa	15.10%				

LITERATURE CITED

Ahrens WH, Cox DJ, Budhwar G. 1990. Use of the Arcsine and Square Root Transformations for Subjectively Determined Percentage Data. *Weed Science* 38(4/5): 452-458.

Albert DA. 1995. Regional landscape ecosystems of Michigan, Minnesota, and Wisconsin: a working map and classification. Gen. Tech. Rep. NC-178. St. Paul, MN: U.S. Department of Agriculture, Forest Service, North Central Forest Experiment Station. Jamestown, ND: Northern Prairie Wildlife Research Center Online. <http://www.npwrc.usgs.gov/resource/habitat/rlandscp/index.htm> (Version 03JUN1998).

Anderson SC, Kupfer JA, Wilson RR, Cooper RJ. 2000. Estimating forest crown area removed by selection cutting: a linked regression-GIS approach based on stump diameters. *Forest Ecology and Management* 137: 171-177.

Baker ME, Wiley MJ. 2004. Characterization of Woody Species Distribution in Riparian Forests of Lower Michigan, USA Using Map-Based models. *Wetlands* 24(3): 550-561.

Baker ME, Wiley MJ. 2009. Multiscale control of flooding and riparian-forest composition in Lower Michigan, USA. *Ecology* 90(1): 145-159.

Barnes BV, Wagner WH. 2002. Michigan Trees: A Guide to the Trees of Michigan and the Great Lakes Region. Ann Arbor (MI). The University of Michigan Press 383 p. Upper Saddle River (NJ). Prentice-Hall Inc. p. 278-280.

Battaglia LL, Sharitz RR. 2006. Responses of floodplain forest species to spatially condensed gradients: a test of the flood-shade tolerance tradeoff hypothesis. *Oecologia* 147: 108-118.

Bergen K, Wang J. 2010. LAB 7: Radiometric and Atmospheric Correction. NRE 541 Remote Sensing of Environment (Winter 2010). University of Michigan, Ann Arbor.

Beyer HL. 2006. Hawth's Analysis Tools for ArcGIS v 3.27. Available at <http://www.spatial ecology.com/htools>.

Birnbaum ZW, Hall RA. 1960. Small Sample Distributions for Multi-Sample Statistics of the Smirnov Type. *Annals of Mathematical Statistics* 31(3): 710-720.

Borkowski J. Undated. Nonparametric Statistics (STAT 431), Course Notes: Goodness-of-Fit Tests (pages 29-34) (Part 2). University of Montana; [cited 2012 March 11]. Available from <http://www.math.montana.edu/~jobo/st431/> and

<http://www.math.montana.edu/~jobo/st431/ho2.pdf>

Brown D. 2009. Personal communication (in person). Professor, University of Michigan School of Natural Resources and Environment, Ann Arbor, MI 48109.

Brown D. 2010. Lab 1: ArcGIS Refresher and Terrain Analysis. NRE 534 GIS and Landscape Modeling (Fall 2010). University of Michigan, Ann Arbor.

Brady NC, Weil RR. 2002. The Nature and Properties of Soils, Thirteenth Edition. Pearson Education, Inc. Upper Saddle River: New Jersey. P 213

Busch DE, Ingraham NL, Smith SD. 1992. Water Uptake in Woody Riparian Phreatophytes of the Southwestern United States: A Stable Isotope Study. *Ecological Applications* 2(4): 450-459.

Chavez PS. 1996. Image-Based Atmospheric Corrections—Revisited and Improved. *Photogrammetric Engineering and Remote Sensing* 62(9): 1025-1036.

Congalton RG, Green K. 1999. Assessing the Accuracy of Remotely Sensed Data: Principles and Practices. New York (NY). CRC Press, Inc. p. 17-22.

Crist EP, Cicone RC. 1984a. A Physically-Based Transformation of Thematic Mapper Data-The TM Tasseled Cap. *IEEE TRANSACTIONS ON GEOSCIENCE AND REMOTE SENSING* GE-22(3): 256-263

Crist EP, Cicone RC. 1984b. Application of the Tasseled Cap to Simulated Thematic Mapper Data. *Photogrammetric Engineering and Remote Sensing* 50(3): 343-352.

Crist, EP, Kauth RJ. 1986. The Tasseled Cap De-Mystified. *Photogrammetric Engineering and Remote Sensing* 52(1): 81-86

(EAB) Emerald Ash Borer. 2012 Administered by Michigan State University. Available online at www.emeraldashborer.info. Accessed 14 July 2012.

ESRI. 2009. ArcGIS 9.3.1, License type: ArcEditor.

Gallant JC, Wilson JP. 2000. Chapter 3: Primary Topographic Attributes. In: Wilson JP, Gallant JC editors. *Terrain Analysis: Principles and Applications*. New York (NY). John Wiley & Sons, Inc. p. 51-85.

Gotelli NJ, Ellison AM. 2004. A Primer of Ecological Statistics. Sunderland (MA). Sinauer Associates, Inc. p. 231-232, 400, 406-415.

Guisan A, Zimmerman NE. 2000. Predictive habitat distribution models in ecology. *Ecological Modeling* 135: 147-186.

Hale BW, Alsum EM, Adams MS. 2008. Changes in the Floodplain Forest Vegetation of the Lower Wisconsin River over the Last Fifty Years. *American Midland Naturalist* 160: 454-476.

Hallet R. 2009. Personal communication (phone). September 18, 2009. USDA Forest Service Northern Research Station, Durham, NH 03824.

Haukos DA, Sun HZ, Westeff DB, Smith LM. 1998. Sample size, power, and analytical considerations for vertical structure data from profile boards in wetland vegetation. *Wetlands* 18(2): 203-215.

Haug C, Wylie B, Yang L, Homer C, Zylstra G. 2002. Derivation of a tasseled cap transformation based on Landsat 7 at-satellite reflectance. *International Journal of Remote Sensing* 23(8): 1741-1748. doi: 10.1080/01431160110106113

Iverson LR, Prasad AM, Sydnor D, Bossenbroek J, Schwartz MW. 2006. Modeling potential emerald ash borer spread through GIS/cell-based/gravity models with data bolstered by web-based inputs [abstract]. In: Emerald Ash Borer Research and Technology Development Meeting; 2005 Sep 26-27; Pittsburgh. Morgantown, (WV): Forest Health Technology Enterprise Team. FHTET-2005-16.

Kauth RJ, Thomas GS. 1976. The Tasseled Cap -- A Graphic Description of the Spectral-Temporal Development of Agricultural Crops as Seen by LANDSAT. LARS Symposia. Paper 159. http://docs.lib.purdue.edu/lars_symp/159

King SL, Antrobus TJ. 2005. Relationships between gap makers and gap fillers in an Arkansas floodplain forest. *Journal of Vegetation Science* 16: 471-480.

Kupfer JA, Malanson GP. 1993. Observed and modeled direction change in riparian forest composition at a cutbank edge. *Landscape Ecology* 8(3): 185-199.

(Leica) Leica Geosystems Geospatial Imaging, LLC. 2008. ERDAS Field Guide: Volume 2. Norcross (GA): Leica Geosystems Geospatial Imaging, LLC, p. 105-153.

(Leica) Leica Geosystems Geospatial Imaging, LLC. 2009. ERDAS IMAGINE 2010. Norcross (GA).

Lillesand TM, Kiefer RW, Chipman JW. 2008. Remote Sensing and Image Interpretation, sixth edition. Biostatistical Analysis, fourth edition. Hoboken (NJ). John Wiley & Sons, Inc. p. 535.

Mann LE, Harcombe PA, Elsik IS, Hall RBW. 2008. The trade-off between flood- and shade-tolerance: A mortality episode in *Carpinus caroliniana* in a floodplain forest, Texas. *Journal of Vegetation Science* 19: 739-746.

McCullough DG, Siegert NW. 2007. Estimating Potential Emerald Ash Borer (Coleoptera: Buprestidae) Populations Using Ash Inventory Data. *Journal of Economic Entomology* 100(5): 1577-1586).

McCullough DG, Schneeberger NF, Katovich SA. 2008. Pest Alert: Emerald Ash Borer. NA-PR-02-04. U.S. Department of Agriculture, Forest Service, Northeastern Area State and Private Forestry. Newton Square, PA. http://www.na.fs.fed.us/spfo/pubs/pest_al/eab/eab.pdf. Accessed 5 August 2010.

McCullough DG, Poland TM, Cappaert D. 2009. Attraction of the emerald ash borer to ash trees stressed by girdling, herbicide treatment, or wounding. *Canadian Journal of Forest Research* 39: 1331-1345.

(MDNR) Michigan Department of Natural Resources, Forest, Mineral and Fire Management Division. 2003. IFMAP/GAP Lower Peninsula Land Cover. Available at <http://www.mcgi.state.mi.us/mgdl/?rel=thext&action=thmname&cid=5&cat=Land+Cover+2001> Accessed 12 March 2012.

(NRCS) Natural Resources Conservation Service, United States Department of Agriculture. Undated. SSURGO Metadata 2.1.1, p. 8 http://www.dnr.state.oh.us/Portals/12/soils/pdf/surrgo_metadata/Table%20Column%20Descriptions.pdf. Accessed 11 March 2012.

Petrice TB, Haack RA. 2007. Can emerald ash borer, *Agrilus plannipennis* (Coleoptera: Buprestidae), emerge from cut logs two summers after infested trees are cut? *The Great Lakes Entomologist* 40(1-2): 92-95.

Poland TM, McCullough DG. 2006. Emerald Ash Borer: Invasion of the Urban Forest and the Threat to North America's Ash Resource. *Journal of Forestry* (April/May): 118-124.

Pontius J, Martin M, Plourde L, Hallett R. 2008. Ash decline assessment in emerald ash borer-infested regions: A test of tree-level, hyperspectral technologies. *Remote Sensing of Environment* 112: 2665-2676.

(RRWC) River Raisin Watershed Council, Lenawee Conservation District, University of Michigan School of Natural Resources and Environment, Stantec, JFNew. 2009. River Raisin Watershed Management Plan. http://www.michigan.gov/deq/0,1607,7-135-3313_3682_3714_31581-228325--,00.html. Accessed 10 July 2012.

(RS&GIS) Remote Sensing and GIS Research and Outreach Services, Michigan State University. 2005. Michigan Georef NAIP Digital Ortho Photo Image: Manchester SW.ecw. East Lansing, MI. <http://www.rsgis.msu.edu/> Accessed 20 November 2009.

Schilling KE, Jacobson P. 2009. Water uptake and nutrient concentrations under a floodplain oak savannah during a non-flood period, lower Cedar River, Iowa. *Hydrological Processes* 23: 3006-3016.

Smitely D, Davis T, Rebek E. 2008. Progression of Ash Canopy Thinning and Dieback Outward from the Initial Infestation of Emerald Ash Borer (Coleoptera: Buprestidae) in Southeastern Michigan. *Journal of Economic Entomology* 101(5): 1643-1650.

Sorenson R, Zinko U, Seibert J. 2006. On the calculation of the topographic wetness index: evaluation of different methods based on field observations. *Hydrology and Earth System Sciences* 10: 101-112.

Sorenson R, Seibert J. 2007. Effects of DEM resolution on the calculation of topographic indices: TWI and its components. *Journal of Hydrology* 347: 79-89.

(SPSS) SPSS, Inc. 2010. IBM SPSS Statistics, Version 19.0.0.

(StataCorp) StataCorp LP. 2011. STATA Statistics/ Data Analysis, Version 12.0 Special Edition.

(USGS) U.S. Geological Survey. 2009. National Elevation Dataset scene Latitude N43, Longitude W85. Available at <http://seamless.usgs.gov>. Accessed 3 November 2010.

(USGS) U.S. Geological Survey. 2010. Landsat 7 ETM+ scene L71020031_03119990715. Product type: L1T, Acquisition Date: 1999-07-15, Path 20, Row 31. Available at <http://edcns17.cr.usgs.gov/EarthExplorer/> Accessed 4 October 2010.

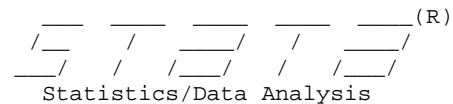
(USGS) U.S. Geological Survey. 2012. National Water Information System: Web Interface. Peak Streamflow for Michigan: USGS 04175600 Raisin River near Manchester, MI. Available at nwis.waterdata.usgs.gov/mi/nwis/peak?site_no=04175600&agency_cd=USGS&format=html. Accessed 8 August 2012.

Wright JW. 1959. Silvical Characteristics of Green Ash (*Fraxinus pennsylvanica*). U.S. Forest Service. 18 p.

Zar JH. 1999. Biostatistical Analysis, fourth edition. Upper Saddle River (NJ). Prentice-Hall Inc. p. 278-280.

Appendix A. Master list of response variable regression tables

Saturday August 11 13:37:13 2012 Page 1



```

_____ (R)
/___ / ___/ / ___/
___/ / ___/ / ___/ 12.1 Copyright 1985-2011 StataCo
> rp LP
Statistics/Data Analysis StataCorp
4905 Lakeway Drive
Special Edition College Station, Texas 7784
> 5 USA 800-STATA-PC http://
www.stata.com 979-696-4600 stata@s
tata.com 979-696-4601 (fax)

400-user Stata network license expires 4 May 2013:
Serial number: 40120520081
Licensed to: University of Michigan
Campus Computing Sites

```

Notes:

1. (/v# option or -set maxvar-) 5000 maximum variables

running Q:\STATA.12\sysprofile.do ...

```
1 . insheet using "M:\thesis\input_table_v3.txt", tab
(23 vars, 60 obs)
```

MLR(p,>0%,>10%,>20%)

```
2 . stepwise, pr(.05): regress crown_arcsine dem slope twi awc brightness greenness wetness
begin with full model
p = 0.8953 >= 0.0500 removing wetness
p = 0.7056 >= 0.0500 removing slope
p = 0.3977 >= 0.0500 removing brightness
p = 0.5605 >= 0.0500 removing greenness
p = 0.2094 >= 0.0500 removing awc
```

Source	SS	df	MS	Number of obs = 60		
Model	1.71038003	2	.855190013	F(2, 57) =	29.17	
Residual	1.67110776	57	.02931768	Prob > F =	0.0000	
Total	3.38148779	59	.057313352	R-squared =	0.5058	
				Adj R-squared =	0.4885	
				Root MSE =	.17122	

crown_arcs~e	Coef.	Std. Err.	t	P> t	[95% Conf. Interval]	
dem	-.0174797	.0032209	-5.43	0.000	-.0239295	-.01103
twi	.0323878	.0092218	3.51	0.001	.0139214	.0508542
_cons	4.89588	.9483704	5.16	0.000	2.996801	6.794959

LR>0%

```
3 . stepwise, pr(.05): logit presence dem slope twi awc brightness greenness wetness
begin with full model
p = 0.7245 >= 0.0500 removing awc
p = 0.5532 >= 0.0500 removing wetness
p = 0.3755 >= 0.0500 removing brightness
p = 0.2782 >= 0.0500 removing slope
p = 0.1963 >= 0.0500 removing twi
```

Logistic regression	Number of obs =	60
	LR chi2(2) =	52.55
	Prob > chi2 =	0.0000
Log likelihood = -15.181695	Pseudo R2 =	0.6338

presence	Coef.	Std. Err.	z	P> z	[95% Conf. Interval]
dem	-1.024682	.3269815	-3.13	0.002	-1.665554 - .3838099
greenness	.2327206	.1121871	2.07	0.038	.012838 .4526033
_cons	275.9972	88.23634	3.13	0.002	103.0572 448.9373

Note: 3 failures and 0 successes completely determined.

4 . estat classification, all

Logistic model for presence

Classified	True		Total
	D	~D	
+	29	3	32
-	3	25	28
Total	32	28	60

Classified + if predicted Pr(D) >= .5
True D defined as presence != 0

Sensitivity	Pr(+ D)	90.63%
Specificity	Pr(- ~D)	89.29%
Positive predictive value	Pr(D +)	90.63%
Negative predictive value	Pr(~D -)	89.29%
False + rate for true ~D	Pr(+ ~D)	10.71%
False - rate for true D	Pr(- D)	9.38%
False + rate for classified +	Pr(~D +)	9.38%
False - rate for classified -	Pr(D -)	10.71%
Correctly classified		90.00%

5 . lroc, nograph all

Logistic model for presence

number of observations = 60
area under ROC curve = 0.9609

LR>10%

6 . stepwise, pr(.05): logit presence10 dem slope twi awc brightness greenness wetness

begin with full model
p = 0.5742 >= 0.0500 removing twi
p = 0.3104 >= 0.0500 removing awc
p = 0.4842 >= 0.0500 removing wetness
p = 0.3364 >= 0.0500 removing brightness
p = 0.2708 >= 0.0500 removing greenness

Logistic regression
Log likelihood = -17.052082
Number of obs = 60
LR chi2(2) = 33.38
Prob > chi2 = 0.0000
Pseudo R2 = 0.4946

presence10	Coef.	Std. Err.	z	P> z	[95% Conf. Interval]
dem	-.4729051	.1643037	-2.88	0.004	-.7949344 -.1508758
slope	-.6212272	.2678619	-2.32	0.020	-1.146227 -.0962276
_cons	134.1341	46.47295	2.89	0.004	43.04878 225.2194

7 . estat classification, all

Logistic model for presence10

Classified	True		Total
	D	~D	
+	8	3	11
-	7	42	49
Total	15	45	60

Classified + if predicted Pr(D) >= .5
True D defined as presence10 != 0

Sensitivity	Pr(+ D)	53.33%
Specificity	Pr(- ~D)	93.33%
Positive predictive value	Pr(D +)	72.73%
Negative predictive value	Pr(~D -)	85.71%
False + rate for true ~D	Pr(+ ~D)	6.67%
False - rate for true D	Pr(- D)	46.67%
False + rate for classified +	Pr(~D +)	27.27%
False - rate for classified -	Pr(D -)	14.29%
Correctly classified		83.33%

8 . lroc, nograph all

Logistic model for presence10

number of observations = 60
area under ROC curve = 0.9259

```

LR>20%
9 . stepwise, pr(.05): logit presence20 dem slope twi awc brightness greenness wetness
    begin with full model
p = 0.3700 >= 0.0500 removing brightness
p = 0.4033 >= 0.0500 removing twi
p = 0.2303 >= 0.0500 removing greenness
p = 0.1545 >= 0.0500 removing wetness
p = 0.1721 >= 0.0500 removing awc
p = 0.0549 >= 0.0500 removing slope

Logistic regression
Number of obs = 60
LR chi2( 1) = 20.60
Prob > chi2 = 0.0000
Pseudo R2 = 0.4371
Log likelihood = -13.261594

presence20 | Coef. Std. Err. z P>|z| [95% Conf. Interval]
-----+-----
dem | -.619925 .2192988 -2.83 0.005 [-1.049743, -.1901072]
_cons | 172.3402 61.19411 2.82 0.005 [52.40197, 292.2785]
    
```

Note: 1 failure and 0 successes completely determined.

10 . estat classification, all

Logistic model for presence20

Classified	True		Total
	D	~D	
+	6	3	9
-	2	49	51
Total	8	52	60

Classified + if predicted Pr(D) >= .5
True D defined as presence20 != 0

Sensitivity	Pr(+ D)	75.00%
Specificity	Pr(- ~D)	94.23%
Positive predictive value	Pr(D +)	66.67%
Negative predictive value	Pr(~D -)	96.08%
False + rate for true ~D	Pr(+ ~D)	5.77%
False - rate for true D	Pr(- D)	25.00%
False + rate for classified +	Pr(~D +)	33.33%
False - rate for classified -	Pr(D -)	3.92%
Correctly classified		91.67%

11 . lroc, nograph all

Logistic model for presence20

number of observations = 60
area under ROC curve = 0.9423

IFMAP_MLR

12 . stepwise, pr(.05): regress crown_arcsine dem slope twi awc ifmap
begin with full model
p = 0.9836 >= 0.0500 removing ifmap
p = 0.5606 >= 0.0500 removing slope
p = 0.2094 >= 0.0500 removing awc

Source	SS	df	MS	Number of obs =	60
Model	1.71038003	2	.855190013	F(2, 57) =	29.17
Residual	1.67110776	57	.02931768	Prob > F =	0.0000
Total	3.38148779	59	.057313352	R-squared =	0.5058
				Adj R-squared =	0.4885
				Root MSE =	.17122

crown_arcs~e	Coef.	Std. Err.	t	P> t	[95% Conf. Interval]
dem	-.0174797	.0032209	-5.43	0.000	-.0239295 - .01103
twi	.0323878	.0092218	3.51	0.001	.0139214 .0508542
_cons	4.89588	.9483704	5.16	0.000	2.996801 6.794959

IFMAP_LR>0%

```
13 . stepwise, pr(.05): logit presence dem slope twi awc ifmap
      begin with full model
p = 0.9877 >= 0.0500 removing ifmap
p = 0.6885 >= 0.0500 removing awc
p = 0.3131 >= 0.0500 removing slope
p = 0.2194 >= 0.0500 removing twi
```

```
Logistic regression      Number of obs =      60
                        LR chi2( 1) =      46.56
                        Prob > chi2 =      0.0000
Log likelihood = -18.173615      Pseudo R2 =      0.5616
```

presence	Coef.	Std. Err.	z	P> z	[95% Conf. Interval]	
dem	-.7340369	.2340483	-3.14	0.002	-1.192763	-.2753106
_cons	209.1679	66.63193	3.14	0.002	78.57167	339.764

IFMAP_LR>10%

```
14 . stepwise, pr(.05): logit presence10 dem slope twi awc ifmap
      begin with full model
p = 0.4983 >= 0.0500 removing awc
p = 0.3375 >= 0.0500 removing twi
p = 0.0984 >= 0.0500 removing ifmap
```

```
Logistic regression      Number of obs =      60
                        LR chi2( 2) =      33.38
                        Prob > chi2 =      0.0000
Log likelihood = -17.052082      Pseudo R2 =      0.4946
```

presence10	Coef.	Std. Err.	z	P> z	[95% Conf. Interval]	
dem	-.4729051	.1643037	-2.88	0.004	-.7949344	-.1508758
slope	-.6212272	.2678619	-2.32	0.020	-1.146227	-.0962276
_cons	134.1341	46.47295	2.89	0.004	43.04878	225.2194

IFMAP_LR>20%

```
15 . stepwise, pr(.05): logit presence20 dem slope twi awc ifmap
      begin with full model
p = 0.4153 >= 0.0500 removing ifmap
p = 0.4031 >= 0.0500 removing twi
p = 0.1721 >= 0.0500 removing awc
p = 0.0549 >= 0.0500 removing slope
```

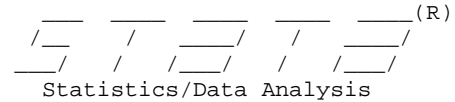
```
Logistic regression      Number of obs =      60
                        LR chi2( 1) =      20.60
                        Prob > chi2 =      0.0000
Log likelihood = -13.261594      Pseudo R2 =      0.4371
```

presence20	Coef.	Std. Err.	z	P> z	[95% Conf. Interval]	
dem	-.619925	.2192988	-2.83	0.005	-1.049743	-.1901072
_cons	172.3402	61.19411	2.82	0.005	52.40197	292.2785

Note: 1 failure and 0 successes completely determined.

16 .

Appendix B. Master list of all investigated regression tables



```

_____ (R)
/_____/ /_____/ /_____/ /_____/
_____/ /_____/ /_____/ /_____/ 12.1 Copyright 1985-2011 StataCo
> rp LP
Statistics/Data Analysis StataCorp
4905 Lakeway Drive
Special Edition College Station, Texas 7784
> 5 USA 800-STATA-PC http://
www.stata.com 979-696-4600 stata@s
www.stata.com 979-696-4601 (fax)

```

400-user Stata network license expires 4 May 2013:
 Serial number: 40120520081
 Licensed to: University of Michigan
 Campus Computing Sites

Notes:
 1. (/v# option or -set maxvar-) 5000 maximum variables

running Q:\STATA.12\sysprofile.do ...

```
1 . insheet using "M:\thesis\input_table_v3.txt", tab
(23 vars, 60 obs)
```

MLR(p,>0%,>10%,>20%)

```
2 . stepwise, pr(.05): regress crown_arcsine dem slope twi awc brightness greenness wetness
begin with full model
p = 0.8953 >= 0.0500 removing wetness
p = 0.7056 >= 0.0500 removing slope
p = 0.3977 >= 0.0500 removing brightness
p = 0.5605 >= 0.0500 removing greenness
p = 0.2094 >= 0.0500 removing awc
```

Source	SS	df	MS	Number of obs =	60
Model	1.71038003	2	.855190013	F(2, 57) =	29.17
Residual	1.67110776	57	.02931768	Prob > F =	0.0000
Total	3.38148779	59	.057313352	R-squared =	0.5058
				Adj R-squared =	0.4885
				Root MSE =	.17122

crown_arcsine	Coef.	Std. Err.	t	P> t	[95% Conf. Interval]
dem	-.0174797	.0032209	-5.43	0.000	-.0239295 - .01103
twi	.0323878	.0092218	3.51	0.001	.0139214 .0508542
_cons	4.89588	.9483704	5.16	0.000	2.996801 6.794959

LR>0%

```
3 . stepwise, pr(.05): logit presence dem slope twi awc brightness greenness wetness
begin with full model
p = 0.7245 >= 0.0500 removing awc
p = 0.5532 >= 0.0500 removing wetness
p = 0.3755 >= 0.0500 removing brightness
p = 0.2782 >= 0.0500 removing slope
p = 0.1963 >= 0.0500 removing twi
```

Logistic regression	Number of obs =	60
	LR chi2(2) =	52.55
	Prob > chi2 =	0.0000
Log likelihood = -15.181695	Pseudo R2 =	0.6338

presence	Coef.	Std. Err.	z	P> z	[95% Conf. Interval]	
dem	-1.024682	.3269815	-3.13	0.002	-1.665554	-.3838099
greenness	.2327206	.1121871	2.07	0.038	.012838	.4526033
_cons	275.9972	88.23634	3.13	0.002	103.0572	448.9373

Note: 3 failures and 0 successes completely determined.

4 . estat classification, all

Logistic model for presence

Classified	True		Total
	D	~D	
+	29	3	32
-	3	25	28
Total	32	28	60

Classified + if predicted Pr(D) >= .5
True D defined as presence != 0

Sensitivity	Pr(+ D)	90.63%
Specificity	Pr(- ~D)	89.29%
Positive predictive value	Pr(D +)	90.63%
Negative predictive value	Pr(~D -)	89.29%

False + rate for true ~D	Pr(+ ~D)	10.71%
False - rate for true D	Pr(- D)	9.38%
False + rate for classified +	Pr(~D +)	9.38%
False - rate for classified -	Pr(D -)	10.71%

Correctly classified 90.00%

5 . lroc, nograph all

Logistic model for presence

number of observations = 60
area under ROC curve = 0.9609

LR>10%

6 . stepwise, pr(.05): logit presence10 dem slope twi awc brightness greenness wetness

begin with full model
p = 0.5742 >= 0.0500 removing twi
p = 0.3104 >= 0.0500 removing awc
p = 0.4842 >= 0.0500 removing wetness
p = 0.3364 >= 0.0500 removing brightness
p = 0.2708 >= 0.0500 removing greenness

Logistic regression
Log likelihood = -17.052082
Number of obs = 60
LR chi2(2) = 33.38
Prob > chi2 = 0.0000
Pseudo R2 = 0.4946

presence10	Coef.	Std. Err.	z	P> z	[95% Conf. Interval]	
dem	-.4729051	.1643037	-2.88	0.004	-.7949344	-.1508758
slope	-.6212272	.2678619	-2.32	0.020	-1.146227	-.0962276
_cons	134.1341	46.47295	2.89	0.004	43.04878	225.2194

7 . estat classification, all

Logistic model for presence10

Classified	True		Total
	D	~D	
+	8	3	11
-	7	42	49
Total	15	45	60

Classified + if predicted Pr(D) >= .5
 True D defined as presence10 != 0

Sensitivity	Pr(+ D)	53.33%
Specificity	Pr(- ~D)	93.33%
Positive predictive value	Pr(D +)	72.73%
Negative predictive value	Pr(~D -)	85.71%
False + rate for true ~D	Pr(+ ~D)	6.67%
False - rate for true D	Pr(- D)	46.67%
False + rate for classified +	Pr(~D +)	27.27%
False - rate for classified -	Pr(D -)	14.29%
Correctly classified		83.33%

8 . lroc, nograph all

Logistic model for presence10

number of observations = 60
 area under ROC curve = 0.9259

LR>20%

```
9 . stepwise, pr(.05): logit presence20 dem slope twi awc brightness greenness wetness
    begin with full model
p = 0.3700 >= 0.0500 removing brightness
p = 0.4033 >= 0.0500 removing twi
p = 0.2303 >= 0.0500 removing greenness
p = 0.1545 >= 0.0500 removing wetness
p = 0.1721 >= 0.0500 removing awc
p = 0.0549 >= 0.0500 removing slope
```

```
Logistic regression      Number of obs =      60
                        LR chi2( 1) =      20.60
                        Prob > chi2 =      0.0000
Log likelihood = -13.261594      Pseudo R2 =      0.4371
```

presence20	Coef.	Std. Err.	z	P> z	[95% Conf. Interval]
dem	-.619925	.2192988	-2.83	0.005	-1.049743 - .1901072
_cons	172.3402	61.19411	2.82	0.005	52.40197 292.2785

Note: 1 failure and 0 successes completely determined.

10 . estat classification, all

Logistic model for presence20

Classified	True		Total
	D	~D	
+	6	3	9
-	2	49	51
Total	8	52	60

Classified + if predicted Pr(D) >= .5
True D defined as presence20 != 0

Sensitivity	Pr(+ D)	75.00%
Specificity	Pr(- ~D)	94.23%
Positive predictive value	Pr(D +)	66.67%
Negative predictive value	Pr(~D -)	96.08%
False + rate for true ~D	Pr(+ ~D)	5.77%
False - rate for true D	Pr(- D)	25.00%
False + rate for classified +	Pr(~D +)	33.33%
False - rate for classified -	Pr(D -)	3.92%
Correctly classified		91.67%

11 . lroc, nograph all

Logistic model for presence20

number of observations = 60
area under ROC curve = 0.9423

IFMAPp

12 . stepwise, pr(.05): regress crown_arcsine dem slope twi awc ifmap
begin with full model
p = 0.9836 >= 0.0500 removing ifmap
p = 0.5606 >= 0.0500 removing slope
p = 0.2094 >= 0.0500 removing awc

Source	SS	df	MS	Number of obs =	60
Model	1.71038003	2	.855190013	F(2, 57) =	29.17
Residual	1.67110776	57	.02931768	Prob > F =	0.0000
Total	3.38148779	59	.057313352	R-squared =	0.5058
				Adj R-squared =	0.4885
				Root MSE =	.17122

crown_arcs~e	Coef.	Std. Err.	t	P> t	[95% Conf. Interval]
dem	-.0174797	.0032209	-5.43	0.000	-.0239295 - .01103
twi	.0323878	.0092218	3.51	0.001	.0139214 .0508542
_cons	4.89588	.9483704	5.16	0.000	2.996801 6.794959

IFMAP_LR>0%

```
13 . stepwise, pr(.05): logit presence dem slope twi awc ifmap
      begin with full model
p = 0.9877 >= 0.0500 removing ifmap
p = 0.6885 >= 0.0500 removing awc
p = 0.3131 >= 0.0500 removing slope
p = 0.2194 >= 0.0500 removing twi
```

```
Logistic regression      Number of obs =      60
                        LR chi2( 1) =      46.56
                        Prob > chi2 =      0.0000
Log likelihood = -18.173615      Pseudo R2 =      0.5616
```

presence	Coef.	Std. Err.	z	P> z	[95% Conf. Interval]	
dem	-.7340369	.2340483	-3.14	0.002	-1.192763	-.2753106
_cons	209.1679	66.63193	3.14	0.002	78.57167	339.764

IFMAP_LR>10%

```
14 . stepwise, pr(.05): logit presence10 dem slope twi awc ifmap
      begin with full model
p = 0.4983 >= 0.0500 removing awc
p = 0.3375 >= 0.0500 removing twi
p = 0.0984 >= 0.0500 removing ifmap
```

```
Logistic regression      Number of obs =      60
                        LR chi2( 2) =      33.38
                        Prob > chi2 =      0.0000
Log likelihood = -17.052082      Pseudo R2 =      0.4946
```

presence10	Coef.	Std. Err.	z	P> z	[95% Conf. Interval]	
dem	-.4729051	.1643037	-2.88	0.004	-.7949344	-.1508758
slope	-.6212272	.2678619	-2.32	0.020	-1.146227	-.0962276
_cons	134.1341	46.47295	2.89	0.004	43.04878	225.2194

IFMAP_LR>20%

```
15 . stepwise, pr(.05): logit presence20 dem slope twi awc ifmap
      begin with full model
p = 0.4153 >= 0.0500 removing ifmap
p = 0.4031 >= 0.0500 removing twi
p = 0.1721 >= 0.0500 removing awc
p = 0.0549 >= 0.0500 removing slope
```

```
Logistic regression      Number of obs =      60
                        LR chi2( 1) =      20.60
                        Prob > chi2 =      0.0000
Log likelihood = -13.261594      Pseudo R2 =      0.4371
```

presence20	Coef.	Std. Err.	z	P> z	[95% Conf. Interval]	
dem	-.619925	.2192988	-2.83	0.005	-1.049743	-.1901072
_cons	172.3402	61.19411	2.82	0.005	52.40197	292.2785

Note: 1 failure and 0 successes completely determined.

```
16 . stepwise, pr(.05): regress crown_arcsine dem slope twi awc etm1
      begin with full model
p = 0.6279 >= 0.0500 removing etm1
p = 0.5606 >= 0.0500 removing slope
p = 0.2094 >= 0.0500 removing awc
```

Source	SS	df	MS	Number of obs = 60		
Model	1.71038003	2	.855190013	F(2, 57) =	29.17	
Residual	1.67110776	57	.02931768	Prob > F =	0.0000	
Total	3.38148779	59	.057313352	R-squared =	0.5058	
				Adj R-squared =	0.4885	
				Root MSE =	.17122	

crown_arcs~e	Coef.	Std. Err.	t	P> t	[95% Conf. Interval]	
dem	-.0174797	.0032209	-5.43	0.000	-.0239295	-.01103
twi	.0323878	.0092218	3.51	0.001	.0139214	.0508542
_cons	4.89588	.9483704	5.16	0.000	2.996801	6.794959

```
17 . stepwise, pr(.05): regress crown_arcsine dem slope twi awc etm2
      begin with full model
p = 0.7955 >= 0.0500 removing slope
p = 0.2628 >= 0.0500 removing etm2
p = 0.2094 >= 0.0500 removing awc
```

Source	SS	df	MS	Number of obs = 60		
Model	1.71038003	2	.855190013	F(2, 57) =	29.17	
Residual	1.67110776	57	.02931768	Prob > F =	0.0000	
Total	3.38148779	59	.057313352	R-squared =	0.5058	
				Adj R-squared =	0.4885	
				Root MSE =	.17122	

crown_arcs~e	Coef.	Std. Err.	t	P> t	[95% Conf. Interval]	
dem	-.0174797	.0032209	-5.43	0.000	-.0239295	-.01103
twi	.0323878	.0092218	3.51	0.001	.0139214	.0508542
_cons	4.89588	.9483704	5.16	0.000	2.996801	6.794959

```
18 . stepwise, pr(.05): regress crown_arcsine dem slope twi awc etm3
      begin with full model
p = 0.8028 >= 0.0500 removing slope
p = 0.2654 >= 0.0500 removing awc
p = 0.0806 >= 0.0500 removing etm3
```

Source	SS	df	MS	Number of obs = 60		
Model	1.71038003	2	.855190013	F(2, 57) =	29.17	
Residual	1.67110776	57	.02931768	Prob > F =	0.0000	
Total	3.38148779	59	.057313352	R-squared =	0.5058	
				Adj R-squared =	0.4885	
				Root MSE =	.17122	

crown_arcs~e	Coef.	Std. Err.	t	P> t	[95% Conf. Interval]	
dem	-.0174797	.0032209	-5.43	0.000	-.0239295	-.01103
twi	.0323878	.0092218	3.51	0.001	.0139214	.0508542
_cons	4.89588	.9483704	5.16	0.000	2.996801	6.794959

```
19 . stepwise, pr(.05): regress crown_arcsine dem slope twi awc etm4
      begin with full model
p = 0.7172 >= 0.0500 removing etm4
p = 0.5606 >= 0.0500 removing slope
p = 0.2094 >= 0.0500 removing awc
```

Source	SS	df	MS	Number of obs = 60		
Model	1.71038003	2	.855190013	F(2, 57) =	29.17	
Residual	1.67110776	57	.02931768	Prob > F =	0.0000	
Total	3.38148779	59	.057313352	R-squared =	0.5058	
				Adj R-squared =	0.4885	
				Root MSE =	.17122	

crown_arcs~e	Coef.	Std. Err.	t	P> t	[95% Conf. Interval]	
dem	-.0174797	.0032209	-5.43	0.000	-.0239295	-.01103
twi	.0323878	.0092218	3.51	0.001	.0139214	.0508542
_cons	4.89588	.9483704	5.16	0.000	2.996801	6.794959

```
20 . stepwise, pr(.05): regress crown_arcsine dem slope twi awc etm5
      begin with full model
p = 0.6397 >= 0.0500 removing slope
p = 0.5370 >= 0.0500 removing etm5
p = 0.2094 >= 0.0500 removing awc
```

Source	SS	df	MS	Number of obs = 60		
Model	1.71038003	2	.855190013	F(2, 57) =	29.17	
Residual	1.67110776	57	.02931768	Prob > F =	0.0000	
Total	3.38148779	59	.057313352	R-squared =	0.5058	
				Adj R-squared =	0.4885	
				Root MSE =	.17122	

crown_arcs~e	Coef.	Std. Err.	t	P> t	[95% Conf. Interval]	
dem	-.0174797	.0032209	-5.43	0.000	-.0239295	-.01103
twi	.0323878	.0092218	3.51	0.001	.0139214	.0508542
_cons	4.89588	.9483704	5.16	0.000	2.996801	6.794959

```
21 . stepwise, pr(.05): regress crown_arcsine dem slope twi awc etm6
      begin with full model
p = 0.6941 >= 0.0500 removing slope
p = 0.2615 >= 0.0500 removing etm6
p = 0.2094 >= 0.0500 removing awc
```

Source	SS	df	MS	Number of obs = 60		
Model	1.71038003	2	.855190013	F(2, 57) =	29.17	
Residual	1.67110776	57	.02931768	Prob > F =	0.0000	
Total	3.38148779	59	.057313352	R-squared =	0.5058	
				Adj R-squared =	0.4885	
				Root MSE =	.17122	

crown_arcs~e	Coef.	Std. Err.	t	P> t	[95% Conf. Interval]	
dem	-.0174797	.0032209	-5.43	0.000	-.0239295	-.01103
twi	.0323878	.0092218	3.51	0.001	.0139214	.0508542
_cons	4.89588	.9483704	5.16	0.000	2.996801	6.794959

22 . stepwise, pr(.05): regress crown_arcsine dem slope twi awc NDVI
variable NDVI not found
r(111);

23 . stepwise, pr(.05): regress crown_arcsine dem slope twi awc NDVIv2
variable NDVIv2 not found
r(111);

24 . stepwise, pr(.05): regress crown_arcsine dem slope twi awc NDVI_v2
variable NDVI_v2 not found
r(111);

25 . stepwise, pr(.05): regress crown_arcsine dem slope twi awc ndvi_v2
begin with full model
p = **0.7987** >= 0.0500 removing **slope**
p = **0.3004** >= 0.0500 removing **awc**
p = **0.0897** >= 0.0500 removing **ndvi_v2**

Source	SS	df	MS	Number of obs =	60
Model	1.71038003	2	.855190013	F(2, 57) =	29.17
Residual	1.67110776	57	.02931768	Prob > F =	0.0000
Total	3.38148779	59	.057313352	R-squared =	0.5058
				Adj R-squared =	0.4885
				Root MSE =	.17122

crown_arcs~e	Coef.	Std. Err.	t	P> t	[95% Conf. Interval]	
dem	-.0174797	.0032209	-5.43	0.000	-.0239295	-.01103
twi	.0323878	.0092218	3.51	0.001	.0139214	.0508542
_cons	4.89588	.9483704	5.16	0.000	2.996801	6.794959

26 . stepwise, pr(.05): logit presence dem slope twi awc etm1
begin with full model
p = **0.8191** >= 0.0500 removing **awc**
p = **0.5218** >= 0.0500 removing **slope**
p = **0.1937** >= 0.0500 removing **twi**
p = **0.1845** >= 0.0500 removing **etm1**

Logistic regression
Log likelihood = **-18.173615**
Number of obs = 60
LR chi2(1) = 46.56
Prob > chi2 = 0.0000
Pseudo R2 = 0.5616

presence	Coef.	Std. Err.	z	P> z	[95% Conf. Interval]	
dem	-.7340369	.2340483	-3.14	0.002	-1.192763	-.2753106
_cons	209.1679	66.63193	3.14	0.002	78.57167	339.764

27 . stepwise, pr(.05): logit presence dem slope twi awc etm2
begin with full model
p = **0.6454** >= 0.0500 removing **awc**
p = **0.4697** >= 0.0500 removing **etm2**
p = **0.3131** >= 0.0500 removing **slope**
p = **0.2194** >= 0.0500 removing **twi**

Logistic regression
Log likelihood = **-18.173615**
Number of obs = 60
LR chi2(1) = 46.56
Prob > chi2 = 0.0000
Pseudo R2 = 0.5616

presence	Coef.	Std. Err.	z	P> z	[95% Conf. Interval]	
dem	-.7340369	.2340483	-3.14	0.002	-1.192763	-.2753106
_cons	209.1679	66.63193	3.14	0.002	78.57167	339.764

28 . stepwise, pr(.05): logit presence dem slope twi awc etm3
begin with full model

p = **0.7442** >= 0.0500 removing **awc**
p = **0.2280** >= 0.0500 removing **etm3**
p = **0.3131** >= 0.0500 removing **slope**
p = **0.2194** >= 0.0500 removing **twi**

Logistic regression

Number of obs = 60
LR chi2(1) = 46.56
Prob > chi2 = 0.0000
Pseudo R2 = 0.5616

Log likelihood = **-18.173615**

presence	Coef.	Std. Err.	z	P> z	[95% Conf. Interval]	
dem	-.7340369	.2340483	-3.14	0.002	-1.192763	-.2753106
_cons	209.1679	66.63193	3.14	0.002	78.57167	339.764

29 . stepwise, pr(.05): logit presence dem slope twi awc etm4
begin with full model

p = **0.6441** >= 0.0500 removing **awc**
p = **0.3988** >= 0.0500 removing **slope**
p = **0.1852** >= 0.0500 removing **twi**
p = **0.0568** >= 0.0500 removing **etm4**

Logistic regression

Number of obs = 60
LR chi2(1) = 46.56
Prob > chi2 = 0.0000
Pseudo R2 = 0.5616

Log likelihood = **-18.173615**

presence	Coef.	Std. Err.	z	P> z	[95% Conf. Interval]	
dem	-.7340369	.2340483	-3.14	0.002	-1.192763	-.2753106
_cons	209.1679	66.63193	3.14	0.002	78.57167	339.764

30 . stepwise, pr(.05): logit presence dem slope twi awc etm5
begin with full model

p = **0.7149** >= 0.0500 removing **etm5**
p = **0.6885** >= 0.0500 removing **awc**
p = **0.3131** >= 0.0500 removing **slope**
p = **0.2194** >= 0.0500 removing **twi**

Logistic regression

Number of obs = 60
LR chi2(1) = 46.56
Prob > chi2 = 0.0000
Pseudo R2 = 0.5616

Log likelihood = **-18.173615**

presence	Coef.	Std. Err.	z	P> z	[95% Conf. Interval]	
dem	-.7340369	.2340483	-3.14	0.002	-1.192763	-.2753106
_cons	209.1679	66.63193	3.14	0.002	78.57167	339.764

```
31 . stepwise, pr(.05): logit presence dem slope twi awc etm6
      begin with full model
```

```
p = 0.6665 >= 0.0500 removing awc
p = 0.6071 >= 0.0500 removing etm6
p = 0.3131 >= 0.0500 removing slope
p = 0.2194 >= 0.0500 removing twi
```

```
Logistic regression              Number of obs   =           60
LR chi2(  1)                     =           46.56
Prob > chi2                       =           0.0000
Pseudo R2                         =           0.5616
Log likelihood = -18.173615
```

presence	Coef.	Std. Err.	z	P> z	[95% Conf. Interval]
dem	-.7340369	.2340483	-3.14	0.002	-1.192763 - .2753106
_cons	209.1679	66.63193	3.14	0.002	78.57167 339.764

```
32 . stepwise, pr(.05): logit presence dem slope twi awc ndvi_v2
      begin with full model
```

```
p = 0.6282 >= 0.0500 removing awc
p = 0.2227 >= 0.0500 removing ndvi_v2
p = 0.3131 >= 0.0500 removing slope
p = 0.2194 >= 0.0500 removing twi
```

```
Logistic regression              Number of obs   =           60
LR chi2(  1)                     =           46.56
Prob > chi2                       =           0.0000
Pseudo R2                         =           0.5616
Log likelihood = -18.173615
```

presence	Coef.	Std. Err.	z	P> z	[95% Conf. Interval]
dem	-.7340369	.2340483	-3.14	0.002	-1.192763 - .2753106
_cons	209.1679	66.63193	3.14	0.002	78.57167 339.764

```
33 . stepwise, pr(.05): logit presence10 dem slope twi awc etm1
      begin with full model
```

```
p = 0.9547 >= 0.0500 removing etm1
p = 0.4823 >= 0.0500 removing awc
p = 0.2689 >= 0.0500 removing twi
```

```
Logistic regression              Number of obs   =           60
LR chi2(  2)                     =           33.38
Prob > chi2                       =           0.0000
Pseudo R2                         =           0.4946
Log likelihood = -17.052082
```

presence10	Coef.	Std. Err.	z	P> z	[95% Conf. Interval]
dem	-.4729051	.1643037	-2.88	0.004	-.7949344 - .1508758
slope	-.6212272	.2678619	-2.32	0.020	-1.146227 - .0962276
_cons	134.1341	46.47295	2.89	0.004	43.04878 225.2194


```
34 . stepwise, pr(.05): logit presence10 dem slope twi awc etm2
      begin with full model
p = 0.6391 >= 0.0500 removing twi
p = 0.4395 >= 0.0500 removing awc
p = 0.1522 >= 0.0500 removing etm2
```

```
Logistic regression                               Number of obs   =           60
LR chi2( 2)                                     =           33.38
Prob > chi2                                     =           0.0000
Log likelihood = -17.052082                      Pseudo R2      =           0.4946
```

presence10	Coef.	Std. Err.	z	P> z	[95% Conf. Interval]	
dem	-.4729051	.1643037	-2.88	0.004	-.7949344	-.1508758
slope	-.6212272	.2678619	-2.32	0.020	-1.146227	-.0962276
_cons	134.1341	46.47295	2.89	0.004	43.04878	225.2194

```
35 . stepwise, pr(.05): logit presence10 dem slope twi awc etm3
      begin with full model
p = 0.3620 >= 0.0500 removing twi
p = 0.1932 >= 0.0500 removing awc
p = 0.0799 >= 0.0500 removing etm3
```

```
Logistic regression                               Number of obs   =           60
LR chi2( 2)                                     =           33.38
Prob > chi2                                     =           0.0000
Log likelihood = -17.052082                      Pseudo R2      =           0.4946
```

presence10	Coef.	Std. Err.	z	P> z	[95% Conf. Interval]	
dem	-.4729051	.1643037	-2.88	0.004	-.7949344	-.1508758
slope	-.6212272	.2678619	-2.32	0.020	-1.146227	-.0962276
_cons	134.1341	46.47295	2.89	0.004	43.04878	225.2194

```
36 . stepwise, pr(.05): logit presence10 dem slope twi awc etm4
      begin with full model
p = 0.5386 >= 0.0500 removing awc
p = 0.3803 >= 0.0500 removing etm4
p = 0.2689 >= 0.0500 removing twi
```

```
Logistic regression                               Number of obs   =           60
LR chi2( 2)                                     =           33.38
Prob > chi2                                     =           0.0000
Log likelihood = -17.052082                      Pseudo R2      =           0.4946
```

presence10	Coef.	Std. Err.	z	P> z	[95% Conf. Interval]	
dem	-.4729051	.1643037	-2.88	0.004	-.7949344	-.1508758
slope	-.6212272	.2678619	-2.32	0.020	-1.146227	-.0962276
_cons	134.1341	46.47295	2.89	0.004	43.04878	225.2194

37 . stepwise, pr(.05): logit presence10 dem slope twi awc etm5
begin with full model

p = **0.9523** >= 0.0500 removing **etm5**
p = **0.4823** >= 0.0500 removing **awc**
p = **0.2689** >= 0.0500 removing **twi**

Logistic regression
Number of obs = 60
LR chi2(2) = 33.38
Prob > chi2 = 0.0000
Pseudo R2 = 0.4946
Log likelihood = **-17.052082**

presence10	Coef.	Std. Err.	z	P> z	[95% Conf. Interval]	
dem	-.4729051	.1643037	-2.88	0.004	-.7949344	-.1508758
slope	-.6212272	.2678619	-2.32	0.020	-1.146227	-.0962276
_cons	134.1341	46.47295	2.89	0.004	43.04878	225.2194

38 . stepwise, pr(.05): logit presence10 dem slope twi awc etm6
begin with full model

p = **0.8885** >= 0.0500 removing **etm6**
p = **0.4823** >= 0.0500 removing **awc**
p = **0.2689** >= 0.0500 removing **twi**

Logistic regression
Number of obs = 60
LR chi2(2) = 33.38
Prob > chi2 = 0.0000
Pseudo R2 = 0.4946
Log likelihood = **-17.052082**

presence10	Coef.	Std. Err.	z	P> z	[95% Conf. Interval]	
dem	-.4729051	.1643037	-2.88	0.004	-.7949344	-.1508758
slope	-.6212272	.2678619	-2.32	0.020	-1.146227	-.0962276
_cons	134.1341	46.47295	2.89	0.004	43.04878	225.2194

39 . stepwise, pr(.05): logit presence10 dem slope twi awc ndvi_v2
begin with full model

p = **0.4520** >= 0.0500 removing **twi**
p = **0.3904** >= 0.0500 removing **awc**
p = **0.1665** >= 0.0500 removing **slope**

Logistic regression
Number of obs = 60
LR chi2(2) = 34.93
Prob > chi2 = 0.0000
Pseudo R2 = 0.5177
Log likelihood = **-16.272727**

presence10	Coef.	Std. Err.	z	P> z	[95% Conf. Interval]	
dem	-.7068262	.2092252	-3.38	0.001	-1.1169	-.2967524
ndvi_v2	77.99209	32.20078	2.42	0.015	14.87972	141.1045
_cons	124.5381	42.22539	2.95	0.003	41.77781	207.2983

Note: 1 failure and 0 successes completely determined.


```
46 . stepwise, pr(.05): logit presence20 dem slope twi awc ndvi_v2
      begin with full model
p = 0.7618 >= 0.0500 removing ndvi_v2
p = 0.4031 >= 0.0500 removing twi
p = 0.1721 >= 0.0500 removing awc
p = 0.0549 >= 0.0500 removing slope
```

```
Logistic regression
Log likelihood = -13.261594
Number of obs = 60
LR chi2( 1) = 20.60
Prob > chi2 = 0.0000
Pseudo R2 = 0.4371
```

presence20	Coef.	Std. Err.	z	P> z	[95% Conf. Interval]	
dem	-.619925	.2192988	-2.83	0.005	-1.049743	-.1901072
_cons	172.3402	61.19411	2.82	0.005	52.40197	292.2785

Note: 1 failure and 0 successes completely determined.

47 .

Appendix C. Field Sample Plot Data

Plot_number	Latitude	Longitude	Fraxinus_species	DBH (cm)	Tree_ID	Crown (m2)	Total Coverage (m2)	Total Coverage %
1	42.1615737	-84.1277862	FRAPEN	20.0	1	13.7	489.6	13.6%
1	42.1615737	-84.1277862	FRAPEN	31.6	2	25.2		
1	42.1615737	-84.1277862	FRAPEN	39.0	3	32.5		
1	42.1615737	-84.1277862	FRAPEN	41.5	4	35.0		
1	42.1615737	-84.1277862	FRAPEN	23.6	5	17.3		
1	42.1615737	-84.1277862	FRAPEN	19.0	6	12.7		
1	42.1615737	-84.1277862	FRAPEN	48.5	7	41.9		
1	42.1615737	-84.1277862	FRAPEN	33.3	8	26.9		
1	42.1615737	-84.1277862	FRAPEN	22.2	9	15.9		
1	42.1615737	-84.1277862	FRAPEN	13.3	10	7.1		
1	42.1615737	-84.1277862	FRAPEN	13.8	11	7.6		
1	42.1615737	-84.1277862	FRAPEN	11.5	12	5.3		
1	42.1615737	-84.1277862	FRAPEN	46.4	13	39.8		
1	42.1615737	-84.1277862	FRAPEN	14.5	14	8.3		
1	42.1615737	-84.1277862	FRAPEN	10.9	15	4.7		
1	42.1615737	-84.1277862	FRAPEN	57.5	16	50.8		
1	42.1615737	-84.1277862	FRAPEN	40.7	17	34.2		
1	42.1615737	-84.1277862	FRAPEN	12.2	18	6.0		
1	42.1615737	-84.1277862	FRAPEN	13.6	19	7.4		
1	42.1615737	-84.1277862	FRAPEN	18.7	20	12.4		
1	42.1615737	-84.1277862	FRAPEN	10.7	21	4.5		
1	42.1615737	-84.1277862	FRAPEN	43.0	22	36.5		
1	42.1615737	-84.1277862	FRAPEN	17.9	23	11.6		
1	42.1615737	-84.1277862	FRAPEN	17.8	24	11.5		
1	42.1615737	-84.1277862	FRAPEN	16.8	25	10.5		

Plot_number	Latitude	Longitude	Fraxinus_species	DBH (cm)	Tree_ID	Crown (m2)	Total Coverage (m2)	Total Coverage %
1	42.1615737	-84.1277862	FRAPEN	16.7	26	10.4		
2	42.1615737	-84.1277862	FRAPEN	19.5	27	13.2	17.3	0.5%
2	42.1615737	-84.1277862	FRAPEN	10.3	28	4.1		
3	42.1645939	-84.1243530	FRAPEN	31.0	29	24.6	174.0	4.8%
3	42.1645939	-84.1243530	FRAPEN	54.5	30	47.9		
3	42.1645939	-84.1243530	FRAPEN	27.5	31	21.1		
3	42.1645939	-84.1243530	FRAPEN	20.7	32	14.4		
3	42.1645939	-84.1243530	FRAPEN	31.9	33	25.5		
3	42.1645939	-84.1243530	FRAPEN	10.6	34	4.4		
3	42.1645939	-84.1243530	FRAPEN	17.4	35	11.1		
3	42.1645939	-84.1243530	FRAPEN	31.4	36	25.0		
4	42.1662783	-84.1240365	FRAPEN	45.9	37	39.3	1343.7	37.3%
4	42.1662783	-84.1240365	FRAPEN	43.0	38	36.5		
4	42.1662783	-84.1240365	FRAPEN	60.4	39	53.7		
4	42.1662783	-84.1240365	FRAPEN	58.6	40	51.9		
4	42.1662783	-84.1240365	FRAPEN	46.2	41	39.6		
4	42.1662783	-84.1240365	FRAPEN	67.1	42	60.3		
4	42.1662783	-84.1240365	FRAPEN	60.0	43	53.3		
4	42.1662783	-84.1240365	FRAPEN	49.3	44	42.7		
4	42.1662783	-84.1240365	FRAPEN	25.2	45	18.8		
4	42.1662783	-84.1240365	FRAPEN	12.6	46	6.4		
4	42.1662783	-84.1240365	FRAPEN	61.9	47	55.2		
4	42.1662783	-84.1240365	FRAPEN	16.6	48	10.3		
4	42.1662783	-84.1240365	FRAPEN	30.7	49	24.3		
4	42.1662783	-84.1240365	FRAPEN	94.1	50	87.1		
4	42.1662783	-84.1240365	FRAPEN	14.4	51	8.2		

Plot_number	Latitude	Longitude	Fraxinus_species	DBH (cm)	Tree_ID	Crown (m2)	Total Coverage (m2)	Total Coverage %
4	42.1662783	-84.1240365	FRAPEN	12.0	52	5.8		
4	42.1662783	-84.1240365	FRAPEN	23.5	53	17.2		
4	42.1662783	-84.1240365	FRAPEN	28.4	54	22.0		
4	42.1662783	-84.1240365	FRAPEN	19.1	55	12.8		
4	42.1662783	-84.1240365	FRAPEN	20.1	56	13.8		
4	42.1662783	-84.1240365	FRAPEN	16.0	57	9.7		
4	42.1662783	-84.1240365	FRAPEN	14.0	58	7.8		
4	42.1662783	-84.1240365	FRAPEN	82.5	59	75.6		
4	42.1662783	-84.1240365	FRAPEN	11.5	60	5.3		
4	42.1662783	-84.1240365	FRAPEN	22.0	61	15.7		
4	42.1662783	-84.1240365	FRAPEN	16.6	62	10.3		
4	42.1662783	-84.1240365	FRAPEN	23.5	63	17.2		
4	42.1662783	-84.1240365	FRAPEN	15.2	64	8.9		
4	42.1662783	-84.1240365	FRAPEN	41.8	65	35.3		
4	42.1662783	-84.1240365	FRAPEN	27.3	66	20.9		
4	42.1662783	-84.1240365	FRAPEN	36.4	67	29.9		
4	42.1662783	-84.1240365	FRAPEN	28.2	68	21.8		
4	42.1662783	-84.1240365	FRAPEN	82.0	69	75.1		
4	42.1662783	-84.1240365	FRAPEN	12.3	70	6.1		
4	42.1662783	-84.1240365	FRAPEN	10.5	71	4.3		
4	42.1662783	-84.1240365	FRAPEN	14.6	72	8.4		
4	42.1662783	-84.1240365	FRAPEN	10.2	73	4.0		
4	42.1662783	-84.1240365	FRAPEN	10.6	74	4.4		
4	42.1662783	-84.1240365	FRAPEN	17.4	75	11.1		
4	42.1662783	-84.1240365	FRAPEN	18.0	76	11.7		
4	42.1662783	-84.1240365	FRAPEN	16.8	77	10.5		

Plot_number	Latitude	Longitude	Fraxinus_species	DBH (cm)	Tree_ID	Crown (m2)	Total Coverage (m2)	Total Coverage %
4	42.1662783	-84.1240365	FRAPEN	10.5	78	4.3		
4	42.1662783	-84.1240365	FRAPEN	11.1	79	4.9		
4	42.1662783	-84.1240365	FRAPEN	10.8	80	4.6		
4	42.1662783	-84.1240365	FRAPEN	16.2	81	9.9		
4	42.1662783	-84.1240365	FRAPEN	10.2	82	4.0		
4	42.1662783	-84.1240365	FRAPEN	39.1	83	32.6		
4	42.1662783	-84.1240365	FRAPEN	15.6	84	9.3		
4	42.1662783	-84.1240365	FRAPEN	15.4	85	9.1		
4	42.1662783	-84.1240365	FRAPEN	24.8	86	18.5		
4	42.1662783	-84.1240365	FRAPEN	19.3	87	13.0		
4	42.1662783	-84.1240365	FRAPEN	16.6	88	10.3		
4	42.1662783	-84.1240365	FRAPEN	16.5	89	10.2		
4	42.1662783	-84.1240365	FRAPEN	21.0	90	14.7		
4	42.1662783	-84.1240365	FRAPEN	18.0	91	11.7		
4	42.1662783	-84.1240365	FRAPEN	15.5	92	9.2		
4	42.1662783	-84.1240365	FRAPEN	13.0	93	6.8		
4	42.1662783	-84.1240365	FRAPEN	10.1	94	3.9		
4	42.1662783	-84.1240365	FRAPEN	15.8	95	9.5		
4	42.1662783	-84.1240365	FRAPEN	10.2	96	4.0		
4	42.1662783	-84.1240365	FRAPEN	17.9	97	11.6		
4	42.1662783	-84.1240365	FRAPEN	16.2	98	9.9		
4	42.1662783	-84.1240365	FRAPEN	12.3	99	6.1		
4	42.1662783	-84.1240365	FRAPEN	17.4	100	11.1		
4	42.1662783	-84.1240365	FRAPEN	10.0	101	3.8		
4	42.1662783	-84.1240365	FRAPEN	11.8	102	5.6		
4	42.1662783	-84.1240365	FRAPEN	18.2	103	11.9		

Plot_number	Latitude	Longitude	Fraxinus_species	DBH (cm)	Tree_ID	Crown (m2)	Total Coverage (m2)	Total Coverage %
4	42.1662783	-84.1240365	FRAPEN	10.8	104	4.6		
4	42.1662783	-84.1240365	FRAPEN	15.0	105	8.8		
4	42.1662783	-84.1240365	FRAPEN	13.0	106	6.8		
4	42.1662783	-84.1240365	FRAPEN	12.0	107	5.8		
4	42.1662783	-84.1240365	FRAPEN	15.3	108	9.0		
4	42.1662783	-84.1240365	FRAPEN	11.0	109	4.8		
5	42.1671796	-84.1226471	FRAPEN	24.4	110	18.1	341.6	9.5%
5	42.1671796	-84.1226471	FRAPEN	19.6	111	13.3		
5	42.1671796	-84.1226471	FRAPEN	14.8	112	8.6		
5	42.1671796	-84.1226471	FRAPEN	26.7	113	20.3		
5	42.1671796	-84.1226471	FRAPEN	22.8	114	16.5		
5	42.1671796	-84.1226471	FRAPEN	31.3	115	24.9		
5	42.1671796	-84.1226471	FRAPEN	22.1	116	15.8		
5	42.1671796	-84.1226471	FRAPEN	15.5	117	9.2		
5	42.1671796	-84.1226471	FRAPEN	11.9	118	5.7		
5	42.1671796	-84.1226471	FRAPEN	14.0	119	7.8		
5	42.1671796	-84.1226471	FRAPEN	15.6	120	9.3		
5	42.1671796	-84.1226471	FRAPEN	12.6	121	6.4		
5	42.1671796	-84.1226471	FRAPEN	20.2	122	13.9		
5	42.1671796	-84.1226471	FRAPEN	18.5	123	12.2		
5	42.1671796	-84.1226471	FRAPEN	12.3	124	6.1		
5	42.1671796	-84.1226471	FRAPEN	11.6	125	5.4		
5	42.1671796	-84.1226471	FRAPEN	11.5	126	5.3		
5	42.1671796	-84.1226471	FRAPEN	22.0	127	15.7		
5	42.1671796	-84.1226471	FRAPEN	17.2	128	10.9		
5	42.1671796	-84.1226471	FRAPEN	19.9	129	13.6		

Plot_number	Latitude	Longitude	Fraxinus_species	DBH (cm)	Tree_ID	Crown (m2)	Total Coverage (m2)	Total Coverage %
5	42.1671796	-84.1226471	FRAPEN	26.8	130	20.4		
5	42.1671796	-84.1226471	FRAPEN	18.3	131	12.0		
5	42.1671796	-84.1226471	FRAPEN	22.7	132	16.4		
5	42.1671796	-84.1226471	FRAPEN	30.8	133	24.4		
5	42.1671796	-84.1226471	FRAPEN	36.0	134	29.5		
6	42.1660906	-84.1233284	FRAPEN	26.7	135	20.3	1172.0	32.6%
6	42.1660906	-84.1233284	FRAPEN	18.8	136	12.5		
6	42.1660906	-84.1233284	FRAPEN	43.2	137	36.7		
6	42.1660906	-84.1233284	FRAPEN	49.1	138	42.5		
6	42.1660906	-84.1233284	FRAPEN	14.8	139	8.6		
6	42.1660906	-84.1233284	FRAPEN	24.0	140	17.7		
6	42.1660906	-84.1233284	FRAPEN	12.5	141	6.3		
6	42.1660906	-84.1233284	FRAPEN	14.1	142	7.9		
6	42.1660906	-84.1233284	FRAPEN	31.3	143	24.9		
6	42.1660906	-84.1233284	FRAPEN	28.8	144	22.4		
6	42.1660906	-84.1233284	FRAPEN	22.2	145	15.9		
6	42.1660906	-84.1233284	FRAPEN	20.3	146	14.0		
6	42.1660906	-84.1233284	FRAPEN	17.2	147	10.9		
6	42.1660906	-84.1233284	FRAPEN	23.9	148	17.6		
6	42.1660906	-84.1233284	FRAPEN	24.3	149	18.0		
6	42.1660906	-84.1233284	FRAPEN	20.0	150	13.7		
6	42.1660906	-84.1233284	FRAPEN	13.7	151	7.5		
6	42.1660906	-84.1233284	FRAPEN	25.8	152	19.4		
6	42.1660906	-84.1233284	FRAPEN	16.0	153	9.7		
6	42.1660906	-84.1233284	FRAPEN	23.3	154	17.0		
6	42.1660906	-84.1233284	FRAPEN	31.3	155	24.9		

Plot_number	Latitude	Longitude	Fraxinus_species	DBH (cm)	Tree_ID	Crown (m2)	Total Coverage (m2)	Total Coverage %
6	42.1660906	-84.1233284	FRAPEN	18.2	156	11.9		
6	42.1660906	-84.1233284	FRAPEN	28.5	157	22.1		
6	42.1660906	-84.1233284	FRAPEN	16.3	158	10.0		
6	42.1660906	-84.1233284	FRAPEN	21.3	159	15.0		
6	42.1660906	-84.1233284	FRAPEN	19.0	160	12.7		
6	42.1660906	-84.1233284	FRAPEN	16.6	161	10.3		
6	42.1660906	-84.1233284	FRAPEN	21.5	162	15.2		
6	42.1660906	-84.1233284	FRAPEN	15.8	163	9.5		
6	42.1660906	-84.1233284	FRAPEN	19.5	164	13.2		
6	42.1660906	-84.1233284	FRAPEN	14.0	165	7.8		
6	42.1660906	-84.1233284	FRAPEN	19.0	166	12.7		
6	42.1660906	-84.1233284	FRAPEN	22.4	167	16.1		
6	42.1660906	-84.1233284	FRAPEN	33.5	168	27.1		
6	42.1660906	-84.1233284	FRAPEN	35.7	169	29.2		
6	42.1660906	-84.1233284	FRAPEN	11.0	170	4.8		
6	42.1660906	-84.1233284	FRAPEN	15.5	171	9.2		
6	42.1660906	-84.1233284	FRAPEN	15.3	172	9.0		
6	42.1660906	-84.1233284	FRAPEN	10.8	173	4.6		
6	42.1660906	-84.1233284	FRAPEN	14.0	174	7.8		
6	42.1660906	-84.1233284	FRAPEN	24.0	175	17.7		
6	42.1660906	-84.1233284	FRAPEN	14.2	176	8.0		
6	42.1660906	-84.1233284	FRAPEN	23.5	177	17.2		
6	42.1660906	-84.1233284	FRAPEN	16.5	178	10.2		
6	42.1660906	-84.1233284	FRAPEN	27.6	179	21.2		
6	42.1660906	-84.1233284	FRAPEN	25.6	180	19.2		
6	42.1660906	-84.1233284	FRAPEN	20.9	181	14.6		

Plot_number	Latitude	Longitude	Fraxinus_species	DBH (cm)	Tree_ID	Crown (m2)	Total Coverage (m2)	Total Coverage %
6	42.1660906	-84.1233284	FRAPEN	24.1	182	17.8		
6	42.1660906	-84.1233284	FRAPEN	61.0	183	54.3		
6	42.1660906	-84.1233284	FRAPEN	35.4	184	28.9		
6	42.1660906	-84.1233284	FRAPEN	12.1	185	5.9		
6	42.1660906	-84.1233284	FRAPEN	21.0	186	14.7		
6	42.1660906	-84.1233284	FRAPEN	11.0	187	4.8		
6	42.1660906	-84.1233284	FRAPEN	16.0	188	9.7		
6	42.1660906	-84.1233284	FRAPEN	20.5	189	14.2		
6	42.1660906	-84.1233284	FRAPEN	17.1	190	10.8		
6	42.1660906	-84.1233284	FRAPEN	11.0	191	4.8		
6	42.1660906	-84.1233284	FRAPEN	11.4	192	5.2		
6	42.1660906	-84.1233284	FRAPEN	16.3	193	10.0		
6	42.1660906	-84.1233284	FRAPEN	14.3	194	8.1		
6	42.1660906	-84.1233284	FRAPEN	11.0	195	4.8		
6	42.1660906	-84.1233284	FRAPEN	14.3	196	8.1		
6	42.1660906	-84.1233284	FRAPEN	17.5	197	11.2		
6	42.1660906	-84.1233284	FRAPEN	11.3	198	5.1		
6	42.1660906	-84.1233284	FRAPEN	13.0	199	6.8		
6	42.1660906	-84.1233284	FRAPEN	14.8	200	8.6		
6	42.1660906	-84.1233284	FRAPEN	10.0	201	3.8		
6	42.1660906	-84.1233284	FRAPEN	30.3	202	23.9		
6	42.1660906	-84.1233284	FRAPEN	19.0	203	12.7		
6	42.1660906	-84.1233284	FRAPEN	19.5	204	13.2		
6	42.1660906	-84.1233284	FRAPEN	18.3	205	12.0		
6	42.1660906	-84.1233284	FRAPEN	38.4	206	31.9		
6	42.1660906	-84.1233284	FRAPEN	19.6	207	13.3		

Plot_number	Latitude	Longitude	Fraxinus_species	DBH (cm)	Tree_ID	Crown (m2)	Total Coverage (m2)	Total Coverage %
6	42.1660906	-84.1233284	FRAPEN	15.1	208	8.8		
6	42.1660906	-84.1233284	FRAPEN	19.8	209	13.5		
6	42.1660906	-84.1233284	FRAPEN	10.3	210	4.1		
6	42.1660906	-84.1233284	FRAPEN	33.5	211	27.1		
6	42.1660906	-84.1233284	FRAPEN	16.2	212	9.9		
6	42.1660906	-84.1233284	FRAPEN	22.2	213	15.9		
6	42.1660906	-84.1233284	FRAPEN	30.0	214	23.6		
7	42.1643793	-84.1242028	FRAPEN	33.0	215	26.6	431.9	12.0%
7	42.1643793	-84.1242028	FRAPEN	12.3	216	6.1		
7	42.1643793	-84.1242028	FRAPEN	13.7	217	7.5		
7	42.1643793	-84.1242028	FRAPEN	11.0	218	4.8		
7	42.1643793	-84.1242028	FRAPEN	18.7	219	12.4		
7	42.1643793	-84.1242028	FRAPEN	21.8	220	15.5		
7	42.1643793	-84.1242028	FRAPEN	14.5	221	8.3		
7	42.1643793	-84.1242028	FRAPEN	11.9	222	5.7		
7	42.1643793	-84.1242028	FRAPEN	14.0	223	7.8		
7	42.1643793	-84.1242028	FRAPEN	11.6	224	5.4		
7	42.1643793	-84.1242028	FRAPEN	17.4	225	11.1		
7	42.1643793	-84.1242028	FRAPEN	15.0	226	8.8		
7	42.1643793	-84.1242028	FRAPEN	15.5	227	9.2		
7	42.1643793	-84.1242028	FRAPEN	13.5	228	7.3		
7	42.1643793	-84.1242028	FRAPEN	15.9	229	9.6		
7	42.1643793	-84.1242028	FRAPEN	11.2	230	5.0		
7	42.1643793	-84.1242028	FRAPEN	33.9	231	27.5		
7	42.1643793	-84.1242028	FRAPEN	10.7	232	4.5		
7	42.1643793	-84.1242028	FRAPEN	10.4	233	4.2		

Plot_number	Latitude	Longitude	Fraxinus_species	DBH (cm)	Tree_ID	Crown (m2)	Total Coverage (m2)	Total Coverage %
7	42.1643793	-84.1242028	FRAPEN	10.5	234	4.3		
7	42.1643793	-84.1242028	FRAPEN	11.2	235	5.0		
7	42.1643793	-84.1242028	FRAPEN	16.0	236	9.7		
7	42.1643793	-84.1242028	FRAPEN	17.0	237	10.7		
7	42.1643793	-84.1242028	FRAPEN	10.1	238	3.9		
7	42.1643793	-84.1242028	FRAPEN	11.9	239	5.7		
7	42.1643793	-84.1242028	FRAPEN	16.9	240	10.6		
7	42.1643793	-84.1242028	FRAPEN	13.9	241	7.7		
7	42.1643793	-84.1242028	FRAPEN	21.3	242	15.0		
7	42.1643793	-84.1242028	FRAPEN	12.8	243	6.6		
7	42.1643793	-84.1242028	FRAPEN	20.8	244	14.5		
7	42.1643793	-84.1242028	FRAPEN	21.4	245	15.1		
7	42.1643793	-84.1242028	FRAPEN	14.4	246	8.2		
7	42.1643793	-84.1242028	FRAPEN	16.1	247	9.8		
7	42.1643793	-84.1242028	FRAPEN	10.1	248	3.9		
7	42.1643793	-84.1242028	FRAPEN	16.7	249	10.4		
7	42.1643793	-84.1242028	FRAPEN	24.2	250	17.9		
7	42.1643793	-84.1242028	FRAPEN	16.0	251	9.7		
7	42.1643793	-84.1242028	FRAPEN	10.8	252	4.6		
7	42.1643793	-84.1242028	FRAPEN	23.8	253	17.5		
7	42.1643793	-84.1242028	FRAPEN	23.6	254	17.3		
7	42.1643793	-84.1242028	FRAPEN	16.8	255	10.5		
7	42.1643793	-84.1242028	FRAPEN	22.0	256	15.7		
7	42.1643793	-84.1242028	FRAPEN	11.7	257	5.5		
7	42.1643793	-84.1242028	FRAPEN	11.4	258	5.2		
8	42.1712458	-84.1224862	FRAPEN	19.5	259	13.2	357.7	9.9%

Plot_number	Latitude	Longitude	Fraxinus_species	DBH (cm)	Tree_ID	Crown (m2)	Total Coverage (m2)	Total Coverage %
8	42.1712458	-84.1224862	FRAPEN	54.8	260	48.2		
8	42.1712458	-84.1224862	FRAPEN	35.0	261	28.6		
8	42.1712458	-84.1224862	FRAPEN	12.4	262	6.2		
8	42.1712458	-84.1224862	FRAPEN	27.0	263	20.6		
8	42.1712458	-84.1224862	FRAPEN	22.0	264	15.7		
8	42.1712458	-84.1224862	FRAPEN	41.2	265	34.7		
8	42.1712458	-84.1224862	FRAPEN	24.3	266	18.0		
8	42.1712458	-84.1224862	FRAPEN	42.8	267	36.3		
8	42.1712458	-84.1224862	FRAPEN	22.3	268	16.0		
8	42.1712458	-84.1224862	FRAPEN	35.8	269	29.3		
8	42.1712458	-84.1224862	FRAPEN	37.2	270	30.7		
8	42.1712458	-84.1224862	FRAPEN	43.5	271	37.0		
8	42.1712458	-84.1224862	FRAPEN	29.8	272	23.4		
9	42.1710044	-84.1205711	FRAPEN	20.0	273	13.7	877.4	24.4%
9	42.1710044	-84.1205711	FRAPEN	36.7	274	30.2		
9	42.1710044	-84.1205711	FRAPEN	14.4	275	8.2		
9	42.1710044	-84.1205711	FRAPEN	41.5	276	35.0		
9	42.1710044	-84.1205711	FRAPEN	18.3	277	12.0		
9	42.1710044	-84.1205711	FRAPEN	37.8	278	31.3		
9	42.1710044	-84.1205711	FRAPEN	50.0	279	43.4		
9	42.1710044	-84.1205711	FRAPEN	20.5	280	14.2		
9	42.1710044	-84.1205711	FRAPEN	21.0	281	14.7		
9	42.1710044	-84.1205711	FRAPEN	54.0	282	47.4		
9	42.1710044	-84.1205711	FRAPEN	37.5	283	31.0		
9	42.1710044	-84.1205711	FRAPEN	12.6	284	6.4		
9	42.1710044	-84.1205711	FRAPEN	23.5	285	17.2		

Plot_number	Latitude	Longitude	Fraxinus_species	DBH (cm)	Tree_ID	Crown (m2)	Total Coverage (m2)	Total Coverage %
9	42.1710044	-84.1205711	FRAPEN	13.3	286	7.1		
9	42.1710044	-84.1205711	FRAPEN	12.0	287	5.8		
9	42.1710044	-84.1205711	FRAPEN	14.6	288	8.4		
9	42.1710044	-84.1205711	FRAPEN	20.8	289	14.5		
9	42.1710044	-84.1205711	FRAPEN	23.3	290	17.0		
9	42.1710044	-84.1205711	FRAPEN	31.3	291	24.9		
9	42.1710044	-84.1205711	FRAPEN	16.9	292	10.6		
9	42.1710044	-84.1205711	FRAPEN	41.2	293	34.7		
9	42.1710044	-84.1205711	FRAPEN	31.8	294	25.4		
9	42.1710044	-84.1205711	FRAPEN	37.7	295	31.2		
9	42.1710044	-84.1205711	FRAPEN	20.2	296	13.9		
9	42.1710044	-84.1205711	FRAPEN	15.9	297	9.6		
9	42.1710044	-84.1205711	FRAPEN	14.5	298	8.3		
9	42.1710044	-84.1205711	FRAPEN	22.2	299	15.9		
9	42.1710044	-84.1205711	FRAPEN	24.4	300	18.1		
9	42.1710044	-84.1205711	FRAPEN	28.2	301	21.8		
9	42.1710044	-84.1205711	FRAPEN	21.6	302	15.3		
9	42.1710044	-84.1205711	FRAPEN	17.7	303	11.4		
9	42.1710044	-84.1205711	FRAPEN	15.9	304	9.6		
9	42.1710044	-84.1205711	FRAPEN	24.7	305	18.4		
9	42.1710044	-84.1205711	FRAPEN	13.0	306	6.8		
9	42.1710044	-84.1205711	FRAPEN	40.1	307	33.6		
9	42.1710044	-84.1205711	FRAPEN	53.5	308	46.9		
9	42.1710044	-84.1205711	FRAPEN	17.9	309	11.6		
9	42.1710044	-84.1205711	FRAPEN	19.5	310	13.2		
9	42.1710044	-84.1205711	FRAPEN	12.7	311	6.5		

Plot_number	Latitude	Longitude	Fraxinus_species	DBH (cm)	Tree_ID	Crown (m2)	Total Coverage (m2)	Total Coverage %
9	42.1710044	-84.1205711	FRAPEN	16.2	312	9.9		
9	42.1710044	-84.1205711	FRAPEN	14.3	313	8.1		
9	42.1710044	-84.1205711	FRAPEN	21.9	314	15.6		
9	42.1710044	-84.1205711	FRAPEN	12.9	315	6.7		
9	42.1710044	-84.1205711	FRAPEN	33.6	316	27.2		
9	42.1710044	-84.1205711	FRAPEN	20.4	317	14.1		
9	42.1710044	-84.1205711	FRAPEN	57.7	318	51.0		
10	42.1709829	-84.1209627	FRAPEN	13.6	319	7.4	1051.8	29.2%
10	42.1709829	-84.1209627	FRAPEN	29.6	320	23.2		
10	42.1709829	-84.1209627	FRAPEN	19.1	321	12.8		
10	42.1709829	-84.1209627	FRAPEN	16.8	322	10.5		
10	42.1709829	-84.1209627	FRAPEN	49.3	323	42.7		
10	42.1709829	-84.1209627	FRAPEN	19.4	324	13.1		
10	42.1709829	-84.1209627	FRAPEN	35.2	325	28.7		
10	42.1709829	-84.1209627	FRAPEN	47.8	326	41.2		
10	42.1709829	-84.1209627	FRAPEN	38.5	327	32.0		
10	42.1709829	-84.1209627	FRAPEN	23.2	328	16.9		
10	42.1709829	-84.1209627	FRAPEN	11.5	329	5.3		
10	42.1709829	-84.1209627	FRAPEN	11.0	330	4.8		
10	42.1709829	-84.1209627	FRAPEN	11.6	331	5.4		
10	42.1709829	-84.1209627	FRAPEN	27.8	332	21.4		
10	42.1709829	-84.1209627	FRAPEN	32.4	333	26.0		
10	42.1709829	-84.1209627	FRAPEN	49.7	334	43.1		
10	42.1709829	-84.1209627	FRAPEN	15.0	335	8.8		
10	42.1709829	-84.1209627	FRAPEN	14.5	336	8.3		
10	42.1709829	-84.1209627	FRAPEN	23.1	337	16.8		

Plot_number	Latitude	Longitude	Fraxinus_species	DBH (cm)	Tree_ID	Crown (m2)	Total Coverage (m2)	Total Coverage %
10	42.1709829	-84.1209627	FRAPEN	32.0	338	25.6		
10	42.1709829	-84.1209627	FRAPEN	22.0	339	15.7		
10	42.1709829	-84.1209627	FRAPEN	29.1	340	22.7		
10	42.1709829	-84.1209627	FRAPEN	16.0	341	9.7		
10	42.1709829	-84.1209627	FRAPEN	37.7	342	31.2		
10	42.1709829	-84.1209627	FRAPEN	16.1	343	9.8		
10	42.1709829	-84.1209627	FRAPEN	16.0	344	9.7		
10	42.1709829	-84.1209627	FRAPEN	28.0	345	21.6		
10	42.1709829	-84.1209627	FRAPEN	20.0	346	13.7		
10	42.1709829	-84.1209627	FRAPEN	19.5	347	13.2		
10	42.1709829	-84.1209627	FRAPEN	21.4	348	15.1		
10	42.1709829	-84.1209627	FRAPEN	69.6	349	62.8		
10	42.1709829	-84.1209627	FRAPEN	14.7	350	8.5		
10	42.1709829	-84.1209627	FRAPEN	10.2	351	4.0		
10	42.1709829	-84.1209627	FRAPEN	19.9	352	13.6		
10	42.1709829	-84.1209627	FRAPEN	18.3	353	12.0		
10	42.1709829	-84.1209627	FRAPEN	14.4	354	8.2		
10	42.1709829	-84.1209627	FRAPEN	16.4	355	10.1		
10	42.1709829	-84.1209627	FRAPEN	22.9	356	16.6		
10	42.1709829	-84.1209627	FRAPEN	21.3	357	15.0		
10	42.1709829	-84.1209627	FRAPEN	13.5	358	7.3		
10	42.1709829	-84.1209627	FRAPEN	21.3	359	15.0		
10	42.1709829	-84.1209627	FRAPEN	30.8	360	24.4		
10	42.1709829	-84.1209627	FRAPEN	15.5	361	9.2		
10	42.1709829	-84.1209627	FRAPEN	16.6	362	10.3		
10	42.1709829	-84.1209627	FRAPEN	12.5	363	6.3		

Plot_number	Latitude	Longitude	Fraxinus_species	DBH (cm)	Tree_ID	Crown (m2)	Total Coverage (m2)	Total Coverage %
10	42.1709829	-84.1209627	FRAPEN	14.8	364	8.6		
10	42.1709829	-84.1209627	FRAPEN	41.4	365	34.9		
10	42.1709829	-84.1209627	FRAPEN	35.8	366	29.3		
10	42.1709829	-84.1209627	FRAPEN	17.5	367	11.2		
10	42.1709829	-84.1209627	FRAPEN	26.6	368	20.2		
10	42.1709829	-84.1209627	FRAPEN	18.1	369	11.8		
10	42.1709829	-84.1209627	FRAPEN	10.8	370	4.6		
10	42.1709829	-84.1209627	FRAPEN	16.5	371	10.2		
10	42.1709829	-84.1209627	FRAPEN	11.7	372	5.5		
10	42.1709829	-84.1209627	FRAPEN	17.8	373	11.5		
10	42.1709829	-84.1209627	FRAPEN	12.1	374	5.9		
10	42.1709829	-84.1209627	FRAPEN	23.5	375	17.2		
10	42.1709829	-84.1209627	FRAPEN	18.5	376	12.2		
10	42.1709829	-84.1209627	FRAPEN	23.3	377	17.0		
10	42.1709829	-84.1209627	FRAPEN	25.1	378	18.7		
10	42.1709829	-84.1209627	FRAPEN	45.9	379	39.3		
10	42.1709829	-84.1209627	FRAPEN	20.2	380	13.9		
11	42.1734935	-84.1196430	FRAPEN	19.5	381	13.2	2401.4	66.7%
11	42.1734935	-84.1196430	FRAPEN	33.0	382	26.6		
11	42.1734935	-84.1196430	FRAPEN	34.7	383	28.3		
11	42.1734935	-84.1196430	FRAPEN	38.7	384	32.2		
11	42.1734935	-84.1196430	FRAPEN	30.2	385	23.8		
11	42.1734935	-84.1196430	FRAPEN	22.2	386	15.9		
11	42.1734935	-84.1196430	FRAPEN	12.1	387	5.9		
11	42.1734935	-84.1196430	FRAPEN	26.9	388	20.5		
11	42.1734935	-84.1196430	FRAPEN	16.7	389	10.4		

Plot_number	Latitude	Longitude	Fraxinus_species	DBH (cm)	Tree_ID	Crown (m2)	Total Coverage (m2)	Total Coverage %
11	42.1734935	-84.1196430	FRAPEN	32.9	390	26.5		
11	42.1734935	-84.1196430	FRAPEN	33.2	391	26.8		
11	42.1734935	-84.1196430	FRAPEN	33.2	392	26.8		
11	42.1734935	-84.1196430	FRAPEN	17.9	393	11.6		
11	42.1734935	-84.1196430	FRAPEN	22.8	394	16.5		
11	42.1734935	-84.1196430	FRAPEN	16.7	395	10.4		
11	42.1734935	-84.1196430	FRAPEN	18.8	396	12.5		
11	42.1734935	-84.1196430	FRAPEN	41.1	397	34.6		
11	42.1734935	-84.1196430	FRAPEN	25.0	398	18.7		
11	42.1734935	-84.1196430	FRAPEN	32.9	399	26.5		
11	42.1734935	-84.1196430	FRAPEN	21.7	400	15.4		
11	42.1734935	-84.1196430	FRAPEN	32.0	401	25.6		
11	42.1734935	-84.1196430	FRAPEN	19.0	402	12.7		
11	42.1734935	-84.1196430	FRAPEN	17.3	403	11.0		
11	42.1734935	-84.1196430	FRAPEN	59.8	404	53.1		
11	42.1734935	-84.1196430	FRAPEN	34.7	405	28.3		
11	42.1734935	-84.1196430	FRAPEN	20.3	406	14.0		
11	42.1734935	-84.1196430	FRAPEN	62.0	407	55.3		
11	42.1734935	-84.1196430	FRAPEN	29.9	408	23.5		
11	42.1734935	-84.1196430	FRAPEN	20.3	409	14.0		
11	42.1734935	-84.1196430	FRAPEN	14.2	410	8.0		
11	42.1734935	-84.1196430	FRAPEN	30.8	411	24.4		
11	42.1734935	-84.1196430	FRAPEN	17.0	412	10.7		
11	42.1734935	-84.1196430	FRAPEN	34.0	413	27.6		
11	42.1734935	-84.1196430	FRAPEN	33.7	414	27.3		
11	42.1734935	-84.1196430	FRAPEN	36.0	415	29.5		

Plot_number	Latitude	Longitude	Fraxinus_species	DBH (cm)	Tree_ID	Crown (m2)	Total Coverage (m2)	Total Coverage %
11	42.1734935	-84.1196430	FRAPEN	14.1	416	7.9		
11	42.1734935	-84.1196430	FRAPEN	12.5	417	6.3		
11	42.1734935	-84.1196430	FRAPEN	41.7	418	35.2		
11	42.1734935	-84.1196430	FRAPEN	27.7	419	21.3		
11	42.1734935	-84.1196430	FRAPEN	22.8	420	16.5		
11	42.1734935	-84.1196430	FRAPEN	33.8	421	27.4		
11	42.1734935	-84.1196430	FRAPEN	47.7	422	41.1		
11	42.1734935	-84.1196430	FRAPEN	20.5	423	14.2		
11	42.1734935	-84.1196430	FRAPEN	20.9	424	14.6		
11	42.1734935	-84.1196430	FRAPEN	26.7	425	20.3		
11	42.1734935	-84.1196430	FRAPEN	15.7	426	9.4		
11	42.1734935	-84.1196430	FRAPEN	40.1	427	33.6		
11	42.1734935	-84.1196430	FRAPEN	21.2	428	14.9		
11	42.1734935	-84.1196430	FRAPEN	32.6	429	26.2		
11	42.1734935	-84.1196430	FRAPEN	28.3	430	21.9		
11	42.1734935	-84.1196430	FRAPEN	11.7	431	5.5		
11	42.1734935	-84.1196430	FRAPEN	25.2	432	18.8		
11	42.1734935	-84.1196430	FRAPEN	33.0	433	26.6		
11	42.1734935	-84.1196430	FRAPEN	40.7	434	34.2		
11	42.1734935	-84.1196430	FRAPEN	26.5	435	20.1		
11	42.1734935	-84.1196430	FRAPEN	27.9	436	21.5		
11	42.1734935	-84.1196430	FRAPEN	20.4	437	14.1		
11	42.1734935	-84.1196430	FRAPEN	40.2	438	33.7		
11	42.1734935	-84.1196430	FRAPEN	11.4	439	5.2		
11	42.1734935	-84.1196430	FRAPEN	18.0	440	11.7		
11	42.1734935	-84.1196430	FRAPEN	37.8	441	31.3		

Plot_number	Latitude	Longitude	Fraxinus_species	DBH (cm)	Tree_ID	Crown (m2)	Total Coverage (m2)	Total Coverage %
11	42.1734935	-84.1196430	FRAPEN	38.0	442	31.5		
11	42.1734935	-84.1196430	FRAPEN	10.2	443	4.0		
11	42.1734935	-84.1196430	FRAPEN	13.8	444	7.6		
11	42.1734935	-84.1196430	FRAPEN	22.7	445	16.4		
11	42.1734935	-84.1196430	FRAPEN	16.1	446	9.8		
11	42.1734935	-84.1196430	FRAPEN	36.4	447	29.9		
11	42.1734935	-84.1196430	FRAPEN	25.8	448	19.4		
11	42.1734935	-84.1196430	FRAPEN	16.0	449	9.7		
11	42.1734935	-84.1196430	FRAPEN	10.8	450	4.6		
11	42.1734935	-84.1196430	FRAPEN	14.2	451	8.0		
11	42.1734935	-84.1196430	FRAPEN	15.4	452	9.1		
11	42.1734935	-84.1196430	FRAPEN	36.5	453	30.0		
11	42.1734935	-84.1196430	FRAPEN	39.4	454	32.9		
11	42.1734935	-84.1196430	FRAPEN	15.2	455	8.9		
11	42.1734935	-84.1196430	FRAPEN	14.4	456	8.2		
11	42.1734935	-84.1196430	FRAPEN	23.1	457	16.8		
11	42.1734935	-84.1196430	FRAPEN	31.1	458	24.7		
11	42.1734935	-84.1196430	FRAPEN	26.9	459	20.5		
11	42.1734935	-84.1196430	FRAPEN	14.2	460	8.0		
11	42.1734935	-84.1196430	FRAPEN	32.2	461	25.8		
11	42.1734935	-84.1196430	FRAPEN	14.5	462	8.3		
11	42.1734935	-84.1196430	FRAPEN	13.6	463	7.4		
11	42.1734935	-84.1196430	FRAPEN	11.9	464	5.7		
11	42.1734935	-84.1196430	FRAPEN	21.0	465	14.7		
11	42.1734935	-84.1196430	FRAPEN	21.9	466	15.6		
11	42.1734935	-84.1196430	FRAPEN	32.6	467	26.2		

Plot_number	Latitude	Longitude	Fraxinus_species	DBH (cm)	Tree_ID	Crown (m2)	Total Coverage (m2)	Total Coverage %
11	42.1734935	-84.1196430	FRAPEN	31.7	468	25.3		
11	42.1734935	-84.1196430	FRAPEN	11.9	469	5.7		
11	42.1734935	-84.1196430	FRAPEN	38.2	470	31.7		
11	42.1734935	-84.1196430	FRAPEN	41.8	471	35.3		
11	42.1734935	-84.1196430	FRAPEN	16.4	472	10.1		
11	42.1734935	-84.1196430	FRAPEN	13.9	473	7.7		
11	42.1734935	-84.1196430	FRAPEN	22.5	474	16.2		
11	42.1734935	-84.1196430	FRAPEN	20.4	475	14.1		
11	42.1734935	-84.1196430	FRAPEN	32.5	476	26.1		
11	42.1734935	-84.1196430	FRAPEN	38.2	477	31.7		
11	42.1734935	-84.1196430	FRAPEN	14.7	478	8.5		
11	42.1734935	-84.1196430	FRAPEN	31.1	479	24.7		
11	42.1734935	-84.1196430	FRAPEN	14.9	480	8.7		
11	42.1734935	-84.1196430	FRAPEN	26.8	481	20.4		
11	42.1734935	-84.1196430	FRAPEN	15.9	482	9.6		
11	42.1734935	-84.1196430	FRAPEN	27.2	483	20.8		
11	42.1734935	-84.1196430	FRAPEN	17.5	484	11.2		
11	42.1734935	-84.1196430	FRAPEN	29.8	485	23.4		
11	42.1734935	-84.1196430	FRAPEN	43.1	486	36.6		
11	42.1734935	-84.1196430	FRAPEN	42.7	487	36.2		
11	42.1734935	-84.1196430	FRAPEN	30.9	488	24.5		
11	42.1734935	-84.1196430	FRAPEN	35.1	489	28.6		
11	42.1734935	-84.1196430	FRAPEN	33.9	490	27.5		
11	42.1734935	-84.1196430	FRAPEN	22.2	491	15.9		
11	42.1734935	-84.1196430	FRAPEN	25.3	492	18.9		
11	42.1734935	-84.1196430	FRAPEN	20.2	493	13.9		

Plot_number	Latitude	Longitude	Fraxinus_species	DBH (cm)	Tree_ID	Crown (m2)	Total Coverage (m2)	Total Coverage %
11	42.1734935	-84.1196430	FRAPEN	58.1	494	51.4		
11	42.1734935	-84.1196430	FRAPEN	53.2	495	46.6		
11	42.1734935	-84.1196430	FRAPEN	47.0	496	40.4		
11	42.1734935	-84.1196430	FRAPEN	25.5	497	19.1		
11	42.1734935	-84.1196430	FRAPEN	11.9	498	5.7		
12	42.1772861	-84.1300178	NOASH				0.0	0.0%
13	42.1757036	-84.1284889	NOASH				0.0	0.0%
14	42.1757036	-84.1284889	NOASH				0.0	0.0%
15	42.1752047	-84.1269976	NOASH				0.0	0.0%
16	42.1748131	-84.1306132	NOASH				0.0	0.0%
17	42.1743786	-84.1276789	FRAAME	24.0	499	17.7	17.7	0.5%
18	42.1742123	-84.1261822	NOASH				0.0	0.0%
19	42.1742123	-84.1261822	FRAPEN	12.2	500	6.0	6.0	0.2%
20	42.1748882	-84.1255492	FRAPEN	22.1	501	15.8	94.7	2.6%
20	42.1748882	-84.1255492	FRAPEN	12.6	502	6.4		
20	42.1748882	-84.1255492	FRAPEN	10.2	503	4.0		
20	42.1748882	-84.1255492	FRAPEN	29.8	504	23.4		
20	42.1748882	-84.1255492	FRAPEN	10.9	505	4.7		
20	42.1748882	-84.1255492	FRAPEN	20.4	506	14.1		
20	42.1748882	-84.1255492	FRAPEN	32.8	507	26.4		
21	42.1747112	-84.1248304	FRAPEN	68.8	508	62.0	569.0	15.8%
21	42.1747112	-84.1248304	FRAPEN	15.9	509	9.6		
21	42.1747112	-84.1248304	FRAPEN	19.0	510	12.7		
21	42.1747112	-84.1248304	FRAPEN	40.5	511	34.0		
21	42.1747112	-84.1248304	FRAPEN	40.1	512	33.6		
21	42.1747112	-84.1248304	FRAPEN	25.5	513	19.1		

Plot_number	Latitude	Longitude	Fraxinus_species	DBH (cm)	Tree_ID	Crown (m2)	Total Coverage (m2)	Total Coverage %
21	42.1747112	-84.1248304	FRAPEN	23.0	514	16.7		
21	42.1747112	-84.1248304	FRAPEN	36.6	515	30.1		
21	42.1747112	-84.1248304	FRANIG	17.3	516	11.0		
21	42.1747112	-84.1248304	FRANIG	18.5	517	12.2		
21	42.1747112	-84.1248304	FRANIG	36.6	518	30.1		
21	42.1747112	-84.1248304	FRANIG	12.3	519	6.1		
21	42.1747112	-84.1248304	FRANIG	11.2	520	5.0		
21	42.1747112	-84.1248304	FRANIG	31.3	521	24.9		
21	42.1747112	-84.1248304	FRANIG	21.0	522	14.7		
21	42.1747112	-84.1248304	FRANIG	34.0	523	27.6		
21	42.1747112	-84.1248304	FRANIG	26.6	524	20.2		
21	42.1747112	-84.1248304	FRANIG	12.6	525	6.4		
21	42.1747112	-84.1248304	FRANIG	10.4	526	4.2		
21	42.1747112	-84.1248304	FRANIG	37.6	527	31.1		
21	42.1747112	-84.1248304	FRANIG	28.9	528	22.5		
21	42.1747112	-84.1248304	FRANIG	17.9	529	11.6		
21	42.1747112	-84.1248304	FRANIG	34.8	530	28.4		
21	42.1747112	-84.1248304	FRANIG	12.6	531	6.4		
21	42.1747112	-84.1248304	FRANIG	13.8	532	7.6		
21	42.1747112	-84.1248304	FRANIG	13.5	533	7.3		
21	42.1747112	-84.1248304	FRANIG	12.7	534	6.5		
21	42.1747112	-84.1248304	FRANIG	28.1	535	21.7		
21	42.1747112	-84.1248304	FRANIG	28.0	536	21.6		
21	42.1747112	-84.1248304	FRANIG	30.5	537	24.1		
22	42.1741694	-84.1248197	FRAPEN	34.6	538	28.2	213.6	5.9%
22	42.1741694	-84.1248197	FRAPEN	31.5	539	25.1		

Plot_number	Latitude	Longitude	Fraxinus_species	DBH (cm)	Tree_ID	Crown (m2)	Total Coverage (m2)	Total Coverage %
22	42.1741694	-84.1248197	FRAPEN	28.6	540	22.2		
22	42.1741694	-84.1248197	FRAPEN	30.4	541	24.0		
22	42.1741694	-84.1248197	FRAPEN	30.0	542	23.6		
22	42.1741694	-84.1248197	FRAPEN	25.0	543	18.7		
22	42.1741694	-84.1248197	FRAPEN	11.7	544	5.5		
22	42.1741694	-84.1248197	FRAPEN	14.1	545	7.9		
22	42.1741694	-84.1248197	FRAPEN	18.3	546	12.0		
22	42.1741694	-84.1248197	FRAPEN	19.9	547	13.6		
22	42.1741694	-84.1248197	FRAPEN	19.4	548	13.1		
22	42.1741694	-84.1248197	FRAPEN	26.2	549	19.8		
23	42.1741694	-84.1248197	FRAPEN	38.8	550	32.3	370.6	10.3%
23	42.1741694	-84.1248197	FRAPEN	18.3	551	12.0		
23	42.1741694	-84.1248197	FRAPEN	25.3	552	18.9		
23	42.1741694	-84.1248197	FRAPEN	48.8	553	42.2		
23	42.1741694	-84.1248197	FRAPEN	12.3	554	6.1		
23	42.1741694	-84.1248197	FRAPEN	17.4	555	11.1		
23	42.1741694	-84.1248197	FRAPEN	25.3	556	18.9		
23	42.1741694	-84.1248197	FRAPEN	19.5	557	13.2		
23	42.1741694	-84.1248197	FRAPEN	27.4	558	21.0		
23	42.1741694	-84.1248197	FRAPEN	21.0	559	14.7		
23	42.1741694	-84.1248197	FRAPEN	20.0	560	13.7		
23	42.1741694	-84.1248197	FRAPEN	19.8	561	13.5		
23	42.1741694	-84.1248197	FRAPEN	47.2	562	40.6		
23	42.1741694	-84.1248197	FRAPEN	25.5	563	19.1		
23	42.1741694	-84.1248197	FRAPEN	16.1	564	9.8		
23	42.1741694	-84.1248197	FRAPEN	22.5	565	16.2		

Plot_number	Latitude	Longitude	Fraxinus_species	DBH (cm)	Tree_ID	Crown (m2)	Total Coverage (m2)	Total Coverage %
23	42.1741694	-84.1248197	FRAPEN	15.6	566	9.3		
23	42.1741694	-84.1248197	FRAPEN	20.0	567	13.7		
23	42.1741694	-84.1248197	FRAPEN	17.0	568	10.7		
23	42.1741694	-84.1248197	FRAPEN	26.7	569	20.3		
23	42.1741694	-84.1248197	FRAPEN	19.2	570	12.9		
24	42.1741694	-84.1248197	FRAPEN	22.7	571	16.4	73.6	2.0%
24	42.1741694	-84.1248197	FRAPEN	34.7	572	28.3		
24	42.1741694	-84.1248197	FRAPEN	35.4	573	28.9		
25	42.1799844	-84.1294009	NOASH				0.0	0.0%
26	42.1797484	-84.1280008	NOASH				0.0	0.0%
27	42.1797967	-84.1257531	NOASH				0.0	0.0%
28	42.1803814	-84.1243154	NOASH				0.0	0.0%
29	42.1817976	-84.1218532	NOASH				0.0	0.0%
30	42.1810037	-84.1215152	NOASH				0.0	0.0%
31	42.1810037	-84.1215152	NOASH				0.0	0.0%
32	42.1810412	-84.1192836	NOASH				0.0	0.0%
33	42.1805691	-84.1174436	NOASH				0.0	0.0%
34	42.1817064	-84.1172183	NOASH				0.0	0.0%
35	42.1800649	-84.1181946	FRAPEN	45.0	574	38.5	182.7	5.1%
35	42.1800649	-84.1181946	FRAPEN	50.4	575	43.8		
35	42.1800649	-84.1181946	FRAPEN	47.7	576	41.1		
35	42.1800649	-84.1181946	FRAPEN	25.0	577	18.7		
35	42.1800649	-84.1181946	FRAPEN	47.3	578	40.7		
36	42.1791047	-84.1210324	NOASH				0.0	0.0%
37	42.1792710	-84.1214133	NOASH				0.0	0.0%
38	42.1792710	-84.1214133	FRAPEN	19.3	579	13.0	145.3	4.0%

Plot_number	Latitude	Longitude	Fraxinus_species	DBH (cm)	Tree_ID	Crown (m2)	Total Coverage (m2)	Total Coverage %
38	42.1792710	-84.1214133	FRAPEN	10.5	580	4.3		
38	42.1792710	-84.1214133	FRAPEN	15.1	581	8.8		
38	42.1792710	-84.1214133	FRAPEN	22.3	582	16.0		
38	42.1792710	-84.1214133	FRAPEN	13.2	583	7.0		
38	42.1792710	-84.1214133	FRAPEN	20.3	584	14.0		
38	42.1792710	-84.1214133	FRAPEN	23.0	585	16.7		
38	42.1792710	-84.1214133	FRAPEN	12.1	586	5.9		
38	42.1792710	-84.1214133	FRAPEN	33.1	587	26.7		
38	42.1792710	-84.1214133	FRAPEN	19.5	588	13.2		
38	42.1792710	-84.1214133	FRAPEN	26.1	589	19.7		
39	42.1784824	-84.1220463	NOASH				0.0	0.0%
40	42.1782088	-84.1231782	NOASH				0.0	0.0%
41	42.1769482	-84.1230816	NOASH				0.0	0.0%
42	42.1769911	-84.1202224	FRAPEN	36.0	590	29.5	265.9	7.4%
42	42.1769911	-84.1202224	FRAPEN	29.6	591	23.2		
42	42.1769911	-84.1202224	FRAPEN	32.1	592	25.7		
42	42.1769911	-84.1202224	FRAPEN	25.7	593	19.3		
42	42.1769911	-84.1202224	FRAPEN	10.2	594	4.0		
42	42.1769911	-84.1202224	FRAPEN	11.4	595	5.2		
42	42.1769911	-84.1202224	FRAPEN	10.3	596	4.1		
42	42.1769911	-84.1202224	FRAPEN	20.2	597	13.9		
42	42.1769911	-84.1202224	FRAPEN	19.5	598	13.2		
42	42.1769911	-84.1202224	FRAPEN	42.7	599	36.2		
42	42.1769911	-84.1202224	FRAPEN	36.6	600	30.1		
42	42.1769911	-84.1202224	FRAPEN	41.8	601	35.3		
42	42.1769911	-84.1202224	FRAPEN	21.9	602	15.6		

Plot_number	Latitude	Longitude	Fraxinus_species	DBH (cm)	Tree_ID	Crown (m2)	Total Coverage (m2)	Total Coverage %
42	42.1769911	-84.1202224	FRAPEN	16.8	603	10.5		
43	42.1769911	-84.1202224	FRAPEN	14.6	604	8.4	741.0	20.6%
43	42.1769911	-84.1202224	FRAPEN	17.0	605	10.7		
43	42.1769911	-84.1202224	FRAPEN	22.5	606	16.2		
43	42.1769911	-84.1202224	FRAPEN	14.2	607	8.0		
43	42.1769911	-84.1202224	FRAPEN	50.4	608	43.8		
43	42.1769911	-84.1202224	FRAPEN	15.8	609	9.5		
43	42.1769911	-84.1202224	FRAPEN	22.1	610	15.8		
43	42.1769911	-84.1202224	FRAPEN	24.1	611	17.8		
43	42.1769911	-84.1202224	FRAPEN	23.4	612	17.1		
43	42.1769911	-84.1202224	FRAPEN	14.4	613	8.2		
43	42.1769911	-84.1202224	FRAPEN	10.5	614	4.3		
43	42.1769911	-84.1202224	FRAPEN	16.5	615	10.2		
43	42.1769911	-84.1202224	FRAPEN	23.0	616	16.7		
43	42.1769911	-84.1202224	FRAPEN	10.1	617	3.9		
43	42.1769911	-84.1202224	FRAPEN	16.8	618	10.5		
43	42.1769911	-84.1202224	FRAPEN	19.6	619	13.3		
43	42.1769911	-84.1202224	FRAPEN	14.4	620	8.2		
43	42.1769911	-84.1202224	FRAPEN	12.0	621	5.8		
43	42.1769911	-84.1202224	FRAPEN	20.1	622	13.8		
43	42.1769911	-84.1202224	FRAPEN	19.0	623	12.7		
43	42.1769911	-84.1202224	FRAPEN	30.5	624	24.1		
43	42.1769911	-84.1202224	FRAPEN	27.6	625	21.2		
43	42.1769911	-84.1202224	FRAPEN	15.9	626	9.6		
43	42.1769911	-84.1202224	FRAPEN	13.0	627	6.8		
43	42.1769911	-84.1202224	FRAPEN	15.0	628	8.8		

Plot_number	Latitude	Longitude	Fraxinus_species	DBH (cm)	Tree_ID	Crown (m2)	Total Coverage (m2)	Total Coverage %
43	42.1769911	-84.1202224	FRAPEN	17.9	629	11.6		
43	42.1769911	-84.1202224	FRAPEN	11.0	630	4.8		
43	42.1769911	-84.1202224	FRAPEN	11.5	631	5.3		
43	42.1769911	-84.1202224	FRAPEN	17.5	632	11.2		
43	42.1769911	-84.1202224	FRAPEN	16.9	633	10.6		
43	42.1769911	-84.1202224	FRAPEN	15.8	634	9.5		
43	42.1769911	-84.1202224	FRAPEN	35.1	635	28.6		
43	42.1769911	-84.1202224	FRAPEN	18.9	636	12.6		
43	42.1769911	-84.1202224	FRAPEN	14.3	637	8.1		
43	42.1769911	-84.1202224	FRAPEN	12.9	638	6.7		
43	42.1769911	-84.1202224	FRAPEN	14.7	639	8.5		
43	42.1769911	-84.1202224	FRAPEN	13.9	640	7.7		
43	42.1769911	-84.1202224	FRAPEN	12.2	641	6.0		
43	42.1769911	-84.1202224	FRAPEN	18.7	642	12.4		
43	42.1769911	-84.1202224	FRAPEN	12.0	643	5.8		
43	42.1769911	-84.1202224	FRAPEN	22.0	644	15.7		
43	42.1769911	-84.1202224	FRAPEN	19.3	645	13.0		
43	42.1769911	-84.1202224	FRAPEN	14.8	646	8.6		
43	42.1769911	-84.1202224	FRAPEN	18.3	647	12.0		
43	42.1769911	-84.1202224	FRAPEN	14.4	648	8.2		
43	42.1769911	-84.1202224	FRAPEN	14.1	649	7.9		
43	42.1769911	-84.1202224	FRAPEN	11.9	650	5.7		
43	42.1769911	-84.1202224	FRAPEN	19.0	651	12.7		
43	42.1769911	-84.1202224	FRAPEN	17.1	652	10.8		
43	42.1769911	-84.1202224	FRAPEN	23.5	653	17.2		
43	42.1769911	-84.1202224	FRAPEN	16.0	654	9.7		

Plot_number	Latitude	Longitude	Fraxinus_species	DBH (cm)	Tree_ID	Crown (m2)	Total Coverage (m2)	Total Coverage %
43	42.1769911	-84.1202224	FRAPEN	15.0	655	8.8		
43	42.1769911	-84.1202224	FRAPEN	12.5	656	6.3		
43	42.1769911	-84.1202224	FRAPEN	13.6	657	7.4		
43	42.1769911	-84.1202224	FRAPEN	15.0	658	8.8		
43	42.1769911	-84.1202224	FRAPEN	10.8	659	4.6		
43	42.1769911	-84.1202224	FRAPEN	11.0	660	4.8		
43	42.1769911	-84.1202224	FRAPEN	21.5	661	15.2		
43	42.1769911	-84.1202224	FRAPEN	19.5	662	13.2		
43	42.1769911	-84.1202224	FRAPEN	18.2	663	11.9		
43	42.1769911	-84.1202224	FRAPEN	16.2	664	9.9		
43	42.1769911	-84.1202224	FRAPEN	15.6	665	9.3		
43	42.1769911	-84.1202224	FRAPEN	19.8	666	13.5		
43	42.1769911	-84.1202224	FRAPEN	14.2	667	8.0		
43	42.1769911	-84.1202224	FRAPEN	12.5	668	6.3		
43	42.1769911	-84.1202224	FRAPEN	13.6	669	7.4		
43	42.1769911	-84.1202224	FRAPEN	11.5	670	5.3		
43	42.1769911	-84.1202224	FRAPEN	10.8	671	4.6		
44	42.1767336	-84.1208500	FRAPEN	33.1	672	26.7	971.8	27.0%
44	42.1767336	-84.1208500	FRAPEN	29.1	673	22.7		
44	42.1767336	-84.1208500	FRAPEN	17.1	674	10.8		
44	42.1767336	-84.1208500	FRAPEN	11.1	675	4.9		
44	42.1767336	-84.1208500	FRAPEN	16.1	676	9.8		
44	42.1767336	-84.1208500	FRAPEN	17.8	677	11.5		
44	42.1767336	-84.1208500	FRAPEN	12.8	678	6.6		
44	42.1767336	-84.1208500	FRAPEN	18.2	679	11.9		
44	42.1767336	-84.1208500	FRAPEN	33.8	680	27.4		

Plot_number	Latitude	Longitude	Fraxinus_species	DBH (cm)	Tree_ID	Crown (m2)	Total Coverage (m2)	Total Coverage %
44	42.1767336	-84.1208500	FRAPEN	30.1	681	23.7		
44	42.1767336	-84.1208500	FRAPEN	81.7	682	74.8		
44	42.1767336	-84.1208500	FRAPEN	36.1	683	29.6		
44	42.1767336	-84.1208500	FRAPEN	11.7	684	5.5		
44	42.1767336	-84.1208500	FRAPEN	46.1	685	39.5		
44	42.1767336	-84.1208500	FRAPEN	23.8	686	17.5		
44	42.1767336	-84.1208500	FRAPEN	19.5	687	13.2		
44	42.1767336	-84.1208500	FRAPEN	38.5	688	32.0		
44	42.1767336	-84.1208500	FRAPEN	47.4	689	40.8		
44	42.1767336	-84.1208500	FRAPEN	11.2	690	5.0		
44	42.1767336	-84.1208500	FRAPEN	34.5	691	28.1		
44	42.1767336	-84.1208500	FRAPEN	62.0	692	55.3		
44	42.1767336	-84.1208500	FRAPEN	31.2	693	24.8		
44	42.1767336	-84.1208500	FRAPEN	60.5	694	53.8		
44	42.1767336	-84.1208500	FRAPEN	21.4	695	15.1		
44	42.1767336	-84.1208500	FRAPEN	19.3	696	13.0		
44	42.1767336	-84.1208500	FRAPEN	15.2	697	8.9		
44	42.1767336	-84.1208500	FRAPEN	31.3	698	24.9		
44	42.1767336	-84.1208500	FRAPEN	23.7	699	17.4		
44	42.1767336	-84.1208500	FRAPEN	40.5	700	34.0		
44	42.1767336	-84.1208500	FRAPEN	34.1	701	27.7		
44	42.1767336	-84.1208500	FRAPEN	30.0	702	23.6		
44	42.1767336	-84.1208500	FRAPEN	27.7	703	21.3		
44	42.1767336	-84.1208500	FRAPEN	22.5	704	16.2		
44	42.1767336	-84.1208500	FRAPEN	33.6	705	27.2		
44	42.1767336	-84.1208500	FRAPEN	25.0	706	18.7		

Plot_number	Latitude	Longitude	Fraxinus_species	DBH (cm)	Tree_ID	Crown (m2)	Total Coverage (m2)	Total Coverage %
44	42.1767336	-84.1208500	FRAPEN	22.9	707	16.6		
44	42.1767336	-84.1208500	FRAPEN	14.5	708	8.3		
44	42.1767336	-84.1208500	FRAPEN	14.7	709	8.5		
44	42.1767336	-84.1208500	FRAPEN	78.5	710	71.6		
44	42.1767336	-84.1208500	FRAPEN	24.2	711	17.9		
44	42.1767336	-84.1208500	FRAPEN	16.8	712	10.5		
44	42.1767336	-84.1208500	FRAPEN	13.2	713	7.0		
44	42.1767336	-84.1208500	FRAPEN	14.1	714	7.9		
45	42.1780479	-84.1210056	FRAPEN	22.7	715	16.4	218.6	6.1%
45	42.1780479	-84.1210056	FRAPEN	16.3	716	10.0		
45	42.1780479	-84.1210056	FRAPEN	10.5	717	4.3		
45	42.1780479	-84.1210056	FRAPEN	16.0	718	9.7		
45	42.1780479	-84.1210056	FRAPEN	12.9	719	6.7		
45	42.1780479	-84.1210056	FRAPEN	18.2	720	11.9		
45	42.1780479	-84.1210056	FRAPEN	18.1	721	11.8		
45	42.1780479	-84.1210056	FRAPEN	18.2	722	11.9		
45	42.1780479	-84.1210056	FRAPEN	18.4	723	12.1		
45	42.1780479	-84.1210056	FRAPEN	38.3	724	31.8		
45	42.1780479	-84.1210056	FRAPEN	20.5	725	14.2		
45	42.1780479	-84.1210056	FRAPEN	15.2	726	8.9		
45	42.1780479	-84.1210056	FRAPEN	27.7	727	21.3		
45	42.1780479	-84.1210056	FRAPEN	54.1	728	47.5		
46	42.1764439	-84.1219765	FRAPEN	56.7	729	50.0	610.3	17.0%
46	42.1764439	-84.1219765	FRAPEN	35.0	730	28.6		
46	42.1764439	-84.1219765	FRAPEN	49.1	731	42.5		
46	42.1764439	-84.1219765	FRAPEN	27.5	732	21.1		

Plot_number	Latitude	Longitude	Fraxinus_species	DBH (cm)	Tree_ID	Crown (m2)	Total Coverage (m2)	Total Coverage %
46	42.1764439	-84.1219765	FRAPEN	29.0	733	22.6		
46	42.1764439	-84.1219765	FRAPEN	28.0	734	21.6		
46	42.1764439	-84.1219765	FRAPEN	41.2	735	34.7		
46	42.1764439	-84.1219765	FRAPEN	34.8	736	28.4		
46	42.1764439	-84.1219765	FRAPEN	25.4	737	19.0		
46	42.1764439	-84.1219765	FRAPEN	41.2	738	34.7		
46	42.1764439	-84.1219765	FRAPEN	43.3	739	36.8		
46	42.1764439	-84.1219765	FRAPEN	21.1	740	14.8		
46	42.1764439	-84.1219765	FRAPEN	25.9	741	19.5		
46	42.1764439	-84.1219765	FRAPEN	18.5	742	12.2		
46	42.1764439	-84.1219765	FRAPEN	20.6	743	14.3		
46	42.1764439	-84.1219765	FRAPEN	11.7	744	5.5		
46	42.1764439	-84.1219765	FRAPEN	20.6	745	14.3		
46	42.1764439	-84.1219765	FRAPEN	12.7	746	6.5		
46	42.1764439	-84.1219765	FRAPEN	52.3	747	45.7		
46	42.1764439	-84.1219765	FRAPEN	50.1	748	43.5		
46	42.1764439	-84.1219765	FRAPEN	17.2	749	10.9		
46	42.1764439	-84.1219765	FRAPEN	26.3	750	19.9		
46	42.1764439	-84.1219765	FRAPEN	23.5	751	17.2		
46	42.1764439	-84.1219765	FRAPEN	18.8	752	12.5		
46	42.1764439	-84.1219765	FRAPEN	26.9	753	20.5		
46	42.1764439	-84.1219765	FRAPEN	19.3	754	13.0		
47	42.1758270	-84.1216010	NOASH				0.0	0.0%
48	42.1746468	-84.1175348	FRAPEN	39.2	755	32.7	2243.8	62.3%
48	42.1746468	-84.1175348	FRAPEN	18.0	756	11.7		
48	42.1746468	-84.1175348	FRAPEN	12.7	757	6.5		

Plot_number	Latitude	Longitude	Fraxinus_species	DBH (cm)	Tree_ID	Crown (m2)	Total Coverage (m2)	Total Coverage %
48	42.1746468	-84.1175348	FRAPEN	17.5	758	11.2		
48	42.1746468	-84.1175348	FRAPEN	14.1	759	7.9		
48	42.1746468	-84.1175348	FRAPEN	15.6	760	9.3		
48	42.1746468	-84.1175348	FRAPEN	32.9	761	26.5		
48	42.1746468	-84.1175348	FRAPEN	17.1	762	10.8		
48	42.1746468	-84.1175348	FRAPEN	21.4	763	15.1		
48	42.1746468	-84.1175348	FRAPEN	18.9	764	12.6		
48	42.1746468	-84.1175348	FRAPEN	10.8	765	4.6		
48	42.1746468	-84.1175348	FRAPEN	14.2	766	8.0		
48	42.1746468	-84.1175348	FRAPEN	21.4	767	15.1		
48	42.1746468	-84.1175348	FRAPEN	15.2	768	8.9		
48	42.1746468	-84.1175348	FRAPEN	24.7	769	18.4		
48	42.1746468	-84.1175348	FRAPEN	15.7	770	9.4		
48	42.1746468	-84.1175348	FRAPEN	12.2	771	6.0		
48	42.1746468	-84.1175348	FRAPEN	22.6	772	16.3		
48	42.1746468	-84.1175348	FRAPEN	11.6	773	5.4		
48	42.1746468	-84.1175348	FRAPEN	11.4	774	5.2		
48	42.1746468	-84.1175348	FRAPEN	15.4	775	9.1		
48	42.1746468	-84.1175348	FRAPEN	23.0	776	16.7		
48	42.1746468	-84.1175348	FRAPEN	24.0	777	17.7		
48	42.1746468	-84.1175348	FRAPEN	15.4	778	9.1		
48	42.1746468	-84.1175348	FRAPEN	13.5	779	7.3		
48	42.1746468	-84.1175348	FRAPEN	20.4	780	14.1		
48	42.1746468	-84.1175348	FRAPEN	18.8	781	12.5		
48	42.1746468	-84.1175348	FRAPEN	20.0	782	13.7		
48	42.1746468	-84.1175348	FRAPEN	24.7	783	18.4		

Plot_number	Latitude	Longitude	Fraxinus_species	DBH (cm)	Tree_ID	Crown (m2)	Total Coverage (m2)	Total Coverage %
48	42.1746468	-84.1175348	FRAPEN	65.6	784	58.8		
48	42.1746468	-84.1175348	FRAPEN	20.6	785	14.3		
48	42.1746468	-84.1175348	FRAPEN	59.3	786	52.6		
48	42.1746468	-84.1175348	FRAPEN	38.7	787	32.2		
48	42.1746468	-84.1175348	FRAPEN	28.8	788	22.4		
48	42.1746468	-84.1175348	FRAPEN	15.0	789	8.8		
48	42.1746468	-84.1175348	FRAPEN	36.2	790	29.7		
48	42.1746468	-84.1175348	FRAPEN	11.9	791	5.7		
48	42.1746468	-84.1175348	FRAPEN	20.3	792	14.0		
48	42.1746468	-84.1175348	FRAPEN	39.9	793	33.4		
48	42.1746468	-84.1175348	FRAPEN	11.9	794	5.7		
48	42.1746468	-84.1175348	FRAPEN	11.2	795	5.0		
48	42.1746468	-84.1175348	FRAPEN	14.7	796	8.5		
48	42.1746468	-84.1175348	FRAPEN	14.9	797	8.7		
48	42.1746468	-84.1175348	FRAPEN	20.2	798	13.9		
48	42.1746468	-84.1175348	FRAPEN	14.1	799	7.9		
48	42.1746468	-84.1175348	FRAPEN	13.5	800	7.3		
48	42.1746468	-84.1175348	FRAPEN	15.1	801	8.8		
48	42.1746468	-84.1175348	FRAPEN	12.3	802	6.1		
48	42.1746468	-84.1175348	FRAPEN	46.5	803	39.9		
48	42.1746468	-84.1175348	FRAPEN	16.5	804	10.2		
48	42.1746468	-84.1175348	FRAPEN	25.8	805	19.4		
48	42.1746468	-84.1175348	FRAPEN	13.0	806	6.8		
48	42.1746468	-84.1175348	FRAPEN	11.8	807	5.6		
48	42.1746468	-84.1175348	FRAPEN	19.8	808	13.5		
48	42.1746468	-84.1175348	FRAPEN	14.0	809	7.8		

Plot_number	Latitude	Longitude	Fraxinus_species	DBH (cm)	Tree_ID	Crown (m2)	Total Coverage (m2)	Total Coverage %
48	42.1746468	-84.1175348	FRAPEN	14.2	810	8.0		
48	42.1746468	-84.1175348	FRAPEN	11.3	811	5.1		
48	42.1746468	-84.1175348	FRAPEN	20.7	812	14.4		
48	42.1746468	-84.1175348	FRAPEN	22.0	813	15.7		
48	42.1746468	-84.1175348	FRAPEN	13.7	814	7.5		
48	42.1746468	-84.1175348	FRAPEN	28.3	815	21.9		
48	42.1746468	-84.1175348	FRAPEN	16.8	816	10.5		
48	42.1746468	-84.1175348	FRAPEN	21.1	817	14.8		
48	42.1746468	-84.1175348	FRAPEN	17.9	818	11.6		
48	42.1746468	-84.1175348	FRAPEN	23.1	819	16.8		
48	42.1746468	-84.1175348	FRAPEN	25.6	820	19.2		
48	42.1746468	-84.1175348	FRAPEN	11.1	821	4.9		
48	42.1746468	-84.1175348	FRAPEN	19.9	822	13.6		
48	42.1746468	-84.1175348	FRAPEN	35.0	823	28.6		
48	42.1746468	-84.1175348	FRAPEN	19.5	824	13.2		
48	42.1746468	-84.1175348	FRAPEN	27.8	825	21.4		
48	42.1746468	-84.1175348	FRAPEN	25.4	826	19.0		
48	42.1746468	-84.1175348	FRAPEN	40.2	827	33.7		
48	42.1746468	-84.1175348	FRAPEN	24.8	828	18.5		
48	42.1746468	-84.1175348	FRAPEN	29.2	829	22.8		
48	42.1746468	-84.1175348	FRAPEN	23.3	830	17.0		
48	42.1746468	-84.1175348	FRAPEN	10.1	831	3.9		
48	42.1746468	-84.1175348	FRAPEN	21.7	832	15.4		
48	42.1746468	-84.1175348	FRAPEN	13.6	833	7.4		
48	42.1746468	-84.1175348	FRAPEN	21.5	834	15.2		
48	42.1746468	-84.1175348	FRAPEN	23.3	835	17.0		

Plot_number	Latitude	Longitude	Fraxinus_species	DBH (cm)	Tree_ID	Crown (m2)	Total Coverage (m2)	Total Coverage %
48	42.1746468	-84.1175348	FRAPEN	20.5	836	14.2		
48	42.1746468	-84.1175348	FRAPEN	40.1	837	33.6		
48	42.1746468	-84.1175348	FRAPEN	13.5	838	7.3		
48	42.1746468	-84.1175348	FRAPEN	12.5	839	6.3		
48	42.1746468	-84.1175348	FRAPEN	12.6	840	6.4		
48	42.1746468	-84.1175348	FRAPEN	11.1	841	4.9		
48	42.1746468	-84.1175348	FRAPEN	18.8	842	12.5		
48	42.1746468	-84.1175348	FRAPEN	15.6	843	9.3		
48	42.1746468	-84.1175348	FRAPEN	19.0	844	12.7		
48	42.1746468	-84.1175348	FRAPEN	12.9	845	6.7		
48	42.1746468	-84.1175348	FRAPEN	24.4	846	18.1		
48	42.1746468	-84.1175348	FRAPEN	47.3	847	40.7		
48	42.1746468	-84.1175348	FRAPEN	27.9	848	21.5		
48	42.1746468	-84.1175348	FRAPEN	51.7	849	45.1		
48	42.1746468	-84.1175348	FRAPEN	23.8	850	17.5		
48	42.1746468	-84.1175348	FRAPEN	21.8	851	15.5		
48	42.1746468	-84.1175348	FRAPEN	12.1	852	5.9		
48	42.1746468	-84.1175348	FRAPEN	16.6	853	10.3		
48	42.1746468	-84.1175348	FRAPEN	31.4	854	25.0		
48	42.1746468	-84.1175348	FRAPEN	19.9	855	13.6		
48	42.1746468	-84.1175348	FRAPEN	21.5	856	15.2		
48	42.1746468	-84.1175348	FRAPEN	14.9	857	8.7		
48	42.1746468	-84.1175348	FRAPEN	54.8	858	48.2		
48	42.1746468	-84.1175348	FRAPEN	24.2	859	17.9		
48	42.1746468	-84.1175348	FRAPEN	12.9	860	6.7		
48	42.1746468	-84.1175348	FRAPEN	12.1	861	5.9		

Plot_number	Latitude	Longitude	Fraxinus_species	DBH (cm)	Tree_ID	Crown (m2)	Total Coverage (m2)	Total Coverage %
48	42.1746468	-84.1175348	FRAPEN	14.1	862	7.9		
48	42.1746468	-84.1175348	FRAPEN	34.0	863	27.6		
48	42.1746468	-84.1175348	FRAPEN	24.2	864	17.9		
48	42.1746468	-84.1175348	FRAPEN	11.3	865	5.1		
48	42.1746468	-84.1175348	FRAPEN	10.9	866	4.7		
48	42.1746468	-84.1175348	FRAPEN	13.2	867	7.0		
48	42.1746468	-84.1175348	FRAPEN	17.7	868	11.4		
48	42.1746468	-84.1175348	FRAPEN	24.4	869	18.1		
48	42.1746468	-84.1175348	FRAPEN	13.5	870	7.3		
48	42.1746468	-84.1175348	FRAPEN	34.4	871	28.0		
48	42.1746468	-84.1175348	FRAPEN	21.3	872	15.0		
48	42.1746468	-84.1175348	FRAPEN	16.0	873	9.7		
48	42.1746468	-84.1175348	FRAPEN	21.8	874	15.5		
48	42.1746468	-84.1175348	FRAPEN	14.4	875	8.2		
48	42.1746468	-84.1175348	FRAPEN	22.4	876	16.1		
48	42.1746468	-84.1175348	FRAPEN	10.2	877	4.0		
48	42.1746468	-84.1175348	FRAPEN	21.9	878	15.6		
48	42.1746468	-84.1175348	FRAPEN	43.5	879	37.0		
48	42.1746468	-84.1175348	FRAPEN	16.1	880	9.8		
48	42.1746468	-84.1175348	FRAPEN	15.5	881	9.2		
48	42.1746468	-84.1175348	FRAPEN	26.8	882	20.4		
48	42.1746468	-84.1175348	FRAPEN	11.2	883	5.0		
48	42.1746468	-84.1175348	FRAPEN	17.7	884	11.4		
48	42.1746468	-84.1175348	FRAPEN	32.8	885	26.4		
48	42.1746468	-84.1175348	FRAPEN	20.5	886	14.2		
48	42.1746468	-84.1175348	FRAPEN	35.7	887	29.2		

Plot_number	Latitude	Longitude	Fraxinus_species	DBH (cm)	Tree_ID	Crown (m2)	Total Coverage (m2)	Total Coverage %
48	42.1746468	-84.1175348	FRAPEN	13.8	888	7.6		
48	42.1746468	-84.1175348	FRAPEN	35.5	889	29.0		
48	42.1746468	-84.1175348	FRAPEN	11.3	890	5.1		
48	42.1746468	-84.1175348	FRAPEN	31.7	891	25.3		
48	42.1746468	-84.1175348	FRAPEN	11.8	892	5.6		
48	42.1746468	-84.1175348	FRAPEN	12.6	893	6.4		
48	42.1746468	-84.1175348	FRAPEN	18.0	894	11.7		
48	42.1746468	-84.1175348	FRAPEN	23.0	895	16.7		
48	42.1746468	-84.1175348	FRAPEN	39.0	896	32.5		
48	42.1746468	-84.1175348	FRAPEN	14.9	897	8.7		
48	42.1746468	-84.1175348	FRAPEN	37.9	898	31.4		
48	42.1746468	-84.1175348	FRAPEN	20.4	899	14.1		
48	42.1746468	-84.1175348	FRAPEN	24.5	900	18.2		
48	42.1746468	-84.1175348	FRAPEN	23.3	901	17.0		
49	42.1750331	-84.1316969	NOASH				0.0	0.0%
50	42.1679091	-84.1266543	NOASH				0.0	0.0%
51	42.1694916	-84.1266865	FRAPEN	42.2	902	35.7	227.0	6.3%
51	42.1694916	-84.1266865	FRAPEN	41.3	903	34.8		
51	42.1694916	-84.1266865	FRAPEN	24.7	904	18.4		
51	42.1694916	-84.1266865	FRAPEN	30.1	905	23.7		
51	42.1694916	-84.1266865	FRAPEN	33.0	906	26.6		
51	42.1694916	-84.1266865	FRAPEN	38.0	907	31.5		
51	42.1694916	-84.1266865	FRAPEN	29.3	908	22.9		
51	42.1694916	-84.1266865	FRAPEN	40.0	909	33.5		
52	42.1705806	-84.1260642	NOASH				0.0	0.0%
53	42.1708488	-84.1268045	NOASH				0.0	0.0%

Plot_number	Latitude	Longitude	Fraxinus_species	DBH (cm)	Tree_ID	Crown (m2)	Total Coverage (m2)	Total Coverage %
54	42.1645027	-84.1315788	NOASH				0.0	0.0%
55	42.1608281	-84.1280705	FRAPEN	19.7	910	13.4	539.8	15.0%
55	42.1608281	-84.1280705	FRAPEN	23.8	911	17.5		
55	42.1608281	-84.1280705	FRAPEN	23.7	912	17.4		
55	42.1608281	-84.1280705	FRAPEN	38.6	913	32.1		
55	42.1608281	-84.1280705	FRAPEN	32.0	914	25.6		
55	42.1608281	-84.1280705	FRAPEN	27.5	915	21.1		
55	42.1608281	-84.1280705	FRAPEN	21.9	916	15.6		
55	42.1608281	-84.1280705	FRAPEN	62.0	917	55.3		
55	42.1608281	-84.1280705	FRAPEN	43.5	918	37.0		
55	42.1608281	-84.1280705	FRAPEN	40.3	919	33.8		
55	42.1608281	-84.1280705	FRAPEN	31.0	920	24.6		
55	42.1608281	-84.1280705	FRAPEN	19.4	921	13.1		
55	42.1608281	-84.1280705	FRAPEN	32.1	922	25.7		
55	42.1608281	-84.1280705	FRAPEN	25.6	923	19.2		
55	42.1608281	-84.1280705	FRAPEN	29.2	924	22.8		
55	42.1608281	-84.1280705	FRAPEN	29.2	925	22.8		
55	42.1608281	-84.1280705	FRAPEN	42.2	926	35.7		
55	42.1608281	-84.1280705	FRAPEN	21.6	927	15.3		
55	42.1608281	-84.1280705	FRAPEN	25.0	928	18.7		
55	42.1608281	-84.1280705	FRAPEN	45.8	929	39.2		
55	42.1608281	-84.1280705	FRAPEN	40.5	930	34.0		
56	42.1744537	-84.1127658	FRAPEN	11.4	931	5.2	190.7	5.3%
56	42.1744537	-84.1127658	FRAPEN	39.0	932	32.5		
56	42.1744537	-84.1127658	FRAPEN	19.6	933	13.3		
56	42.1744537	-84.1127658	FRAPEN	27.8	934	21.4		

Plot_number	Latitude	Longitude	Fraxinus_species	DBH (cm)	Tree_ID	Crown (m2)	Total Coverage (m2)	Total Coverage %
56	42.1744537	-84.1127658	FRAPEN	19.4	935	13.1		
56	42.1744537	-84.1127658	FRAPEN	28.8	936	22.4		
56	42.1744537	-84.1127658	FRAPEN	53.7	937	47.1		
56	42.1744537	-84.1127658	FRAPEN	13.1	938	6.9		
56	42.1744537	-84.1127658	FRAPEN	22.7	939	16.4		
56	42.1744537	-84.1127658	FRAPEN	12.8	940	6.6		
56	42.1744537	-84.1127658	FRAPEN	12.1	941	5.9		
57	42.1719324	-84.1177333	FRAPEN	15.7	942	9.4	63.3	1.8%
57	42.1719324	-84.1177333	FRAPEN	26.2	943	19.8		
57	42.1719324	-84.1177333	FRAPEN	13.6	944	7.4		
57	42.1719324	-84.1177333	FRAPEN	14.6	945	8.4		
57	42.1719324	-84.1177333	FRAPEN	13.3	946	7.1		
57	42.1719324	-84.1177333	FRAPEN	12.7	947	6.5		
57	42.1719324	-84.1177333	FRAPEN	11.0	948	4.8		
58	42.1713209	-84.1192139	FRAPEN	45.0	949	38.5	691.3	19.2%
58	42.1713209	-84.1192139	FRAPEN	56.9	950	50.2		
58	42.1713209	-84.1192139	FRAPEN	42.2	951	35.7		
58	42.1713209	-84.1192139	FRAPEN	22.7	952	16.4		
58	42.1713209	-84.1192139	FRAPEN	21.0	953	14.7		
58	42.1713209	-84.1192139	FRAPEN	50.1	954	43.5		
58	42.1713209	-84.1192139	FRAPEN	50.7	955	44.1		
58	42.1713209	-84.1192139	FRAPEN	38.0	956	31.5		
58	42.1713209	-84.1192139	FRAPEN	20.0	957	13.7		
58	42.1713209	-84.1192139	FRAPEN	18.7	958	12.4		
58	42.1713209	-84.1192139	FRAPEN	37.9	959	31.4		
58	42.1713209	-84.1192139	FRAPEN	35.7	960	29.2		

Plot_number	Latitude	Longitude	Fraxinus_species	DBH (cm)	Tree_ID	Crown (m2)	Total Coverage (m2)	Total Coverage %
58	42.1713209	-84.1192139	FRAPEN	32.8	961	26.4		
58	42.1713209	-84.1192139	FRAPEN	35.8	962	29.3		
58	42.1713209	-84.1192139	FRAPEN	30.7	963	24.3		
58	42.1713209	-84.1192139	FRAPEN	31.0	964	24.6		
58	42.1713209	-84.1192139	FRAPEN	37.3	965	30.8		
58	42.1713209	-84.1192139	FRAPEN	43.0	966	36.5		
58	42.1713209	-84.1192139	FRAPEN	31.3	967	24.9		
58	42.1713209	-84.1192139	FRAPEN	29.9	968	23.5		
58	42.1713209	-84.1192139	FRAPEN	39.8	969	33.3		
58	42.1713209	-84.1192139	FRAPEN	28.1	970	21.7		
58	42.1713209	-84.1192139	FRAPEN	27.4	971	21.0		
58	42.1713209	-84.1192139	FRAPEN	40.2	972	33.7		
59	42.1708113	-84.1191495	FRAPEN	21.3	973	15.0	27.3	0.8%
59	42.1708113	-84.1191495	FRAPEN	18.6	974	12.3		
60	42.1646476	-84.1166604	NOASH				0.0	0.0%
Average				23.9		17.6	285.4	7.9%
Median				20.3		14.0	17.5	0.5%
Std Dev				12.3		12.2	505.8	13.8%
Sum							17122.3	7.9%